Thermo Electron Engineering Corporation, 85 First Avenue, Waltham, Massachusetts 02154

Contract No. 950671

Task II

Report No. TE 34-65

FINAL REPORT - TASK II
SOLAR ENERGY THERMIONIC (SET) PROGRAM

December 1964

Prepared for:

Jet Propulsion Laboratory
Pasadena, California

Approved by: Peter G. Pantazelos

Peter G. Pantazelos
Manager
Engineering Department

64-771

Thermo Electron Engineering Corporation, 85 First Avenue, Waltham, Massachusetts 02154

Contract No. 950671

Task II

Report No. TE 34-65

FINAL REPORT - TASK II
SOLAR ENERGY THERMIONIC (SET) PROGRAM

December 1964

by

Pierre J. Brosens

This work was performed for the Jet Propulsion Laboratory, California Institute of Technology, sponsored by the National Aeronautics and Space Administration under Contract NAS7-100.

Approved by: Peter G Pantazelos

Peter G. Pantazelos
Manager
Engineering Department

TABLE OF CONTENTS

TABLE OF CONTENTS

TABLE OF CONTENTS

LIST OF ILLUSTRATIONS

LIST OF ILLUSTRATIONS

LIST OF ILLUSTRATIONS

LIST OF ILLUSTRATIONS

1. PROGRAM REVIEW

Under Task I of Contract 950671, Thermo Electron has designed for fabrication and delivery to JPL a Solar Thermionic Generator suitable for evaluation at the Table Mountain Solar Facility, and capable of meeting flight qualification tests, particularly with regard to resistance to shock and vibration. This Task II, of this same contract, was undertaken on October 27, 1963 to: (1) develop an advanced converter structure capable of satisfying the geometrical constraints of a variety of generator designs, including those that use as many as 16 converters, and (2) improve converter performance, particularly at higher output voltages, by reducing the interelectrode spacing. This last goal was selected because the improvement in performance at higher output voltages has been recognized as the way to improve state-of-the-art converter efficiency; increases in power density at low voltages result in rather small improvement because of the large heat transfer penalty which must be paid for the corresponding increases in the output current.

The original statement of work called for the fabrication and test of:

1 converter prototype with a tantalum emitter

2 identical converters with tantalum emitters

2 identical converters with rhenium emitters

This effort was slightly redirected, according to Thermo Electron's request dated May 6, 1964, when collector deposits in converters with tantalum emitters were found to form, and when the results of rhenium emitter fabrication efforts, undertaken under Task I, demonstrated that rhenium emitter structures could be incorporated in converters earlier than had been anticipated. Consequently, the revised program called for the fabrication and test of two converter prototype iterations with tantalum emitters, followed by 3 converters with rhenium emitters

fabricated in sequence to allow for the incorporation of whatever simple improvements would be suggested by the results of testing. All work under this program was completed December 18, 1964, with the fabrication and test of 7 converters.

A summary of the results obtained with each converter is given below. The converters have been designated with the serial numbers TE-100, TE-101, and so on. A suffix, P, is added to designate additional units which failed before any test data could be obtained.

TE-100: Tantalum Emitter, Molybdenum Collector, Delivered to JPL
This converter had the same basic design as that of all the converters to follow. These indicated that the thermal resistance of the collector structure was excessive and due, mainly, to the incomplete joining of some components.

TE-101: Tantalum Emitter, Molybdenum Collector. Opened for examination.
A refined thermal analysis of the converter design, based on the results obtained from the test of converter TE-100, indicated the need to double the radiator area, and the design was modified accordingly. In test, converter TE-101 suffered a 30% degradation in output, which was traced to the formation of a deposit on the collector surface. As a result, the recommendation was made to JPL to redirect the program to use a rhenium emitter in the fabrication of the next converter.

TE-102P: Rhenium Emitter, Molybdenum Collector. Opened for examination.
This converter had a minute leak at the pinch-off which was not discovered until late in the program. The consequence of this leak was that a substantial amount of the electroplating solution, used to electro-

form a nickel reinforcement over the pinch-off, was aspirated into the converter and the subsequent build-up of gas pressure under converter test conditions deformed the converter structure considerably.

TE-102: Rhenium Emitter, Molybdenum Collector. Delivered to JPL. Considerable testing of this converter demonstrated normal electrode conditions. The observed output, however, was good only at voltages greater than 1.1 volt; below this voltage, the performance observed was less than that observed in Series VIII converters, even though these have an interelectrode spacing twice as large as that of TE-102.

TE-103: Rhenium Emitter, Molybdenum Collector. Opened for examination.

This converter had a collector with a larger lateral area than that provided in converter TE-102. In test, it had the best output and the highest overall efficiency of all the converters tested under Task II. A power density of 11.0 watts/cm^2 was observed at 2000°K at an output voltage of 1.2 volts and the overall measured efficiency at this voltage was 11.0%. The output at lower voltage is, nonetheless, considerably below that which was obtained from variable parameter research converters, and this discrepancy has not been resolved. The converter shorted on the lateral area of the collector after 219 hours of testing when the emitter temperature was lowered to obtain data below 2000°K. Although the location of this short has been clearly identified, there is no satisfactory explanation for this failure except that it is possible that the emitter structure utilized in the fabrication of this converter was one which had been noted to have an appreciable amount of misalignment.

TE-104P: Rhenium Emitter, Molybdenum Collector.
This converter structure was ruined when, in an attempt to simplify the assembly procedure, considerable braze remelting required the removal and rebrazing of several converter components. These additional brazes resulted in the internal flow of braze material with the consequent electrical shorting of the emitter support to the collector structure.

TE-104: Rhenium Emitter, Molybdenum Collector. Delivered to JPL.

The collector of this converter was like that of converter TE-102, except that the internal radiation shield was omitted to avoid the possible loss of output current due to back-emission from this element. The output of converter TE-104 was better than that of TE-102 at output voltages below 0.75 volt or above 1.55 volt, but in the range of practical interest lying between these values the output of TE-104 was less, the difference being 20% at 1.2 volts. The lower performance observed has been tentatively ascribed to the fact that a drill fragment was found to have been left at the bottom of one of the two hohlraums drilled in the emitter structure of this converter and that it subsequently melted and diffused into it. Converter TE-104 was tested for a total of 560 hours at several emitter temperatures, and no evidence of electrical shorting was observed.

The main results of this program may be summarized as follows:

- An advanced converter structure with a 1 mil interelectrode spacing has been developed which meets all the major geometrical conditions for use in multi-converter generators of a variety of designs.
- Interelectrode spacing has been verified in two converters by accurate

measurement of cesium conduction heat transfer.

- Precise calorimetric data on the magnitude of electron cooling losses has been obtained.
- The power output and the efficiency of thermionic converters at voltages above 1.1 volt has been improved considerably.
- Reference data has been obtained for the continued exploration of the effect of changes in converter features, materials and fabrication techniques, on their performance.
- Reference analytic models have been established to facilitate the interpretation of converter performance.
- There has been no opportunity to demonstrate the extent to which the performance of the TE-100 converter series is reproducible.
- A converter life of 560 hours without degradation in output or failure has been demonstrated; it must be recognized, however, that an electrical short was observed in one converter at the end of 219 hours.
- The performance of the TE-100 converter, although attractive compared to that of other hardware converters developed to date, has not reached the level, particularly at voltages below 1.1 volt, which can be expected from the test results obtained with variable parameter research converters.

2. PROTOTYPE DESIGN

2.1 Prototype Design Requirements:

The design of the TE-100 converter series was in large part dictated by the results of a previous study, conducted at Thermo Electron for JPL, to determine optimum generator configurations for use in cislunar space with a 9.5 ft.

diameter parabolic mirror. The design recommended consisted of a single absorber cavity surrounded by two rings of 8 thermionic converters having an emitter area of 2.50 cm^2 each, operating at 2000°K. Such a design, in a series-connected configuration, would be able to deliver maximum power at an output of 72 amperes. Assuming SET Series VIII converter performance, the generator power would be 800 watts at 11.1 volts (corresponding to a power density per converter of 20 watts/cm^2 at 0.7 volts). In earthbound test, this same generator design could operate, assuming a solar constant of 90 watts/sq.ft., at 1900°K, and deliver an output of 400 watts. The pertinent assumptions on the solar concentrator system were:

a. 85% of the flux falling on an area 9.5 ft. in diameter is delivered to a 4 cm diameter generator aperture.
b. the transmissivity of the window used in earthbound test is 85%.

In order for the TE-100 converter series to be able to be used in this generator configuration, as well as in the conventional 4-converter generator design, and many others, the following design requirements were therefore established:

a. emitter area: 2.50 cm^2
b. emitter temperature: 1800°K - 2000°K
c. the entire converter must be encompassed within a truncated conical envelope of 30°, tangent to the edge of the emitter structure, in order to permit the mounting of the converter into 16-converter clusters without mechanical interference.
d. To realize a performance improvement over the previously developed SET converters, the interelectrode spacing is to be reduced from a nominal value of 2 mils to a nominal value of 1.2 mils at operating conditions.

2.2 Prototype Design:

Essentially, the design of the prototype was made in three steps:

a. design an emitter-collector structure capable of producing an interelectrode spacing of 1.2 mils.

b. design the converter radiator.

c. design the remainder of the converter structure.

2.2.1 Design of Emitter Collector Structure:

Previous experience with SET converter designs had indicated that the use of a thermal expansion process from a condition of full contact is the simplest and most reliable way of achieving reproducible small interelectrode spacings. Consequently, the same approach was selected to provide the interelectrode spacing in the TE-100 converter series. However, because of the small value of spacing desired, it was necessary to modify somewhat the design of the elements which contribute to produce the interelectrode spacing, and this is explained below.

Simple analysis of the previous SET VIII design showed that, in a molybdenum-collector-tantalum-emitter structure, the interelectrode spacing, at a given operating temperature distribution, will be proportional to the distance a from the plane of the electrodes to the point where the emitter structure "returns" to the collector structure, as shown in Figure 1a. The minimum attainable value of interelectrode spacing with this configuration, in converters operating at an emitter temperature of 2000°K, is 3.12 mils for a value of d of 1 inch and, therefore, to achieve the value of 1.2 mils it is necessary to have an a of 0.38 inch. This is a relatively small value from the standpoint of reducing the substantial emitter heat loss which occurs in the conducting path created by the emitter support, and a large loss can threaten the integrity of the ceramic

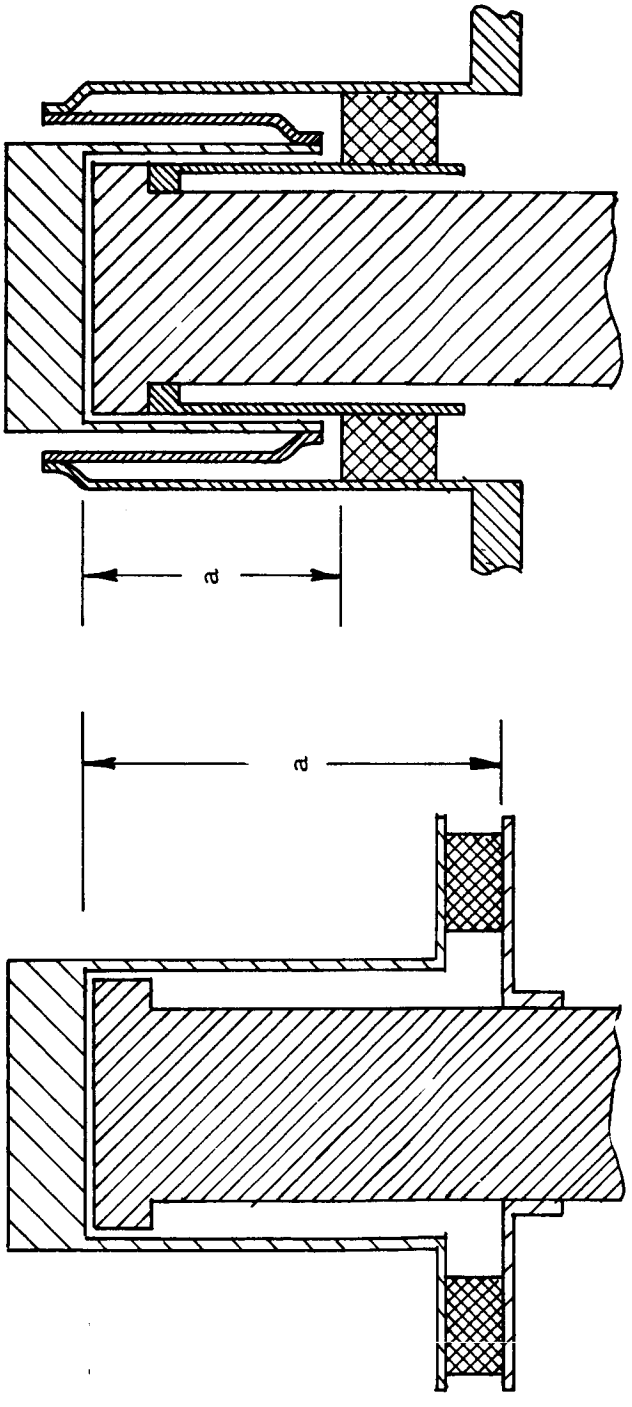

a. Straight

b. Convoluted

Figure 1. Emitter-Collector Structure Designs

seal to which the emitter support must always be attached. For a given value of a, a reduction of this loss can be accomplished only at the expense of strength and fabrication cost by decreasing its thickness. To give an example: at a current density of 15 A/cm^2, the optimum lead loss is of the order of 9 watts/cm^2; to achieve this optimum in a converter with 2.5 cm^2 emitter area and an a of 0.38 inch, it is necessary to use an emitter support having a thickness of 1.5 mils, and this is clearly inconsistent with the achievement of adequate strength. For comparison, the value selected for the Series VIII converter is 3.2 mils, and it is the product of the experience gained in fabricating and testing nearly 100 converters.

To solve the emitter support design problem, a different support design was adopted which is described schematically in Figure 1b. This is a convoluted support which permits increasing the path length for conduction heat transfer while maintaining the desired low value of a. The design also allows an effective reduction of the external radiation losses from the lateral area of the emitter structure by its self-shielding configuration and, moreover, the anular pocket formed by the convoluted structure can be used to lodge therein several additional radiation shields. Thus, the increase in the complexity of the convoluted emitter stucture is offset by the reduction in cost realized in machining thicker cylindrical sleeves, the reduction in conduction loss without sacrificing strength, and the automatic provision of effective means to reduce lateral external radiation.

Figure 2 shows a sketch of the actual emitter structure designed for the Series TE-100 converter. The calculated value of the interelectrode spacing it produces is 1.05 mils which is 2% more than the minimum value which could have been attained in a straight structure (Figure 1a) with the same value of a

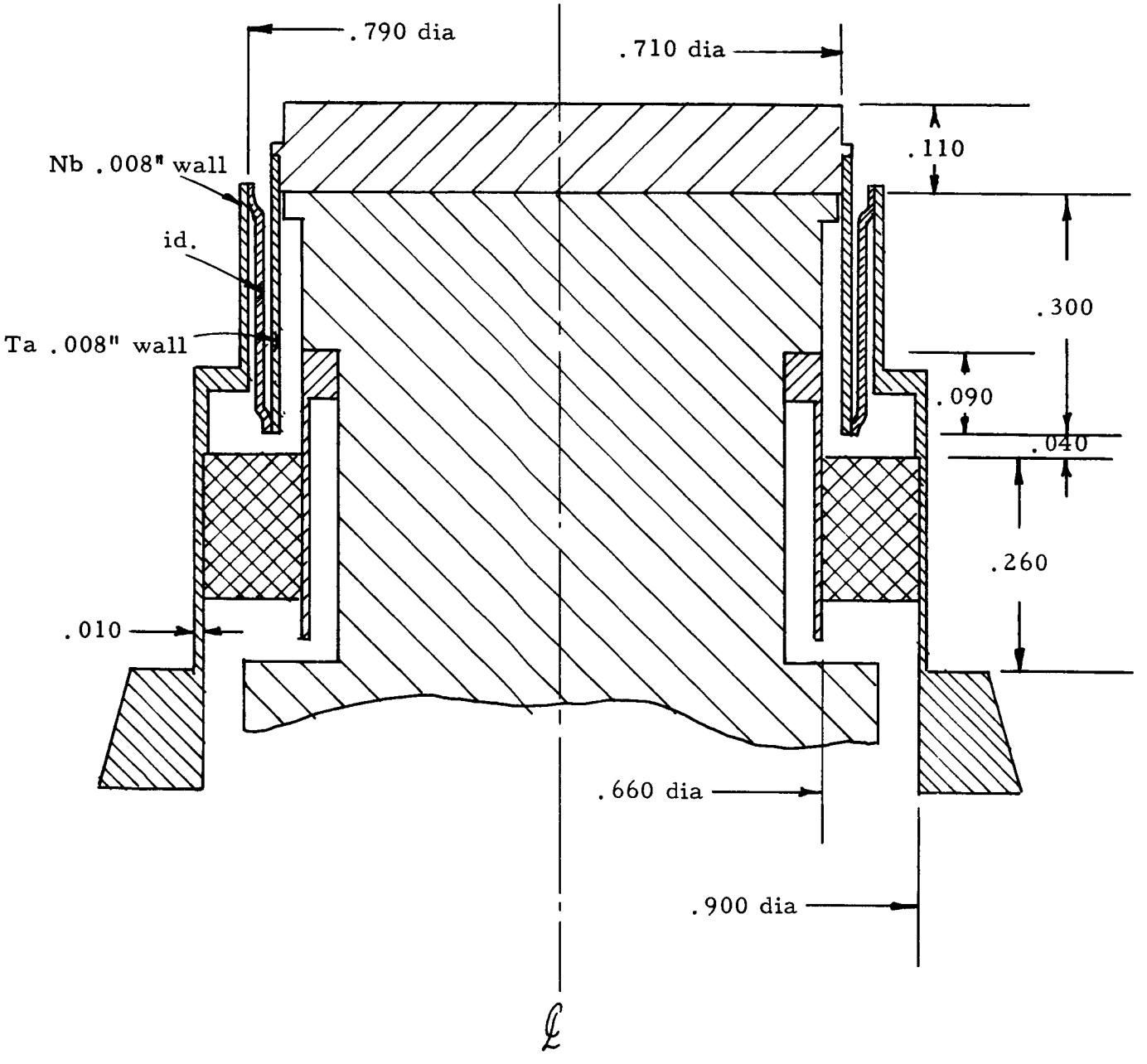

Figure 2. Emitter-Collector Structure Design for Series TE-100 Converters

of 0.33 inch. The calculated values of lead resistance at temperature, and lead conduction at an emitter temperature of 2000°K, are 0.0016 ohm and 58 watts respectively.

It is of interest to compare these lead losses with the lead losses that could be incurred using a fully optimized lead. The losses of a fully optimized lead have been calculated and are presented in Figure 3 as a function of the converter efficiency. There is an ambiguity about the value of converter efficiency that can be selected, and the most appropriate selection is the overall efficiency of the converter that can be expected in individual laboratory electrical test. If a value of 13% is chosen, and the lead is optimized for a total current of 37.5 amperes (15 A/cm^2), Figure 3 indicates that the heat loss of the optimized lead would be 22.5 watts, and its resistance would be .0024 ohm. Thus, it is seen that the lead designed for converter TE-100 is somewhat heavier than optimum. With the use of the convoluted design, however, it is possible to reduce the lead thickness to near-optimum conditions without undermining the strength of the emitter structure.

2.2.2 Design of Converter Radiator:

The radiator design selected for the TE-100 converter is illustrated in Figure 4. It consists of four identical flat fins of a trapezoidal shape which satisfies the requirement, previously mentioned, that the converter structure be encompassed within a 30° conical envelope. Such a design offers two important advantages: (1) it provides support for the free end of the cesium reservoir tube, and (2) the high emissivity surfaces of the radiator have a minimum view angle of the cesium reservoir tube while, at the same time, they allow the

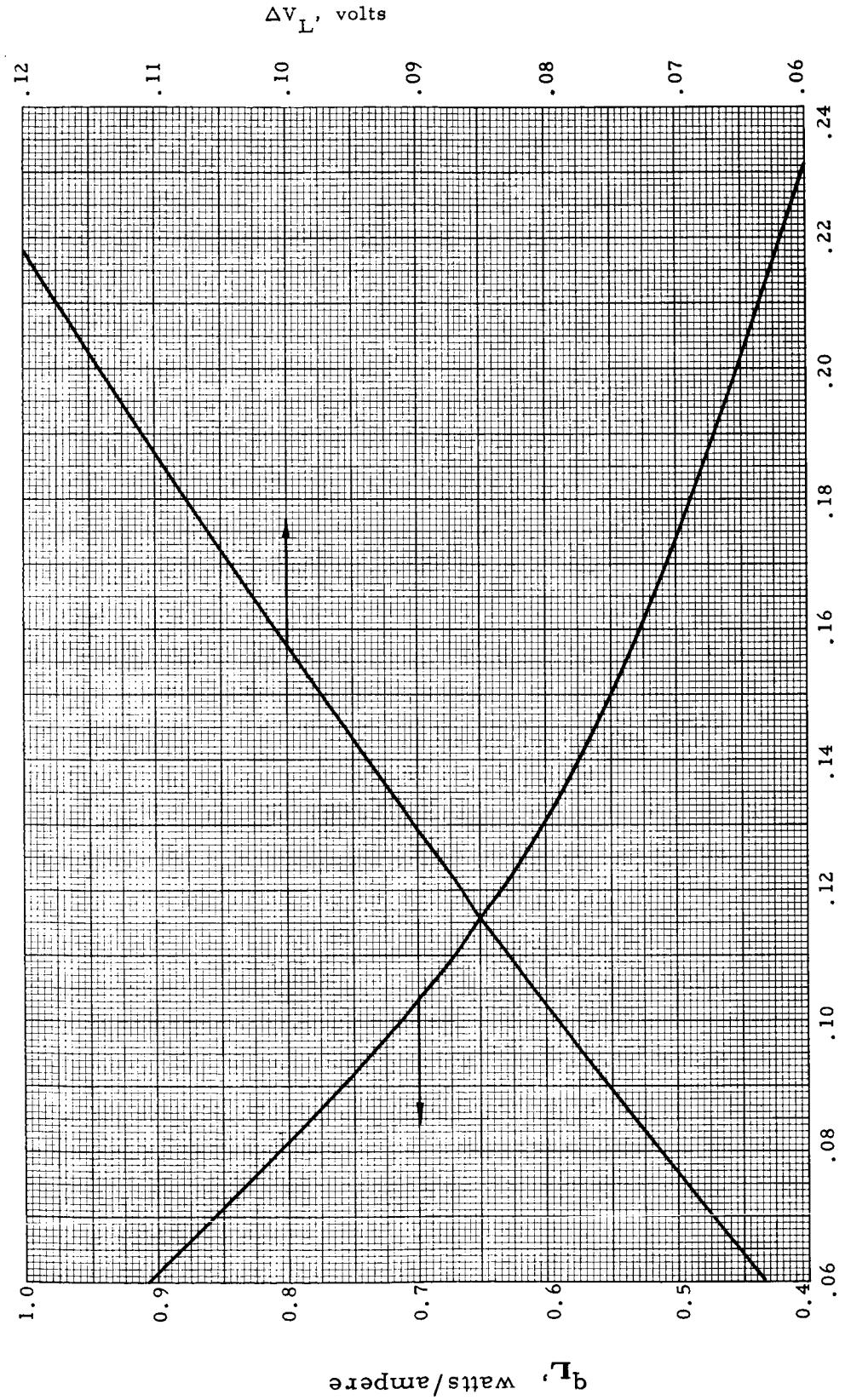

Figure 3. Heat Conduction and Voltage Drop in Optimized Converter Lead

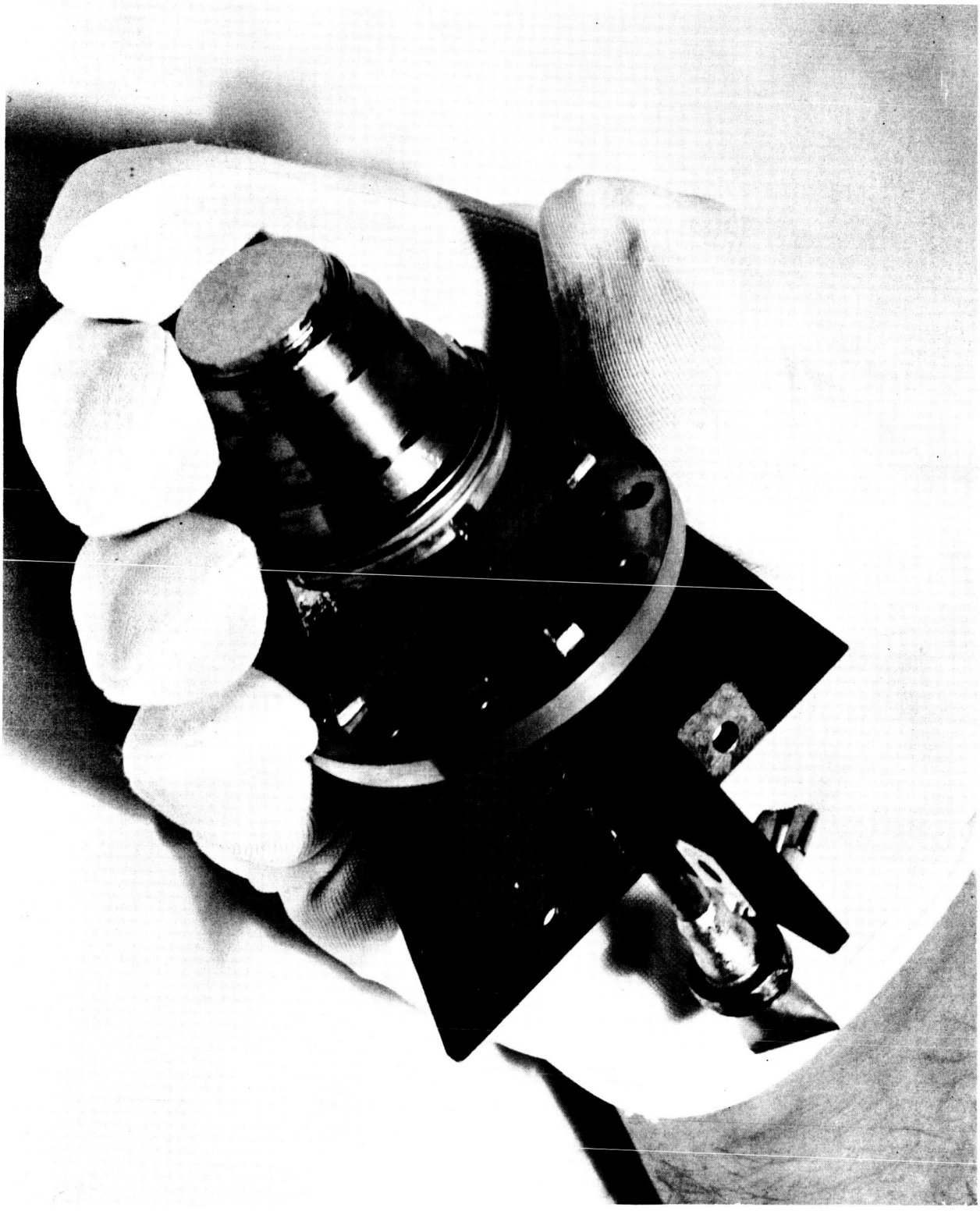

Figure 4. View of Prototype TE-101 and Radiator Structure

entire length of the tube to view the surrounding space, and thus it is possible to reach reservoir temperature with a relatively short length of tube.

The procedure followed to dimension the radiator was to first evaluate the heat transferred to the collector structure; then, for the particular collector structure used, the temperature drop from the collector face to the radiator was calculated, and knowing the desired collector temperature, the radiator temperature was consequently determined. The final step of the design was to develop sufficient radiator area such that at the radiator temperature determined above, it would be possible to radiate the heat transferred to the collector.

2.2.3 Design of Remainder of Converter Structure:

The layout of the TE-100 converter design is shown in Figure 5, and Table 1 gives the list of materials. They apply specifically to the design of prototypes TE-102P and TE-102. The difference between all the prototypes are discussed further on, and can be understood with the help of Figure 5. A simplified view of the layout is presented in Figure 6 to describe the most important design features. The emitter structure has the configuration that was presented in Figure 2, the current collected at the bottom of this structure is directed to a niobium post to which the emitter lead terminal is clamped. To avoid the problem of loosening of this connection which is often encountered in thermionic converters, the terminal clamp is also made of niobium. The collector supports an internal radiation shield and is joined to a cylindrical niobium sleeve which is in turn joined to the ceramic insulator. The cylindrical seal is strong and compact, and by being concealed from the converter environment, it is protected from the condensation of metallic vapors which could lead to a decrease in its electrical resistance. The collector cross-section is grad-

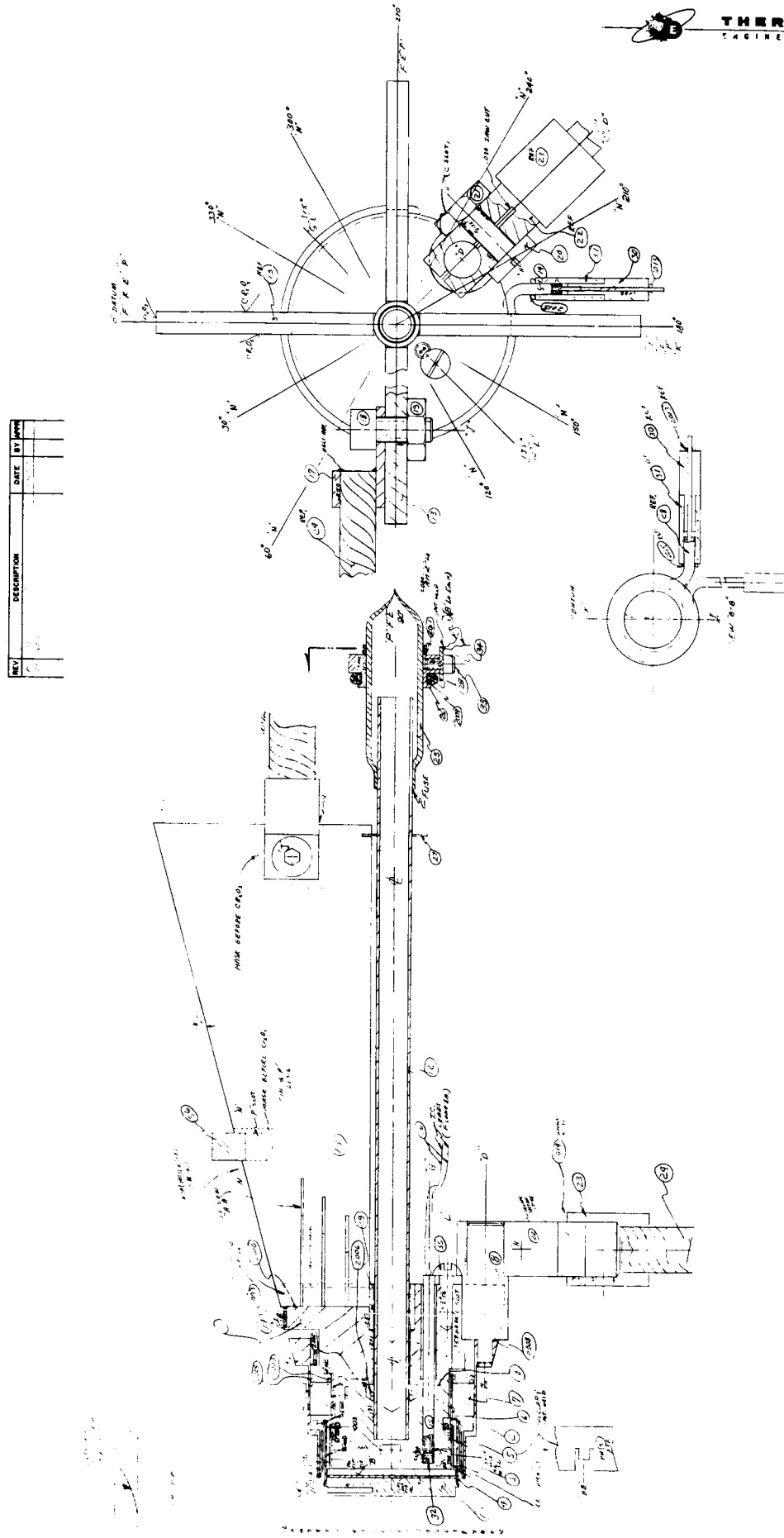

Figure 5. Layout of TE-100 Converter

TABLE I

Parts List - Converter TE-100

Part No.	Description	Material	No. Required
1	Emitter piece	Tantalum & Rhenium	1
2	Outer seal flange	Niobium	1
3	Intermediate emitter support	Niobium	1
4	Emitter support	Tantalum	1
5	Collector shield	Tantalum	1
6	Inner seal flange	Niobium	1
7	Ceramic insulator	Aluminum Oxide	1
8	Terminal post	Niobium	1
10	Collector	Molybdenum	1
11	Radiator support	Molybdenum	1
12	Cesium tube	Nickel	1
13	Radiator fin	Copper	4
14	Collector heater wire	Stainless Steel	1
15	Collector thermocouple insulator	Aluminum Oxide	2
16	Thermocouple	Chromel-Alumel	4
17	Collector lead terminal	Stainless Steel	1
18	Collector terminal screw	Stainless Steel	1
19	Collector terminal nut	Stainless Steel	1
20	Emitter terminal screw	Titanium	1
21	Emitter terminal nut	Stainless Steel	1
22	Emitter lead terminal clamp	Niobium	1
23	Emitter lead connector	Copper	1
24	Stranded Lead (AWG No. 4)	Copper	2
25	Cesium Reservoir	Copper	1
26	Cesium Reservoir ring	Nickel	1
27	Cesium tube support disc	Niobium	1
28	Cesium Reservoir Heater	Stainless Steel	1
29	Radiator Fin stop	Nickel	1
30	Heater Terminal	Nickel	4
31	Heater Terminal insulator	Aluminum Oxide	4
32	Collector thermal slug	Stainless Steel	2
33	Reservoir thermocouple screw	Stainless Steel	2
34	Reservoir thermocouple washer	Stainless Steel	2
35	Collector thermocouple screw	Stainless Steel	2
36	Converter mounting ring	Stainless Steel	1

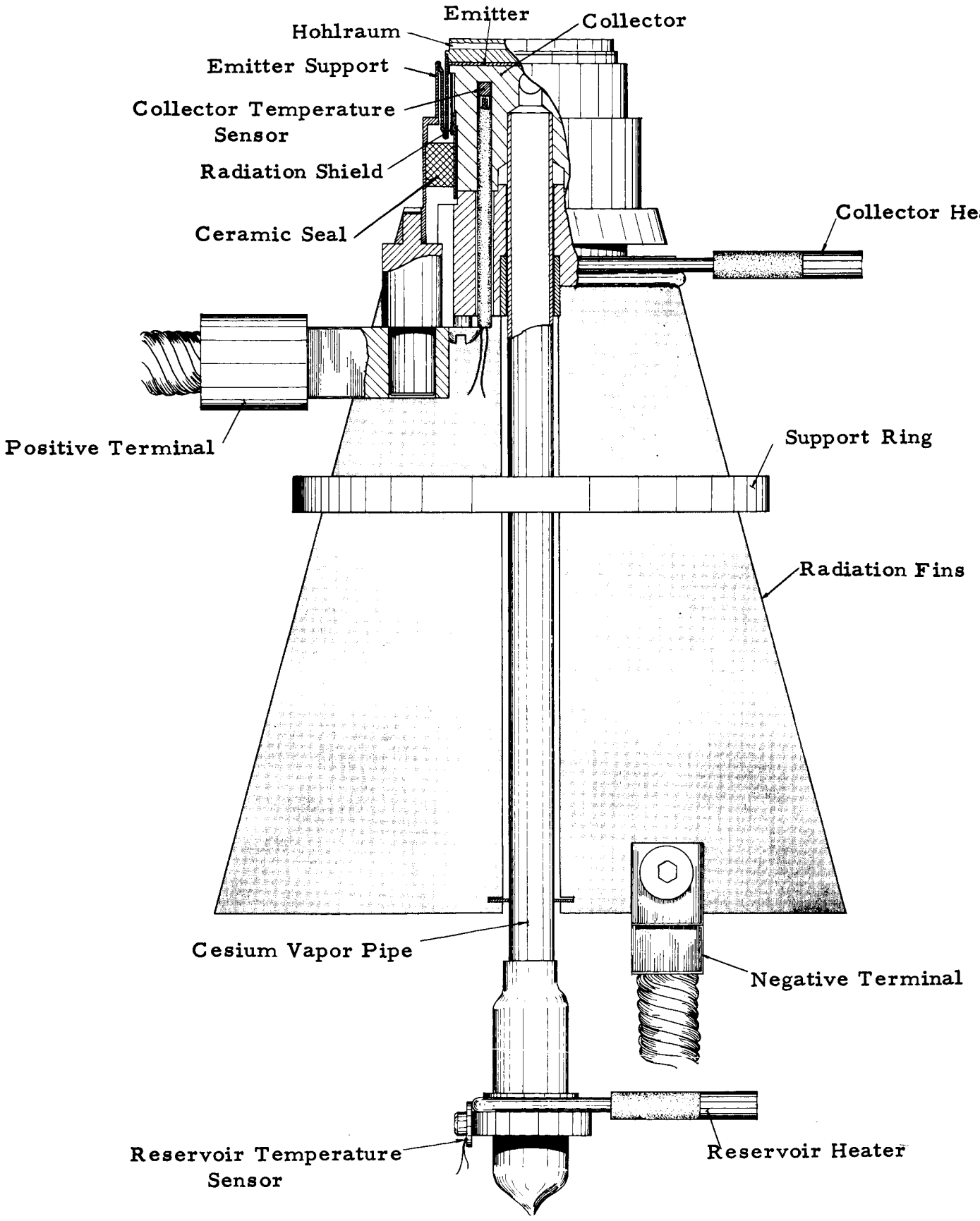

Figure 6. Pictorial Sketch of TE-100 Converter

ually enlarged by means of the element used to support the radiator fins. The cesium reservoir can be inverted without allowing the liquid cesium to drip out of it. The entire converter is supported from the radiator fins by means of a support ring located at the plane of the center of gravity of the converter. Figure 7 shows the converter being supported by a thread from this ring to demonstrate the degree of coincidence between the center of gravity and the plane of the support ring. Temperature sensing is achieved as closely as possible to the desired location with demountable thermocouples. Sheathed heaters are used to allow rapid heating of the collector and the reservoir with minimum encumbering of the converter structure. Initially, the output leads were made with stranded copper wire with an outside diameter of 0.222 in. Converter TE-102P and all that followed were made with #4 stranded copper wire which has an outside diameter of 0.305 in.

3. CONVERTER FABRICATION

Figures 8, 9 and 10 are presented here to show the basic details of a fabricated converter structure. Figure 8 is a side view of Prototype TE-101, Figure 9 presents the top and bottom views of the same converter and Figure 10 shows an x-ray view of converter TE-103 where the actual arrangement of the internal parts achieved can be seen. In this section, the differences in the design, fabrication and treatment of the various prototypes constructed are discussed and the basic assembly procedure is presented.

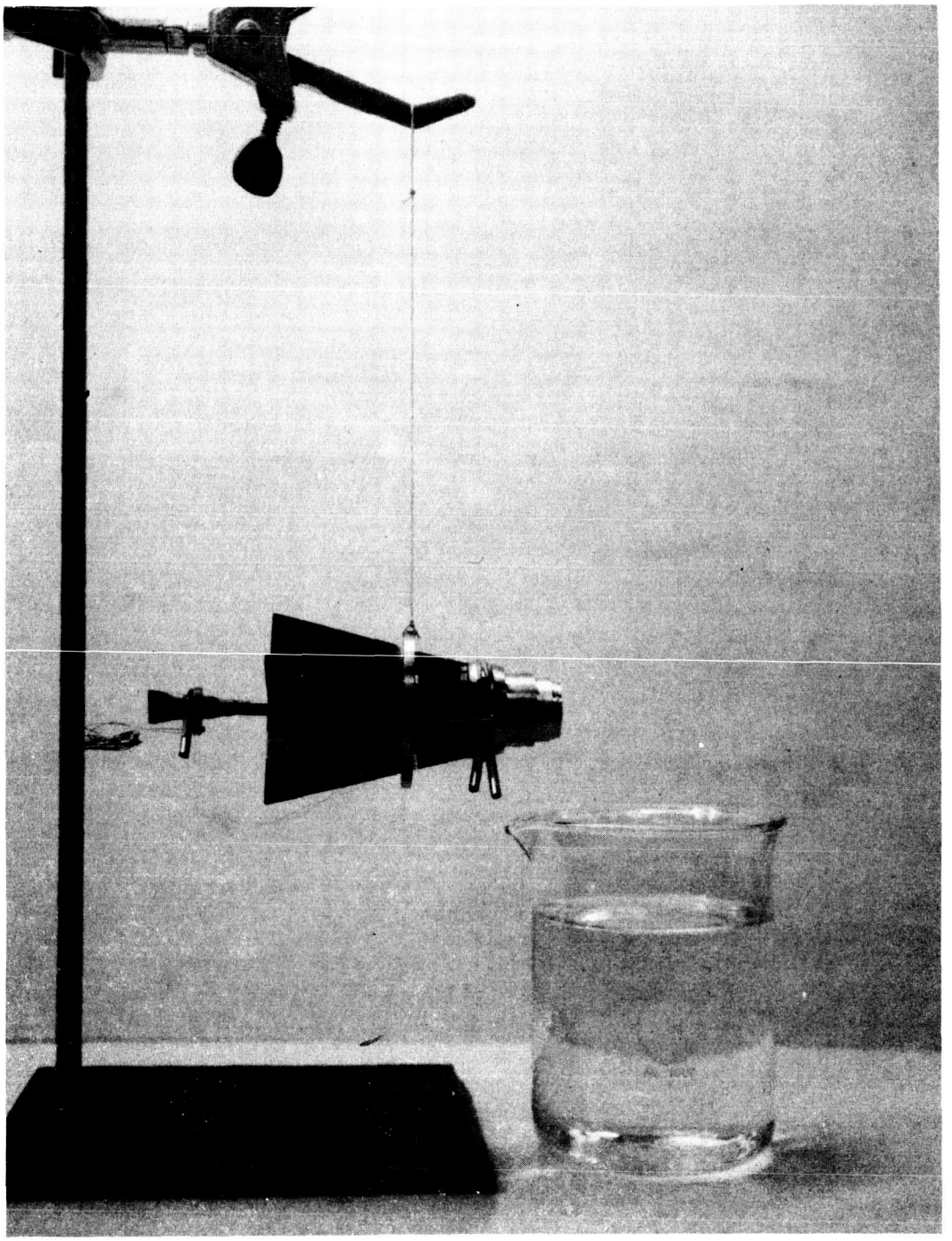

Figure 7. Center of Gravity Support of Modified Prototype Design

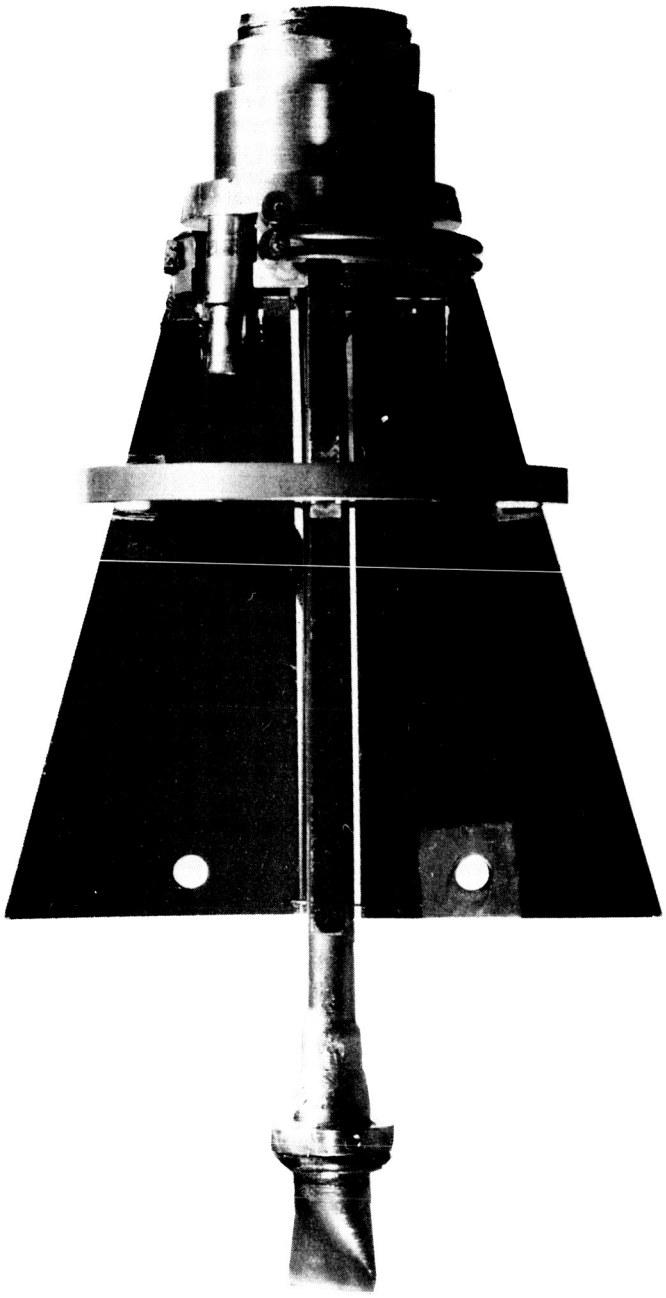

Figure 8 Prototype TE-101, Side View

5815

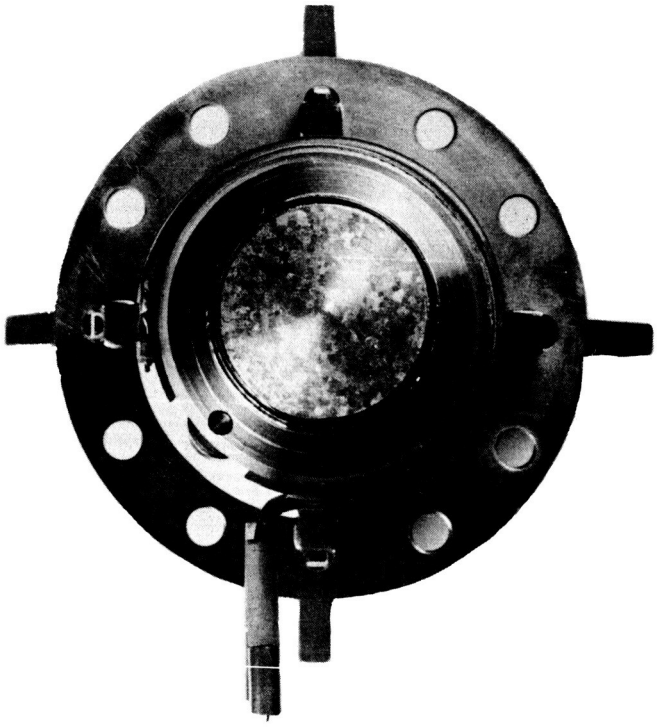

Figure 9a. Prototype TE-101, Top View

5816

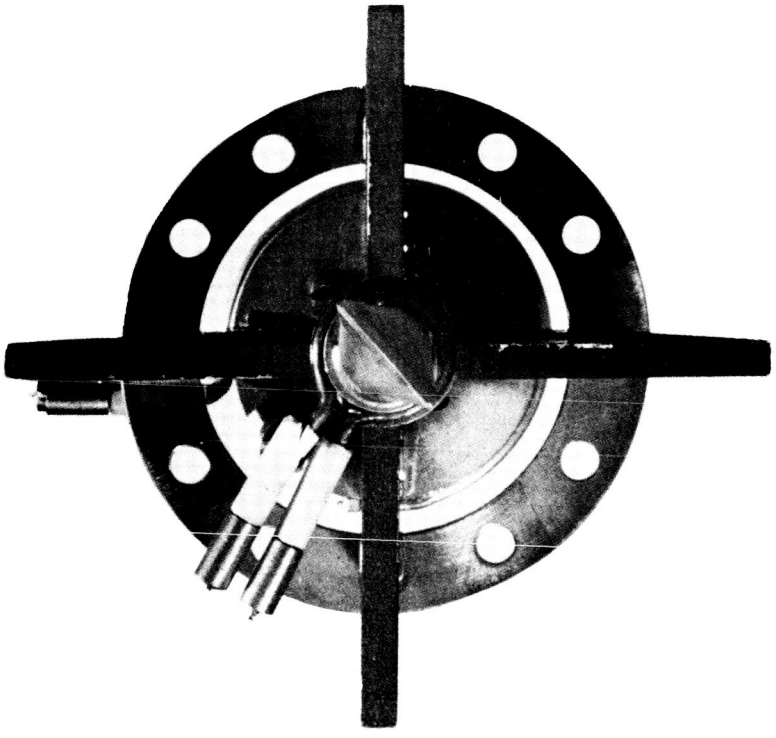

Figure 9b Prototype TE-101, Bottom View

Figure 10. X-Ray View of Converter TE-103

3.1 Converter Materials and Processing Procedures:

Because of the similarity in the design requirements for the TE-100 series of converters, and for the previous series of SET converters, the materials selected for fabrication are basically the same. For instance, niobium is used for the seal flanges in order to match the expansion of the aluminum oxide insulator, molybdenum is used for the collector stem in order to achieve the smallest possible resistance in a structure with a melting point above that of the seal braze material which is copper, copper is used for the radiator fins in order to achieve a minimum radiator weight, and a nickel cesium tube is used to obtain a reliable braze to the molybdenum collector.

3.2 Prototype Variations

As required by the contract, five prototypes were built and tested under this program. In addition, two other prototypes were fabricated but could not be tested due to structural defects. Table II summarizes the principal differences between the seven prototypes thus constructed.

As specified in the contract, prototype TE-100 had a tantalum emitter and was fabricated principally to verify the thermal design of the converter. The thermal test indicated that TE-100 operated at an abnormally high collector temperature. It is calculated that for a design of the structure of converter TE-100 the collector temperature should be 1034°K at a current density of 15 amperes/cm^2. In actual test, the observed collector temperature was 1078°K at a current density of only 10 amperes/cm^2. An x-ray view of the structure of converter TE-100 revealed that the collector and the radiator support, which are supposed to be brazed, were not in intimate contact during assembly because of mechanical

TABLE II

SUMMARY OF PROTOTYPE VARIATIONS

	TE-100	TE-101	TE-102P	TE-102	TE-103	TE-104P	TE-104
Hohlraum L/D	10	8	8	8	8	8	8
*Emitter Material	Ta	Ta	Re	Re	Re	Re	Re
*Emitter Fabrication	one-piece	one-piece	.010" pressure bonded with .001" Nb	.010" pressure bonded with .001" Nb	.010" pressure bonded without Nb	.010" pressure bonded without Nb	.010" pressure bonded without Nb
*Emitter Surface Preparation	ground	ground	ground	ground	ground	ground	ground
*Collector Material	Ta	Mo	Mo	Mo	Mo	Mo	Mo
*Collector Surface Preparation	ground	lapped	lapped	lapped	lapped	lapped	lapped
Collector Planar Area, cm^2	2.50	2.50	2.50	2.50	2.50	2.50	2.50
*Collector Lateral Area, cm^2	0.50	0.50	0.50	0.50	1.28	0.50	0.50
*Interelectrode Spacing, in.	0.001	0.001	0.001	0.001	0.001	0.001	.001
*Lateral Electrode Spacing, in.	0.006	0.006	0.006	0.006	0.006	0.006	.006
*Internal Radiation Shield	one	one	one	one	one	one	omitted
Cesium Capsule	glass	metal	metal	glass	glass	glass	glass
*Cesium Additive	none	none	none	none	none	none	none
Radiator Support Structure	Nb	Mo	Mo	Mo	Mo	Mo	Mo
Collector Heater Turns	1	2 x 1	2	2	2	2	2
Emitter Stud Diameter, in.	0.200	0.250	0.250	0.250	0.250	0.250	0.250
Output Lead Diameter, in.	0.222	0.222	0.305	0.305	0.305	0.305	0.305
Radiation Area, cm^2	66	113	113	113	113	113	113
Demountable Thermocouple	none	4	4	4	4	4	4
C.G. Support Provided	no	yes	yes	yes	yes	yes	yes
Braze Jig	none	rigid	deformable	deformable	deformable	deformable	deformable
Collector Sleeve Braze	Ti	Ti	Pd	Pd	Pd	Pd	Pd
Emitter Sleeve Weld	inert gas	electron beam	electron beam	electron beam	electron beam	electron beam	electron beam
Reservoir Length (beyond radiator fins), in.	1.4	1.4	1.0	1.0	1.0	1.0	1.0
External Radiation Shield	none	none	none	none	one	one	one
Weight (excluding output & TC leads), gms	214	--	318.8	--	323.0	322.5	373.9**

*These features are those which are considered to have the most marked influence on converter performance.

**With TC's and emitter lead

interference, and the discrepancy between the calculated and the observed collector temperatures have therefore been ascribed to the imperfect bond obtained between these two pieces. A further indication provided by the thermal tests was that the interelectrode spacing achieved in converter TE-100 was of the order of 1.4 mils rather than the 1.05 mils expected. The tentative diagnosis made with regard to this last observation was that, because of the large number of concentric elements involved in the fabrication of the collector and the emitter structure, and the attendant accumulation of machining tolerances, there is a tendency for the collector and the emitter planes to be positioned out of parallel during assembly, and that this tendency could be completely corrected only by the application of a longitudinal force which would cause the emitter and the collector to be brought into intimate contact.

As shown in Table II, many changes were made in the fabrication of converter TE-101. For simplicity, the changes are discussed here in the same order in which they appear in the table. The length to diameter ratio of the emitter hohlraum was changed from 10 to 8 in order to accommodate the adoption of a standard at both the Jet Propulsion Laboratory and Thermo Electron for the measurement of emitter temperatures. The collector material was changed from tantalum to molybdenum in order to avoid a braze interface between the collector face and the collector support structure. This change also permitted using a lapping finish on the face of the collector which is difficult to achieve on tantalum surfaces without loss of flatness. As specified in the contract, converter TE-101 was cesiated using a metal cesium capsule. It was felt that the collector temperature achieved in the previous converter TE-100 was relatively high, thereby restricting the range of collector temperature that could be explored

usefully, and possibly preventing satisfactory collector temperature optimization. To reduce the collector temperature and increase the range of collector temperature control, three significant changes were made in the fabrication of converter TE-101: (1) the radiator support structure material was changed from niobium to molybdenum to increase the thermal conductivity of this element. Calculations indicate that with this basic change the overall collector temperature drop changes from 179°K at 15 amperes/cm^2 to 154°K at the greater current density of 25 amperes/cm^2; (2) the collector heater rating was essentially doubled by using two turns of heater wire instead of one; and finally, (3) the radiator area was practically doubled from 66 cm^2 to 113 cm^2 at a cost of the significant increase in converter weight of approximately 82 grams.

It should be noted that this radiator area increase and the associated weight penalty were primarily incurred to increase the range of collector temperature variations; for future reference, it should be assumed that the radiator area and weight of the lighter converter TE-100 are more representative. The emitter stud diameter was increased from .200 inch to .250 inch in order to take advantage of available space in the converter structure and to reduce the emitter lead voltage drop. For convenience, all thermocouples were made demountable. Also, in an attempt to satisfy the requirements of converter support and generator design, a support ring was provided in the plane of the center of gravity in the converter. To apply the force in the longitudinal direction between the emitter and the collector, described above in the description of the results of the thermal test

of converter TE-100, converter TE-101 was brazed using a jig which clamped the emitter and collector into close contact while at braze temperature by a process of differential expansion. The results obtained using this jig are discussed in detail in Section 3.3.4. The joining of the emitter sleeve to the emitter structure which had previously been accomplished by inert gas welding was done by electron beam welding in order to avoid the excessive application of heat to the emitter structure, as discussed in more detail below in Section 3.3.1.

Initially, the converter TE-102, following converter TE-101 was to have been a converter using a tantalum emitter. However, the tests made on converter TE-101 revealed that a deposit had formed on the surface of the collector this was verified later after opening the converter, as shown in Figures 11 and 12. Since the program was aimed at the development of converters with rhenium emitter structures, and since in these converters collector deposits are not observed, Thermo Electron made the recommendation to the Jet Propulsion Laboratory to change the emitter material specified for converter TE-102 from tantalum to rhenium. The recommendation was approved and the emitter structure was made by pressure bonding a .010" sheet of rhenium to tantalum with an intermediate sheet of 1 mil thick niobium. This intermediate sheet of niobium was used to retard the formation of rhenium tantalum intermetallics which have a high hardness and brittleness. To reduce the lead voltage drops the output lead diameter was increased from .222 inch to .305 inch. Since the brazing jig used in the fabrication of converter TE-101 had proven to exert excessive force at the collector-emitter interface, the jig was modified to reduce this force and limit it by means of a deformable member, described in more detail in Section 3.3.4. The use of titanium as a braze between the inner seal flange and the collector had proven to have a very low strength. Consequently, as explained in more detail

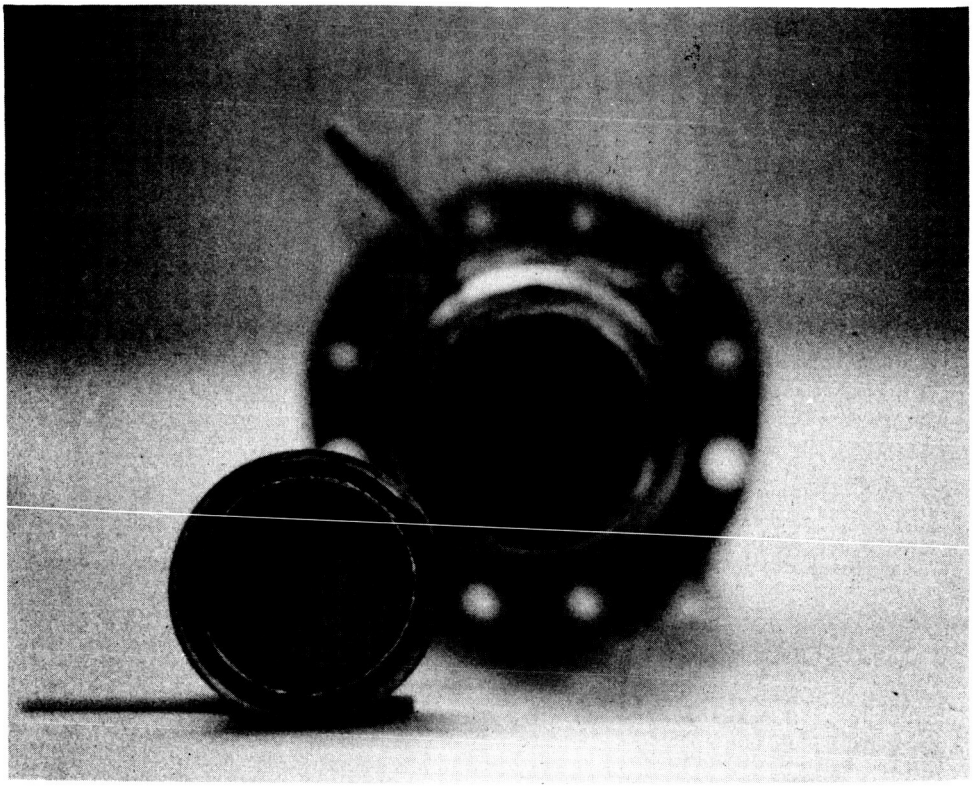

Figure 11. Collector Deposit in Prototype TE-101

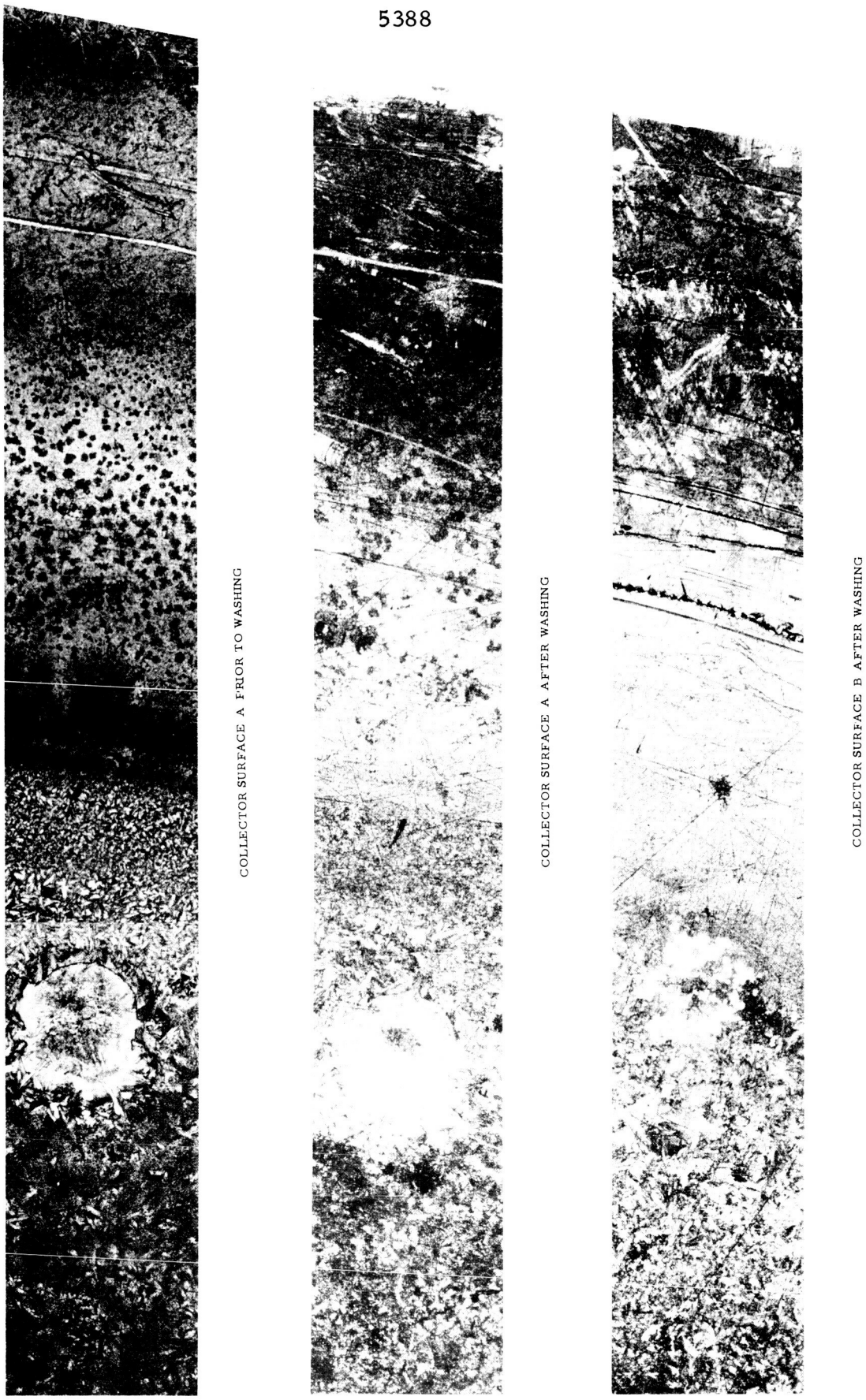

Figure 12. Photomicrograph of Collector Surface, TE-101

in section 3.3.3, a palladium braze was used to join the inner seal flange to the collector material. The length of the reservoir beyond the radiator fins was shortened from 1.4 inch to 1.0 inch in order to render the converter structure more compact. When the first converter TE-102 was tested, its emitter structure bulged out apparently under the effect of extreme internal pressure. Figure 13 shows prototype TE-102P after operation with the emitter structure deformed. Near the end of the program it was discovered that the high internal pressure had been developed by the leakage of nickel plating solution inside the converter structure. This solution was used to electroform a thin cover of nickel over the pinch-off of the converter which is a known point of weakness. In this case the pinch-off leaked and when the converter was placed into the nickel solution, the reduced pressure inside the converter aspirated some of the plating solution inside the converter. In Figure 14 the electrodes of converter TE-102P and the deposits of the nickel salts are shown after opening the converter.

In the second attempt at building converter TE-102, it was not known that the cause of failure of converter TE-102P had been an infiltration of the nickel plating solution. It was suspected that the cesium metal capsule utilized for the fabrication of TE-102P had leaked in the atmosphere, prior to use, and formed some kind of cesium salt which subsequently developed the high pressure. Consequently, in the fabrication of converter TE-102 a glass cesium capsule was used in place of the metal cesium capsule.

Tests of converter TE-102 showed a marked tendency to improve in output over a test period of several hundred hours. It was suspected that this increase in performance may have been related to some process of diffusion of niobium at the interface between the rhenium and the tantalum in the emitter structure. To explore this possibility, the following converters were fabricated omitting the use

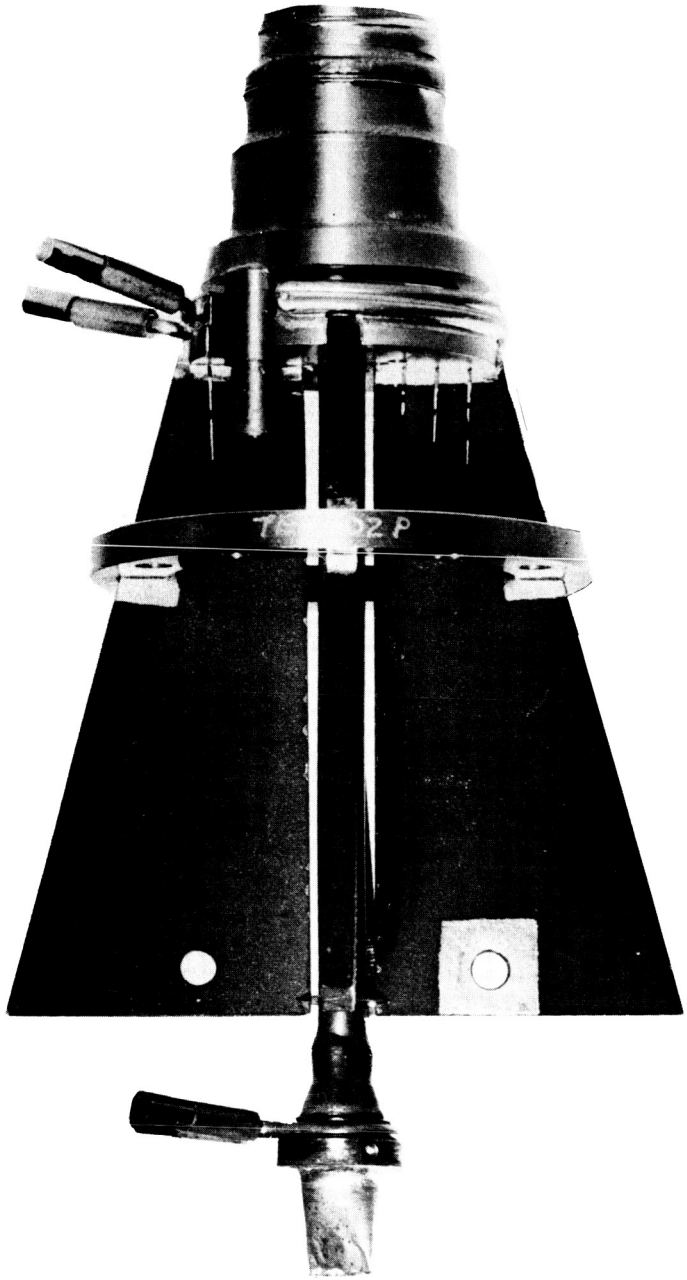

Figure 13. Prototype TE-102P After Operation

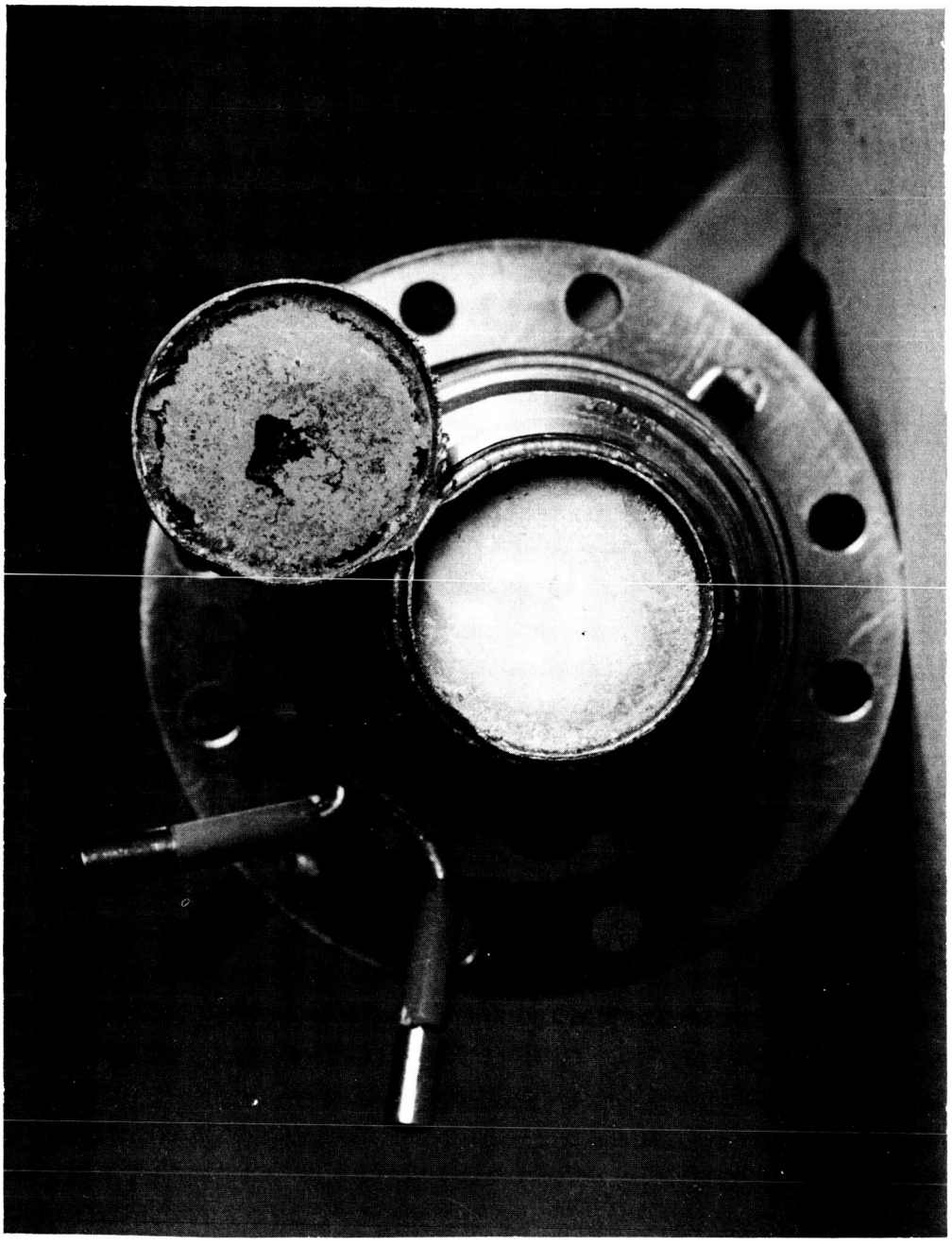

Figure 14. Emitter and Collector Surfaces, Prototype TE-102P

of the .001 inch niobium sheet at the rhenium-tantalum interface.

The fabrication of converters TE-103 and TE-104P

These two structures were identical except for the lateral area of the collector; in converter TE-103 the lateral area of the collector was 1.28 cm^2 as compared to the previous value of .50 cm^2, and in converter TE-104P the collector lateral area was .50 cm^2. The collector geometry details for prototypes TE-101 to TE-104 are given in Figure 15.

The fabrication of converter TE-103 was successful and in test, converter TE-103 gave the best output characteristics observed in the voltage range of interest. However, at the end of about 219 hours of testing,the electrodes of the converter shorted on the lateral area of the collector. Figure 16 shows a photograph of the point of electrical short on this prototype, and Figures 17 and 18 show the planar portion of the electrode surfaces. No signs of electrical shorting were evident on the planar portion of the electrodes.

In the fabrication of converter TE-104P the brazing sequence of the collector heater was altered improperly in an attempt to simplify the fabrication of the converter. The result was that a low melting point braze from the heater wire flowed extensively over the radiator support structure and caused alloying with the cesium tube. Subsequent difficulties made it necessary to take the basic converter assembly three times to the melting point of the seal braze. This resulted in the ultimate flow of braze material from the seal area into the re-entrant emitter sleeve, thus causing both an electrical and a thermal short. Thus, converter TE-104P could not be tested.

The fabrication of converter TE-104 was made identical to that of converter TE-104P, except for the omission of the internal radiation shield between the emitter and the collector structures. It was believed that this shield, being at

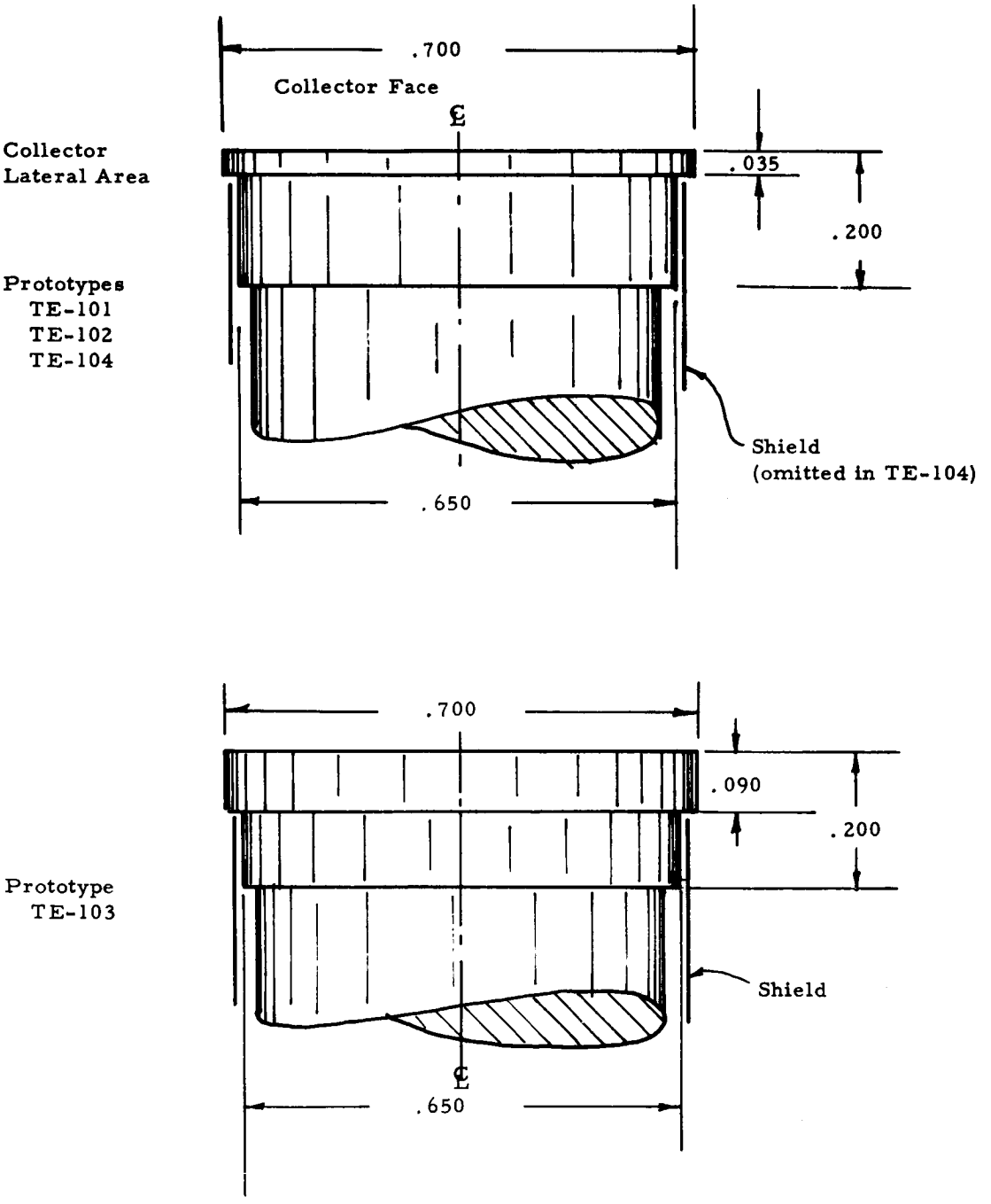

Figure 15. Collector Geometry for Prototypes TE-101 to TE-104

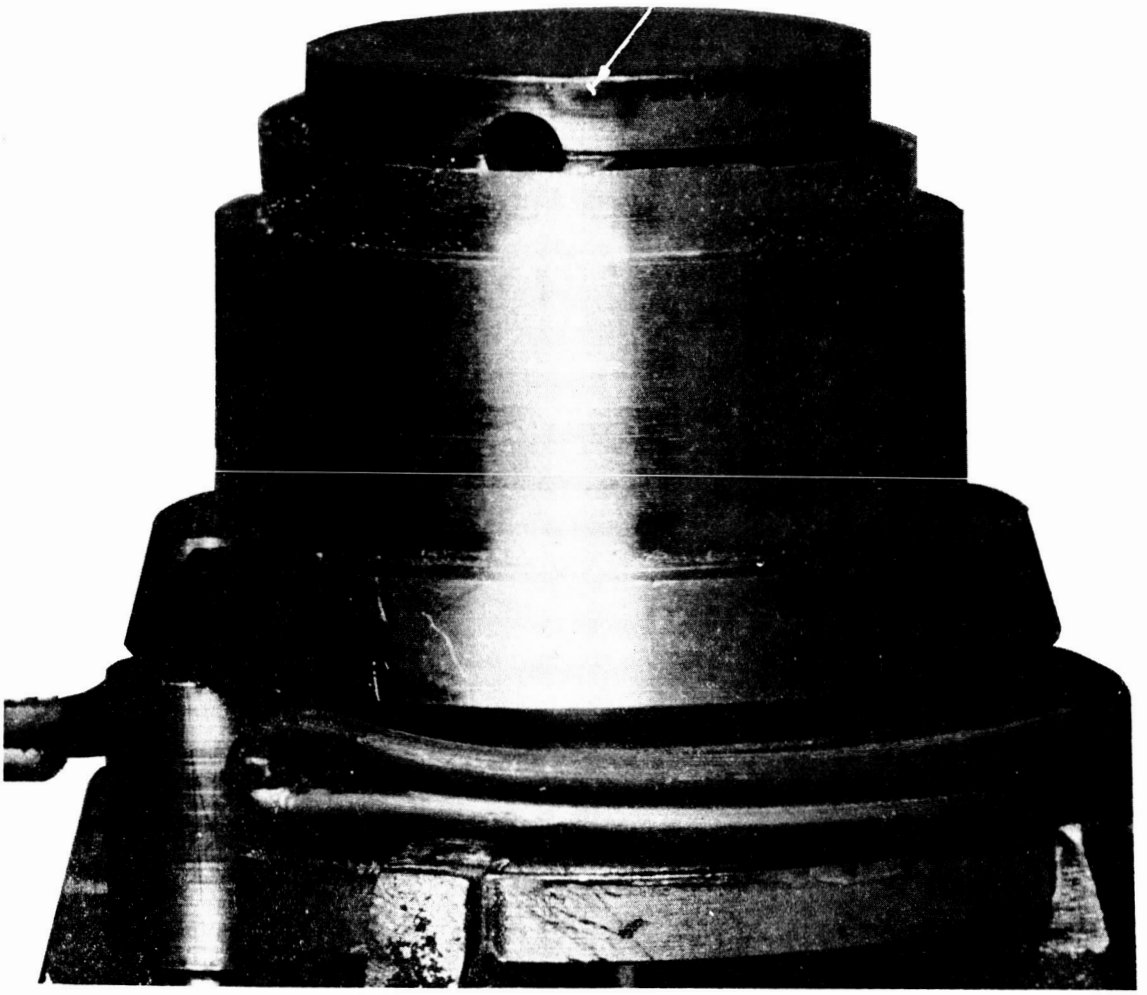

Figure 16. Point of Electrical Short on Collector of Prototype TE-103

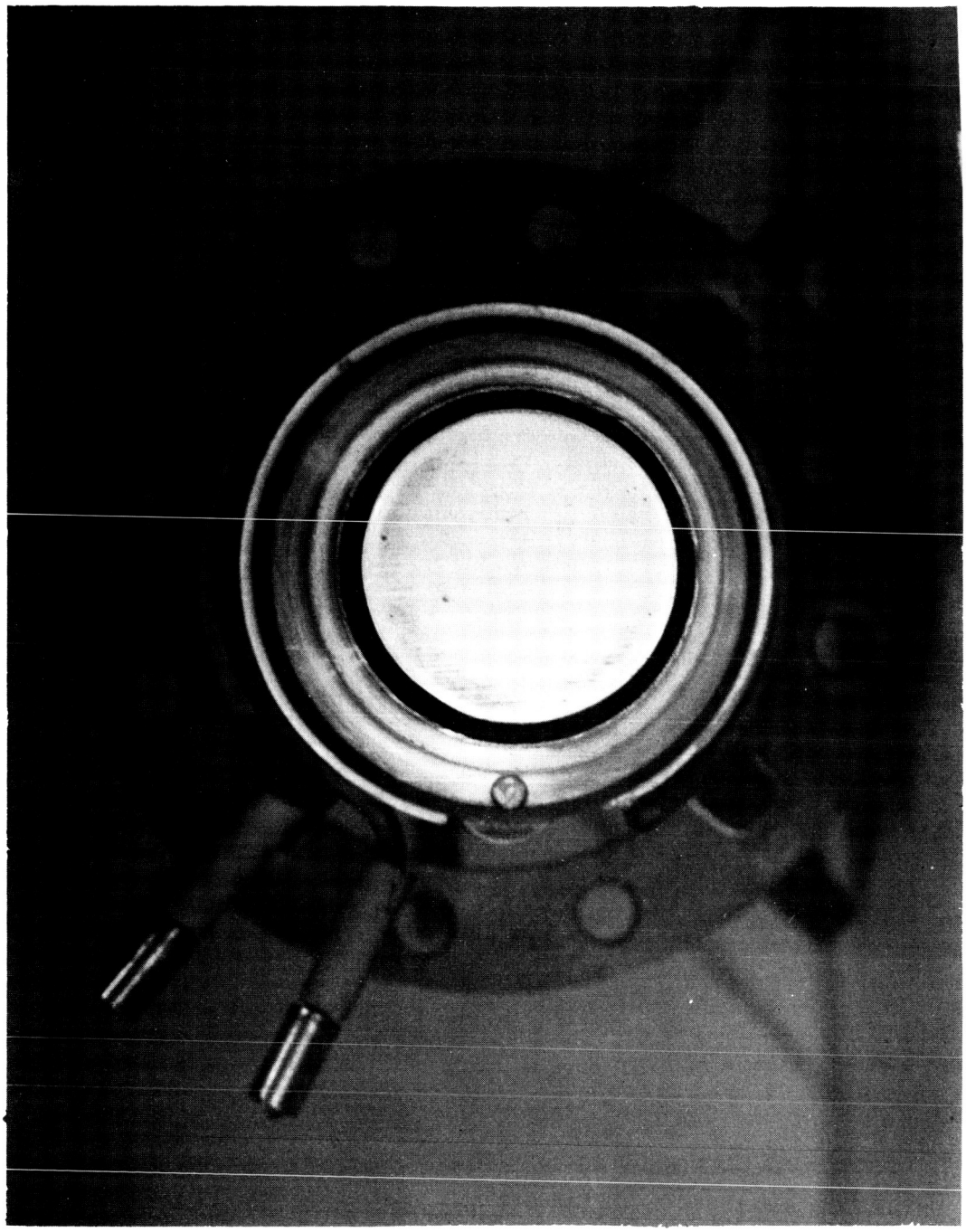

Figure 17. Collector Surface of Prototype TE-103

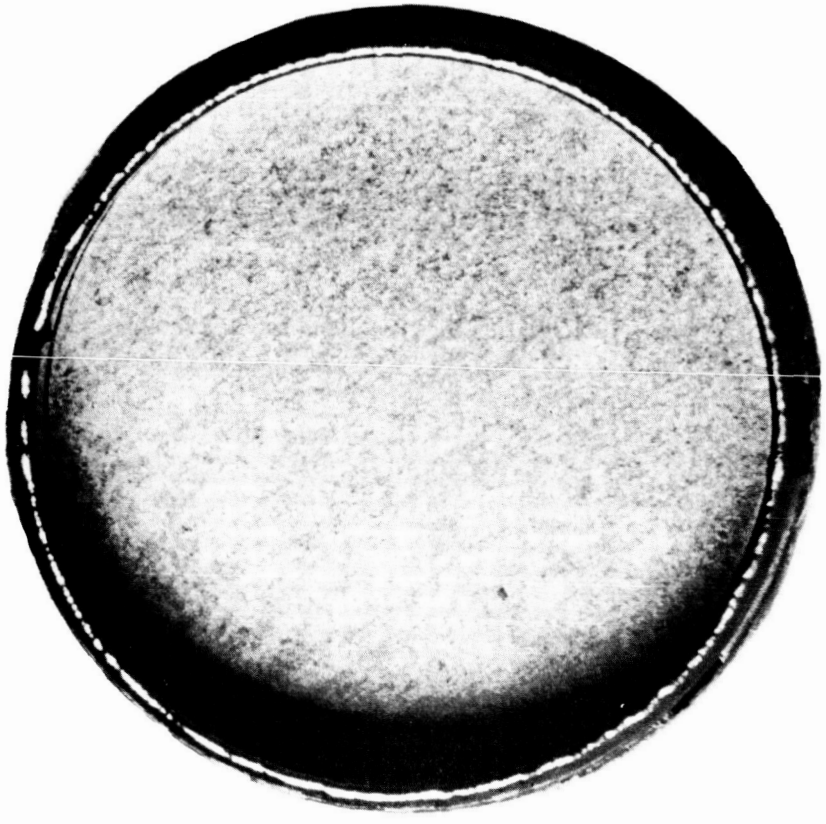

Figure 18. Emitter Surface of Prototype TE-103

collector potential, could contribute significantly to the loss of output current by back emission from the collector to the emitter. Subsequent tests indicated that converter TE-104 indeed was less subject to back emission. However, its output was generally lower than that of converter TE-103. Subsequent inspection revealed that during fabrication of the emitter structure of converter TE-104 the drill used to make the hohlraum in the emitter structure had broken and attempts to remove it had been only partially successful. Thus, in test, this piece of drill remelted and may have resulted in significant diffusion of iron to the surface of the emitter of this converter. Figure 19 shows converter TE-104 at the end of 500 hours of testing.

3.3 Component Development Tests:

During the fabrication of the converter prototypes, a number of component development tests had to be made, and these are described in this section.

3.3.1 Welding of the Emitter Piece

The welding of the emitter piece was initially attempted in an argon atmosphere. The welding conditions were approximatelyas follows:

Argon purity	99.999%
Argon pressure	350 mm Hg, absolute
Welding electrode	.040 inch dia. thoriated tungsten
Gap between electrode & work piece	6 to 10 mils, approximately
Rotating speed	.7 rpm
Preheat time	1/8 to 1/4 turn
Welding time	35 to 50 amperes

Four such assemblies were welded with these settings and only one of these was considered to be approximately perfect. The others were leak tight, but they had to be welded at the higher value of weld current with the result that

Figure 19. Prototype TE-104 After 500 hours of Operation

excessive melting was observed in areas other than the desired weld area with possible distortion of the emitter piece. One of the structures so obtained was used for the fabrication of converter TE-100, but it was decided that for all subsequent converters the use of electron beam welding would be preferable since it is possible with this technique to produce a more effective concentration of heat in the weld area and thereby avoid the considerable distortion that can otherwise result.

3.3.2 Rhenium Pressure Bonding to Tantalum

As described in Section 3.2, the pressure bonding of rhenium to tantalum was effected in some converters using an intermediate layer of niobium .001 inch thick. In other converters this intermediate layer was omitted. As mentioned in Section 3.2, the purpose of this intermediate layer was to retard the formation of a rhenium-tantalum intermetallic which has a high degree of brittleness. Rhenium and niobium also form an intermetallic, but it is reported to have about half the hardness of the rhenium-to-tantalum intermetallic, and it was therefore expected that the use of the niobium interface would result in a stronger bond between the rhenium and the tantalum. The machining of the emitter structure out of the bonded pellets of rhenium and tantalum is made by EDM* in such a manner that an outer ring of the rhenium-tantalum pellet is separated which can be used to test the strength of the rhenium-tantalum bond. The test made consisted of wedging the rhenium and the tantalum apart, and no difference was discerned between the effort required to separate a rhenium-tantalum bond which included the niobium interface and one without this interface. Since converter TE-102 exhibited in test a change in performance which, as explained in section 3.2, is suspected to be related to the diffusion of niobium to the emitter surface, it has been

*Electrical Discharge Machining

tentatively concluded that the use of a niobium interface in the pressure bonding of rhenium to tantalum should be avoided.

3.3.3 Joining of Niobium Flange to Molybdenum Collector

The joining of niobium to molybdenum has always been a source of difficulty in the fabrication of SET converters. In the present case, this was particularly aggravated by the small amount of space available to vary the geometry of the joint in order to arrive at a successful braze attempt. The conventional copper nickel alloys used in other SET converter structures were found inadequate to provide a leak tight joint between the inner seal flange of the TE-100 converter and its collector structure. Some measure of success was obtained using titanium as a filler metal, and, as shown in Table II, converters TE-100 and TE-101 were fabricated using titanium as the braze material for this joint. Further tests showed, however, that the yield of leaktight titanium braze joints is relatively low, even when great care is used in assuring cleanliness of the parts and of the atmosphere in which the braze is made. Also, tests revealed that the adherence achieved between the titanium and molybdenum is extremely poor. Consequently, the titanium braze was rejected. Attempts were next made to use an electron beam weld to seal this joint. In order to avoid over heating the collector piece, it was necessary to provide it with a thin lip at the point where the collector structure joined to the inner seal flange. The welds were made at about one-half rpm with a beam voltage of 20,000 volts and a beam current of 10 milliamperes. The procedure was to preheat the molybdenum collector until red in color and then to move gradually to the welding area favoring the molybdenum collector with the beam. The weld area was then preheated and the beam current was slowly increased until the melting point of the niobium and the molybdenum was reached. Of five welds made in this manner, four were not leak

tight, and only one of the four could be repaired by repeating the procedure a second time. Tests showed, however, that the thin molybdenum lip provided to avoid excessive overheating of the collector was extremely brittle and, therefore, all further efforts at electron beam welding this joint were abandoned. The final approach which proved successful was to use palladium as a braze filler in between the niobium and the molybdenum. This material was found to flow and wet both niobium and molybdenum well. It tends to form a eutectic with niobium, thus causing over-alloying, but any undesirable effects can easily be avoided and the joint remains always ductile.

3.3.4 Use of Compression Jig

As explained in Section 3.2, it was found necessary to use a clamping force between the emitter and the collector during final assembly, in order to insure intimate contact between these surfaces. To achieve this, a compression jig was utilized in the fabrication of converter TE-101 which rigidly restrained the expansion of the converter structure and thus applied a substantial load between the collector and the emitter pieces. With the use of this jig it was found that the force applied was too large, resulting in a tendency for the emitter and the collector to bond partially together. In the case of converter TE-101, this partial bond was broken during converter outgassing by the sudden application of 2 kilowatts of heating power to the emitter. During fabrication of all subsequent converters it was found possible to reduce the magnitude of the clamping force between the emitter and the collector by incorporating a deformable member in the compression jig. This is essentially a disc 1-3/16 inch in diameter, .043" thick, made of molybdenum and which deforms during the emitter-collector assembly by about .013 to .014 inch.

3.3.5 Molybdenum to Molybdenum Braze in Collector Structure

As may be seen in the pictorial sketch presented in Figure 6 of the TE-100 converter, in order to house the compact ceramic seal it is necessary to make the collector structure in two pieces. One of these is the collector proper, Part 10, and the other is the radiator support, Part 11. These two parts are joined by brazing, using a nickel gold eutectic (18% nickel, 82% gold), and, as is generally known in the metal-ceramic tube industry, such butt brazing often includes bubbles caused by entrapped gases which could conceivably affect the ability of the converter to transfer heat across the brazed interface. It was therefore judged of interest to examine metallographically one of these joints, and the collector structure of converter TE-103 was sectioned accordingly. Figure 20 shows typical photomicrographs of sections through this interface, the magnifications for the various views are as follows: Figures 20a and b approximately 150x, Figure 20c approximately 300x. Several cuts were made which accumulated to a total lineal length of 2 inches; and one bubble, shown in Figure 20a, was found. This bubble is approximately ellipsoidal in shape with a diameter of approximately .008 inch and a height of approximately .002 inch. Statistically, it would be expected that about 16 such bubbles would be found over the entire interface in converter TE-103. In order to evaluate accurately the effect of the presence of these bubbles on collector heat transfer, two calculations of the collector temperature drop were made. In the first calculation it was assumed that the braze interface was fully dense and that the converter was operated at 25 amperes/cm^2 corresponding to a total heat flux of 172.5 watts [redacted]. The second calculation was made for the same geometry and heat transfer, except that it was assumed that 100 bubbles of

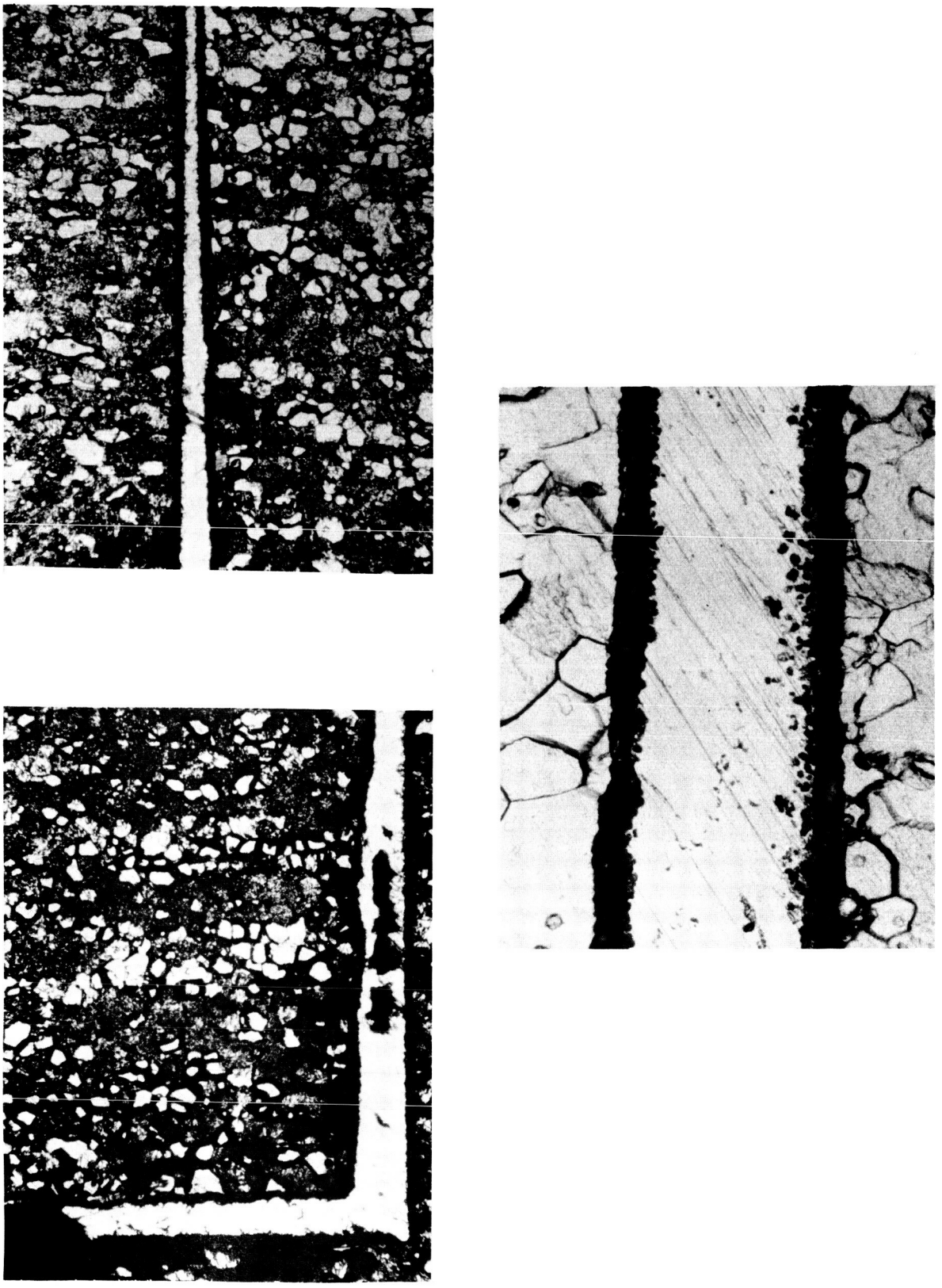

Figure 20. Photomicrographs of Collector Braze, Prototype TE-103

the size described previously were present at the interface. The result of these calculations is that the presence of the bubbles at the interface raises the total collector temperature drop by .02°C. The effect of the voids in the braze is therefore entirely negligible.

3.3.6 Collector Heater Fabrication

As described previously, converter TE-100 used a single loop of heater wire for temperature control of the collector, and in converter TE-101 it was found desirable to double the length of the collector heater wire. The use of a second loop of collector heater wire presented the following problem: the two turns of heater wire could not be simply wrapped around the collector structure because of the presence of the emitter terminal post, and it was therefore required to return the wire over itself before the emitter terminal post. Initially, it was assumed that the heater wire could not be bent completely over itself and therefore a connecting terminal block was used to join the heater wires of the two loops. Subsequently, however, tests showed that the heater wire could be bent completely over itself without effecting an electrical short and the procedure was adopted for the fabrication of all subsequent converters. Figure 19 shows the configuration of the bend of the heater wire on converter TE-104. To date there have been no shorts observed in the region of this bend.

3.3.7 Electroforming of Nickel on Pinch Off

In order to reinforce the converter pinch off which is probably the weakest point in the converter envelope, a thin coat of nickel was electroformed over it by dipping it about 3/8 inch into a standard nickel plating bath* and by applying a negative potential to the pinch off. The electroforms in converter TE-101 and TE-102P were obtained by passing 15 milliamperes of current

*240 gm/ℓ, nickel sulfate; 45 gm/ℓ, nickel chloride; 30 gm/ℓ, boric acid.

for four hours and leaving the solution unagitated. This treatment was found to produce the growth of whiskers of nickel on the pinch off. The approach selected to avoid this whisker formation was to reduce the amount of electroplating current, and this was accomplished by using a 1.5 volt dry cell in series with a 60 ohm resistor as the source of current for the electroforming process. The electroform obtained in converter TE-102, using this set up, still exhibited some whisker formation. The electroforming current was further reduced subsequently by using a 270 ohm resistor in place of the 60 ohm resistor, and the electroforms obtained in converters TE-103 and TE-104 were then of good quality.

3.3.8 Brazing of Emitter Terminal Post

Initially, the emitter terminal post, Part 8, was brazed to the outer seal flange, Part 2, by using a single washer of nickel-gold eutectic .002 inch in thickness. The bond thus obtained was found to be of insufficient strength when, in attaching the emitter lead to converter TE-101, the terminal post broke off in the area of the braze. All subsequent brazes were made using three washers instead of one, and no further difficulties were then encountered.

3.3.9 Attachment of Collector Thermocouple

Figure 6 shows the collector thermocouple insulator held in place by the head of a machine screw bearing on the end face of the collector insulator. As can be appreciated in this figure, this presents the problem of bringing into close proximity of the thermocouple leads a metallic element which can short them. A better method of holding this ceramic in place was devised in the instrumentation of converter TE-104 where instead of using the screw to press against the end of the ceramic insulator, the ceramic insulator was

made substantially longer and the screw was used only for the purpose of acting as a wedge to hold the ceramic in place. This arrangement can be observed in the photograph of converter TE-104 presented in Figure 19.

3.4 Converter Assembly Technique

This section presents a detailed discussion of the methods used for the assembly of the TE-100 prototypes and except for the obvious modifications implied by the prototype differences, as presented in Table II, Section 3.2, it applies to all the prototypes. For illustrative purposes, Figure 21 shows the most important components used in the fabrication of converter TE-100.

3.4.1 Emitter Subassembly

The emitter subassembly consists of Parts 1, 2, 3, and 4 listed in Table I, Section 2.2. The first step of assembly consists in inert gas welding of Part 2, the outer seal flange, to Part 3, the intermediate emitter support. This weld is made in an argon atmosphere 99.999% pure at an absolute pressure of 360 mm Hg at a rotating speed of 1/2 rpm with a .040 inch diameter thoriated tungsten electrode and using a weld current of approximately 20 amperes. The next step in this subassembly is to join the previous two parts to Part 4, the emitter support. This is again done by inert gas welding under the same conditions just described, except that the weld current is about 25 amperes. The final step in the subassembly is to join the re-entrant sleeve structure thus obtained to the emitter piece, Part 1. This is done in an electron beam welder using a beam voltage of 20,000 volts, a beam current of 10 milliamperes, a speed of 1/2 rpm and, in the particular case of the Thermo Electron beam welder, a bias grid voltage of 400 volts, and a focus coil current of 40 milliamperes are applied. After the weld is completed, the assembly is leak checked, degreased and fired at 1400°C for 15 minutes.

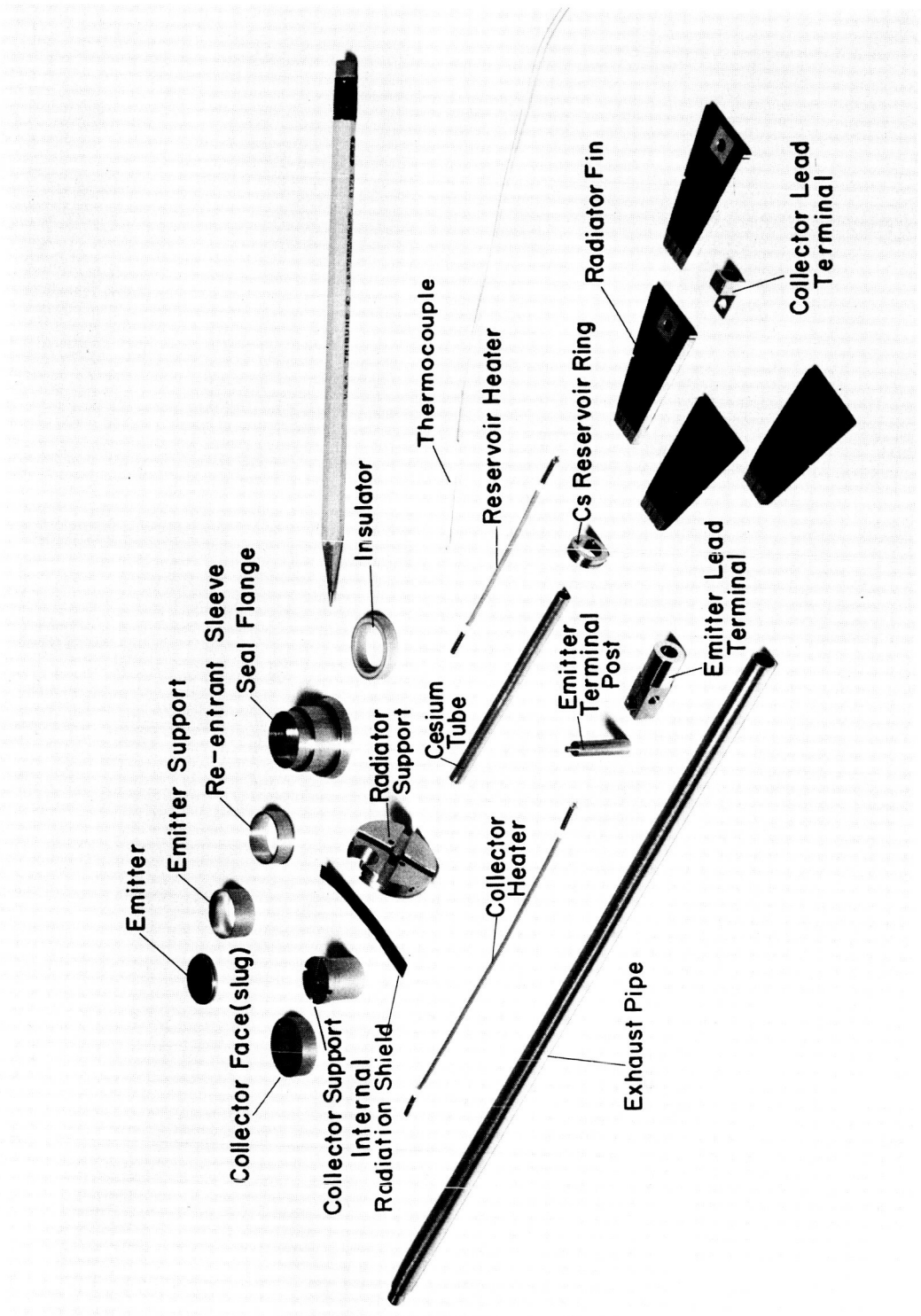

Figure 21. Parts for Prototype TE-100

3.4.2 Collector Subassembly

The collector subassembly consists of joining Parts 5, 6, and 10, also listed in Table I. First, the inner seal flange, Part 6, is brazed to the collector, Part 10, using a palladium braze at 1600°C. After brazing, this partial assembly is leak checked and degreased. Part 5, the collector shield, is formed into a cylinder by spot welding it in a Raytheon Model 2-155 spot welder programmed as follows: up slope, 3 cycles at 37% weld heat; weld, 3 cycles at 70% weld heat; down slope, 3 cycles at 37% weld heat. The shield is then attached to the collector by bending the appropriate tabs into the transverse hole which connects to the cesium tube.

3.4.3 Cesium Tube Subassembly

The cesium tube, Part 12, is connected to the converter exhaust pipe, or cesium reservoir, Part 25, by means of a fuse braze. After brazing, the tubulation is leak checked and degreased.

3.4.4 Subassembly braze

In the converter subassembly braze, the emitter, collector, and cesium tube subassemblies are joined as follows: the collector subassembly is placed into the emitter subassembly and the ceramic insulator, Part 7, is then inserted into its proper position. Braze wire rings of copper .030 inch in diameter are then added at the location where the ceramic seal is to be brazed to the niobium flanges. Next, Part 27, the cesium tube support disc, Part 29, the radiator fin stop, and Part 11, the radiator support, are inserted over the cesium tube in that order so that they will be in place for later assembly. The cesium tube is inserted into the collector, Part 10, and two rings of 6% cupro nickel .015 inch in diameter are placed around the tube and in contact with the collector surface at the location where the tube is inserted into the collector. The parts thus assembled are taken to the compression jig and

the emitter is erected against the deformable molybdenum disc, previously described in Section 3.3.4. The other end of the compression jig is made to bear on Part 11, the radiator support. The subassembly braze is then made at 1150°C until there is indication that all brazes have melted. The subassembly is then allowed to cool for a minimum of 16 hours and it is leak checked.

3.4.5 Final Braze

For the final braze, two washers of nickel-gold eutectic .002 inch in thickness are placed between the collector, Part 10, and the radiator support, Part 11. The radiator fin, Part 13, and the converter mounting ring, Part 36, are then positioned and pieces of .030 inch diameter nickel-gold eutectic wire are added for brazing as required. The collector heater wire is wound around the radiator support and held by means of a small piece of tantalum wire, and two large rings of .030 inch nickel-gold eutectic wire are added for brazing. Heater terminals and heater terminal insulators are slipped over the ends of the heater wire and .015 inch nickel-gold eutectic wire is placed to braze the heater wire ends to the heater terminals. The cesium reservoir ring, Part 26, is slipped over the cesium reservoir exhaust pipe, Part 25, with its heater and heater terminals already pre-brazed with nickel-gold eutectic wire .015 inch in diameter, two turns are used for brazing the heater. Then, two turns of silver-copper eutectic braze wire .015 inch in diameter are placed on either side of the cesium reservoir rings. This entire assembly is then placed in a furnace and heated until all the visible portions of the braze have melted. After brazing, the assembly is leak checked again.

3.4.6 Thermocouple Assembly

The collector thermocouples are made by spot welding the thermocouple leads to the collector thermal slugs, Part 32, inserting the leads through the

thermocouple insulators, Part 15. Similarly, the cesium reservoir thermocouples are made by spot welding the thermocouple leads to the reservoir thermocouple washers, Part 34. The thermocouple assemblies are then attached to the converter structure by means of the appropriate screws.

3.4.7 Converter Outgassing

The cesium capsule is degreased, cleaned ultrasonically and rinsed in ethyl alcohol before insertion into the exhaust tubulation of the converter. It is held in place by appropriate partial crimps made on the exhaust tubulation. The converter is then connected to the outgassing vacuum line for outgassing. A cylindrical shield, 2 inches high and 2-1/4 inches in diameter of .001 inch thick molybdenum is placed around the radiator in order to permit achieving relatively high collector temperatures during converter outgassing. The details of the converter outgassing procedure are discussed in Section 3.5

3.4.8 Cesium Distillation

The actual cesium distillation procedure used for the prototypes TE-100 to TE-104 is discussed in Section 3.7. After cesium distillation, the cesium appendage is pinched off and the pinch off is electroformed in a standard nickel plating solution by connecting the cesium tube to the negative terminal of a circuit comprising a 1.5 volt dry cell in series with a 270 ohm resistor for 24 hours.

3.4.9 Fabrication of Output Leads

The collector output lead is made by passing the end of the #4 stranded copper lead, Part 24, through the collector lead terminal, Part 17, and striking an electric arc on the end of the lead strands so as to cause a localized fusion of the strands with the terminal. One end of the emitter lead is made in the same manner. The other end of the emitter lead is first passed through the emitter lead connector, Part 23, and fuse welded in the manner

explained above, and then the lead connector is brazed to the emitter lead terminal clamps, using a .015 inch diameter wire of nickel-gold eutectic.

3.5 Outgassing of TE-100 Prototypes

The outgassing of each prototype fabricated under this program was recorded in a pressure time plot. The prototypes were outgassed for successively longer periods of time as these records provided more information about the rate at which pressure changes during converter outgassing. The experience accumulated to date indicates that during converter outgassing the emitter should be maintained at a temperature of approximately 1750° C for about 50 hours and that for most of this period of time, the collector should be maintained at 800° C, and the cesium reservoir at 400° C. Figure 22 describes the recommended procedure for future converter fabrication. As it may be noted, it is recommended that the cesium capsule be broken prior to pinching off the converter from the exhaust pump so that any gases in the cesium capsule can be pumped out.

3.6 Cesium Metal Capsules

As described before in Section 3.2, converters TE-101 and TE-102P were charged, using cesium metal capsules. These capsules were made by distilling under vacuum the cesium contained in 350 milligram glass capsules at 200° C for four hours. Four capsules were prepared simultaneously using the apparatus shown in Figure 23. A typical cesium metal capsule is shown in Figure 24. It consists of an embrittled section of molybdenum tube with a copper pinch off at either end. It is obtained by pinching off the extremity of any one of the tubes shown in Figure 23. During the distillation process, the heated glass capsule from which the cesium is distilled is contained in the horizontal portion of the pipes shown in Figure 23. This horizontal portion connects at one end to the

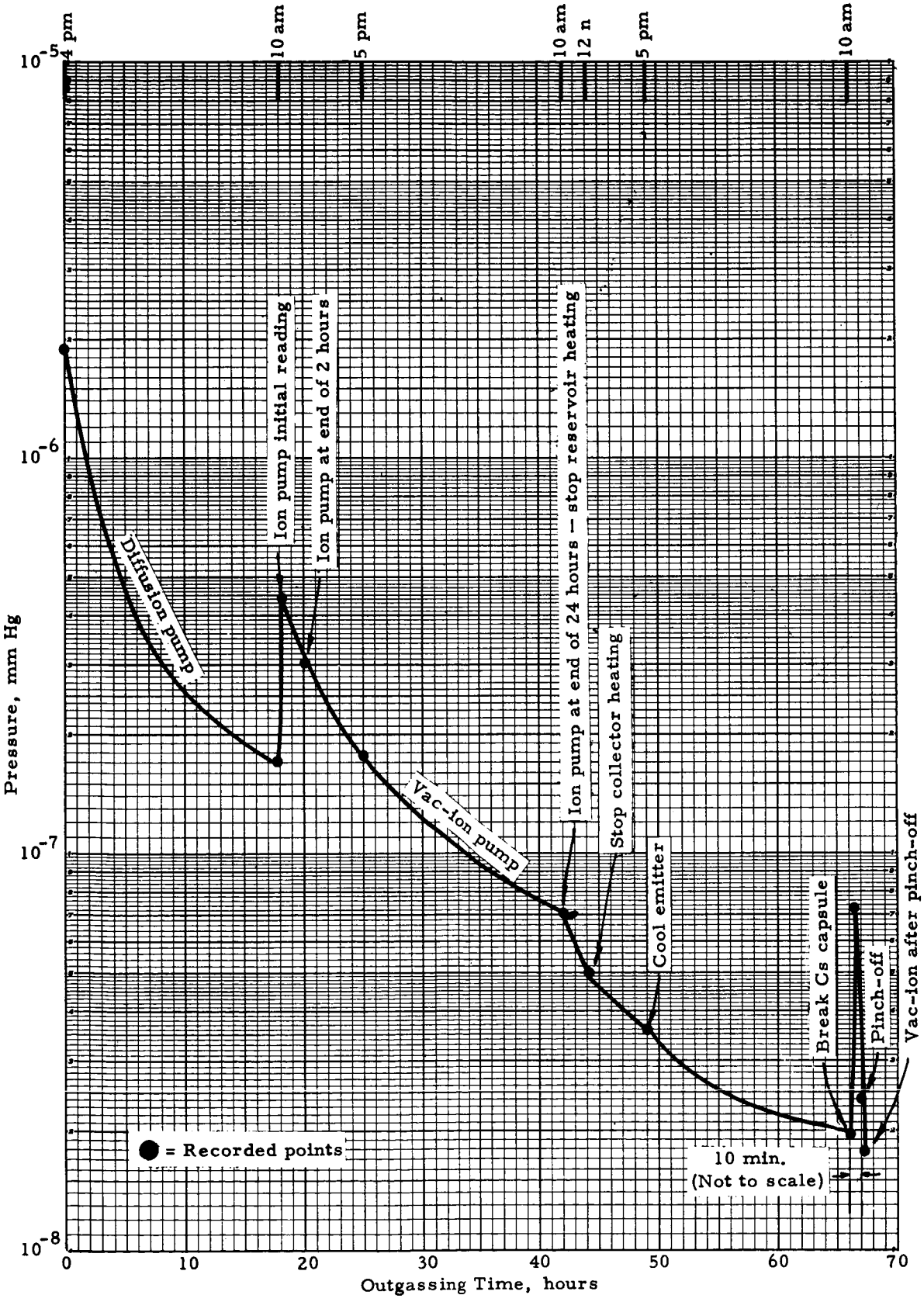

Figure 22. Recommended Outgassing Schedule and Record

T_E = 1750°C
T_C = 800°C
T_R = 400°C

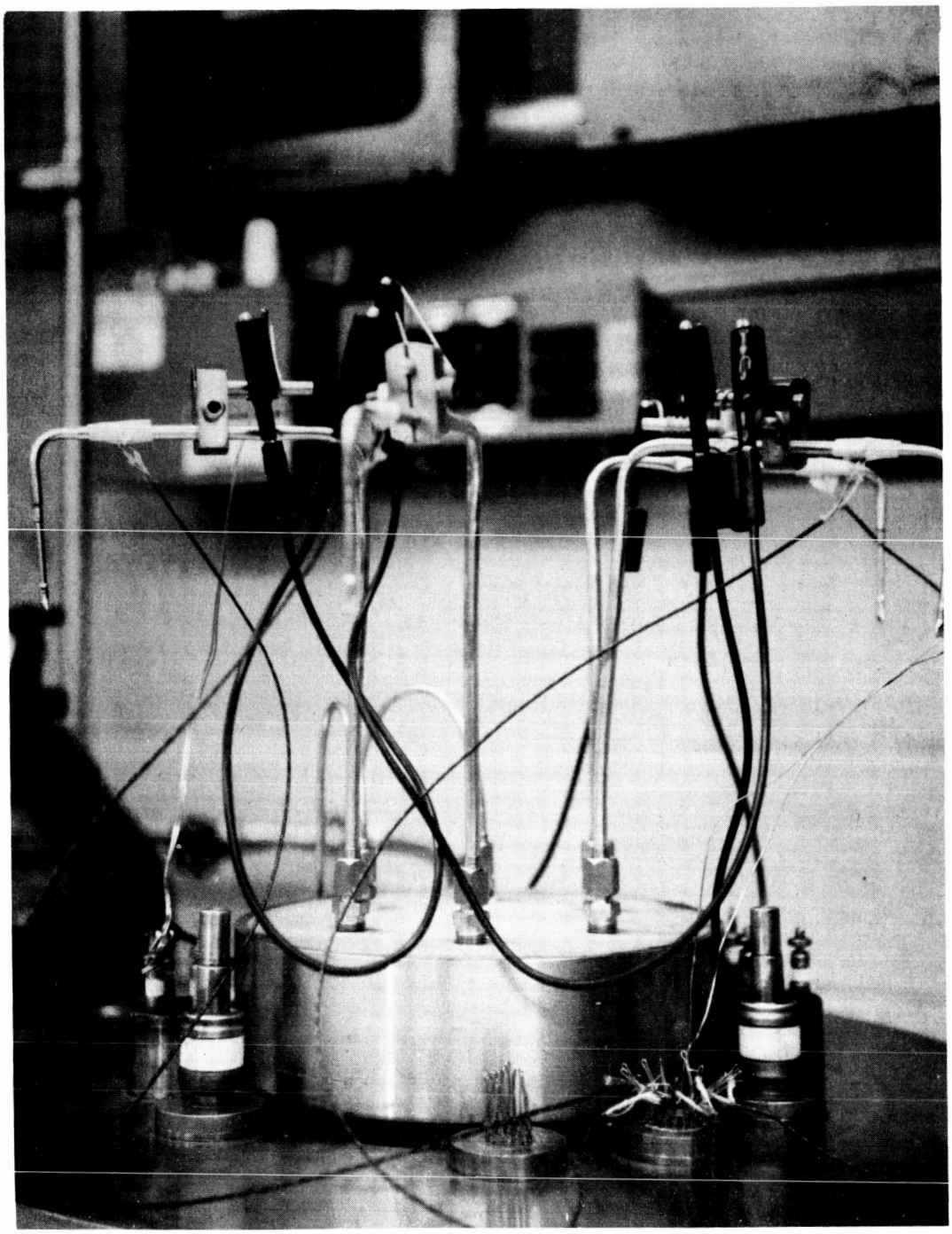

Figure 23. Apparatus for the Vacuum Distillation of Cesium

Figure 24. All-Metal Cesium Capsule

capsule being charged and at the other through a restriction to a vacuum pump. This restriction is dimensioned so that the conductance from the glass capsule to the metal capsule is equal to that from the glass capsule to the vacuum system and about 50% of the cesium initially available is lost to the vacuum pump.

3.7 Cesium Distillation

The cesium distillation procedure used for the TE-100 prototypes is summarized in Table III. The recommended procedure to be used in future converter fabrication is to use a 350 mg cesium capsule, to break it open when the cesium appendix is still connected to the vac-ion pump at the end of the outgassing cycle so as to evacuate the capsule and then to distill the cesium by electrically heating the appendix in vacuum so as to maintain the cesium reservoir of the converter at 200°C for six hours.

3.8 Converter Weight Breakdown

Table IV lists the weights of the major subassemblies, or components, for prototype TE-100 and prototypes TE-101 to 104. As may be noted, prototype TE-100 was considerably lighter because it used the smaller radiator fins previously described in Section 3.2. Also, converter TE-100 did not include a support ring. It should be reiterated that a fully developed hardware converter of the TE-100 design would have a radiator area quite close to that of prototype TE-100 and, therefore, the weight of prototype TE-100 is more representative of what a hardware converter would eventually weigh. If the weight of the support ring is added to that of converter TE-100 it would be anticipated that a hardware converter would weigh 241 grams without the leads and 314.5 grams when fully instrumented for test.

TABLE III

Cesium Distillation Procedure Used for TE-100 Prototypes

Converter	Capsule	Evacuated[1]	Procedure	Cesium Residual
TE-100	glass, 350 mg	yes	Cesium appendix was heated by a torch flame according to the standard technique for cesiating photocell tubes in the vacuum tube industry.	no
TE-101	metal, 175 mg	no	Torch flame as per above.	no
TE-102P	metal, 175 mg	yes	Cesium appendix was heated electrically in vacuum so as to maintain the cesium reservoir of the converter at 200°C for 5.5 hours.	no
TE-102	glass, 300 mg[2]	yes	Same as for TE-102P except that distillation was accomplished overnight at 180°C for 16 hours.	no
TE-103	glass, 350 mg	yes	Same as for TE-102P except that distillation was accomplished overnight at 180°C for 16 hours.	yes
TE-104P	glass, 350 mg	yes	Torch flame as in the distillation for Converter TE-100.	no
TE-104	glass, 350 mg	no[3]	Same as for TE-102P.	yes

NOTES:

(1) The evacuation step consisted in breaking the capsule open when the cesium appendix was still connected to the vac-ion pump, at the end of outgassing.

(2) This capsule was from the batch used for the fabrication of the Series VII life-tested SET converters, and it was used to obtain a future comparison between this converter made using a proven high quality cesium capsule, and converters made with the new batch of 350 mg capsules.

(3) The omission of the capsule evacuation step for converter TE-104 was due to an oversight.

TABLE IV

CONVERTER WEIGHT BREAKDOWN
(grams)

	TE-100	TE-101 to TE-104
Emitter Subassembly	24.3	24.3
Collector Subassembly	23.4	23.4
Radiator Support	54	54
Ceramic Seal	3	3
Radiator Fins	85	167
Support Ring	none	27
Cesium Charge	0.3	0.3
Brazes & Miscellaneous Parts	24	24
Converter Weight without leads	214	323
Four Thermocouples	6.8	6.8
Screws and Ceramics	4.8	4.8
Emitter Lead (.305 dia)	34.7	34.7
Collector Lead (.305 dia)	27.2	27.2
Weight of Converter fully instrumented for test	287.5	396.5

4. TESTING OF TE-100 PROTOTYPES

4.1 Test Equipment

4.1.1 Vacuum System

Figure 25 shows the vacuum system used in the fabrication and test of the TE-100 prototypes. The pump is a 6-inch diameter oil diffusion pump charged with Dow Corning 705 silicon oil, provided with a water cooled first stage jet and with a water cooled optical baffle to prevent back-streaming. With a pyrex 18-inch diameter bell jar and a viton gasket, the system is capable of an ultimate pressure of 4×10^{-8} mm Hg. and with a diode in test and at temperature, the pressure can be as low as 6×10^{-8} mm Hg. It is instrumented with an ultra high vacuum ion gauge and ion gauge amplifier capable of recording pressures as low as 2×10^{-10} mm Hg. It also has an internal fan system for air cooling the bell jar. The vacuum chamber is provided with all the required built-in electrical connections, a secondary ion pumping system for converter outgassing, and connections to provide internal metered flow of cooling water. Figure 25 also shows an instrument mounted on top of the vacuum system in front of the bell jar. This is an optical sight tube provided with a semi-conductor photocell and used for the automatic control of emitter temperatures during converter testing.

4.1.2 Converter Support and Heat Source

To support the converter during testing, it is first mounted on a circular ring with radial webs which are mechanically fastened to the converter mounting ring. This ring is in turn supported by a three-post frame which holds the electron bombardment heat source, as shown in Figure 26. The layout of this structure is shown in Figure 27.

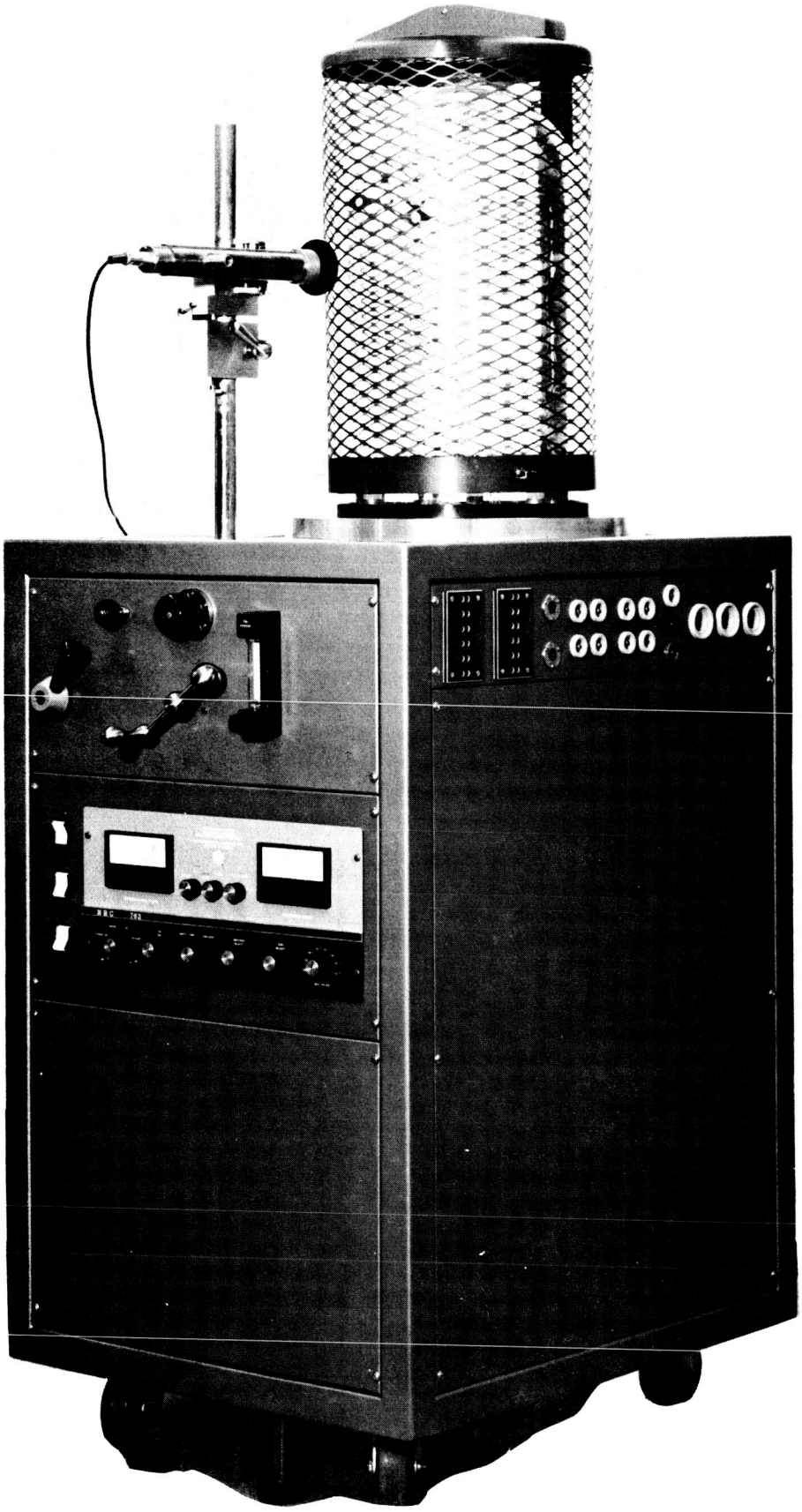

Figure 25. Vacuum System and Photoelectric Temperature Sensor

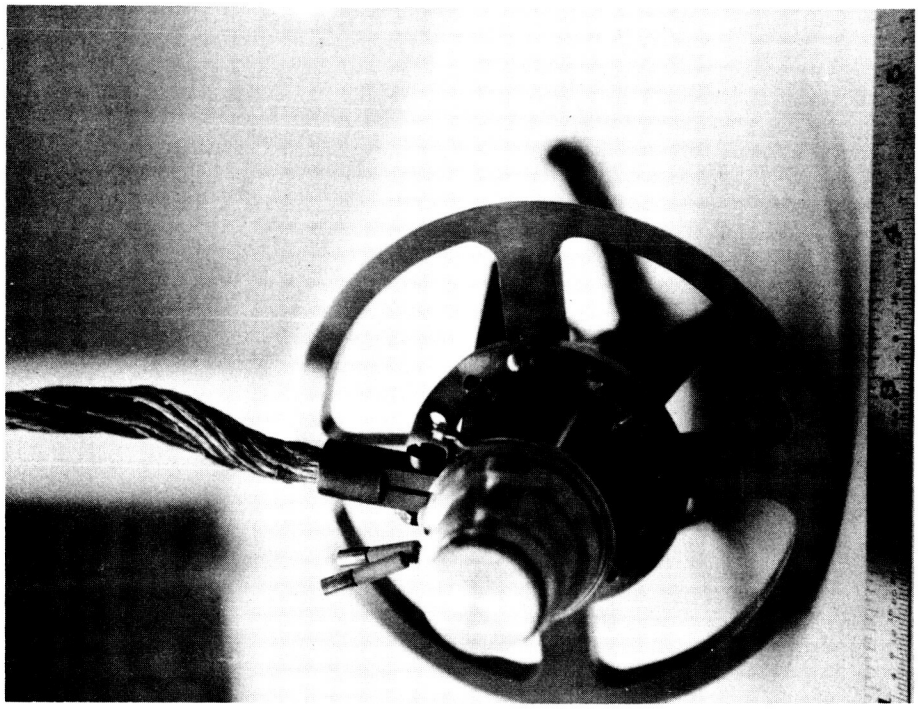

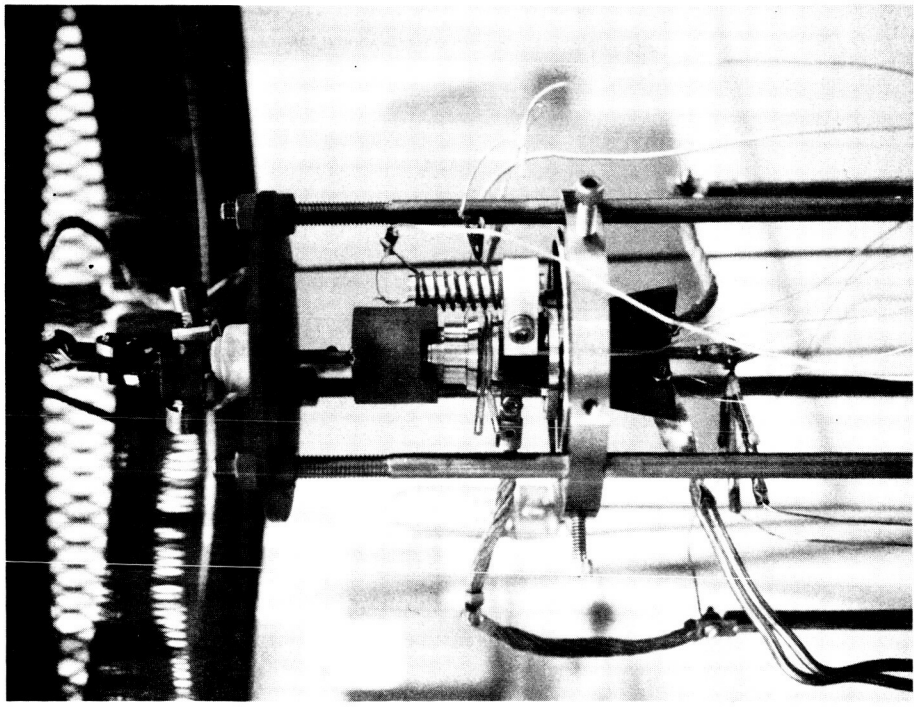

Figure 26. Converter Support and Test Apparatus

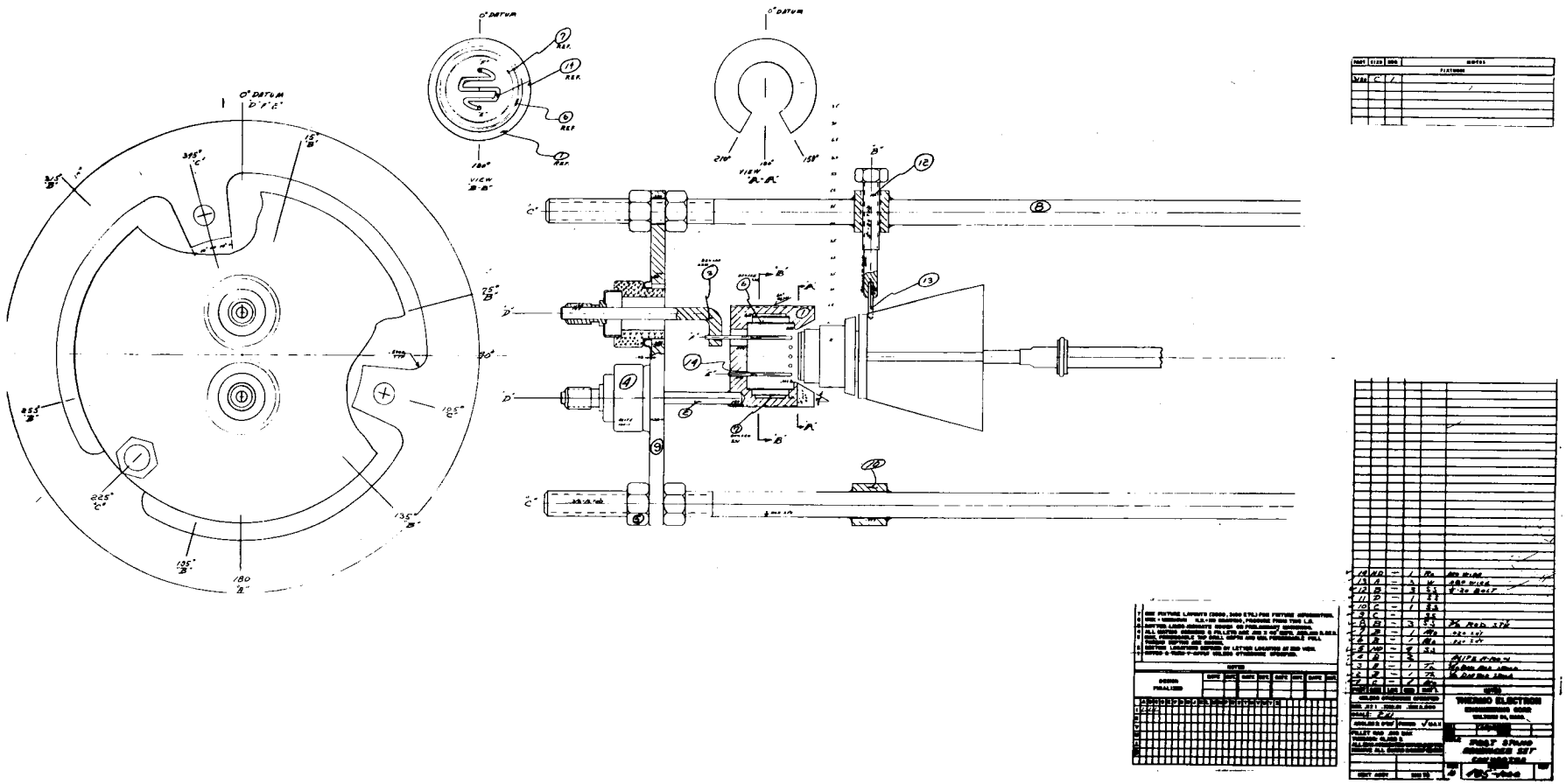

Figure 27. Layout of Converter Test Stand

4.1.3 Main Instrument Console

The main instrument console is shown in Figure 28 and, from top to bottom, it consists of the following:

Vac-ion power supply

Electro Instruments d c Voltmeter 3400A with a sensitivity of 100 microvolst and an accuracy of .1%.

Below the digital voltmeter is an electron bombardment automatic control unit for the filament of the heat source used for converter testing. The unit is provided with sensing circuits which can actuate corrections in filament current according to both changes in electron bombardment current and sensed emitter temperature as signalled by the sensor shown in Figure 25. The unit is also provided with an automatic clock which records the total time that a converter has been on test.

Immediately below, is the converter load panel which includes both a manual carbon disc compression rheostat and a solid state automatically controlled load capable of maintaining constant converter output voltage within 1 millivolt. This load panel also incorporates a channel selector switch which can sample the particular data to be read by the d c digital electron bombardment voltage, the output voltage of the converter the output current of the converter and the emf of all thermocouples. The 0°C reference used is a thermoelectric unit made by Joseph Kaye & Co., Model RJA1C, capable of maintaining 0°C within .01°C.

The units appearing below the load panel are the reservoir temperatur control and the collector temperature control units, respectively. These are a combination of an a c power supply and a West digital set point

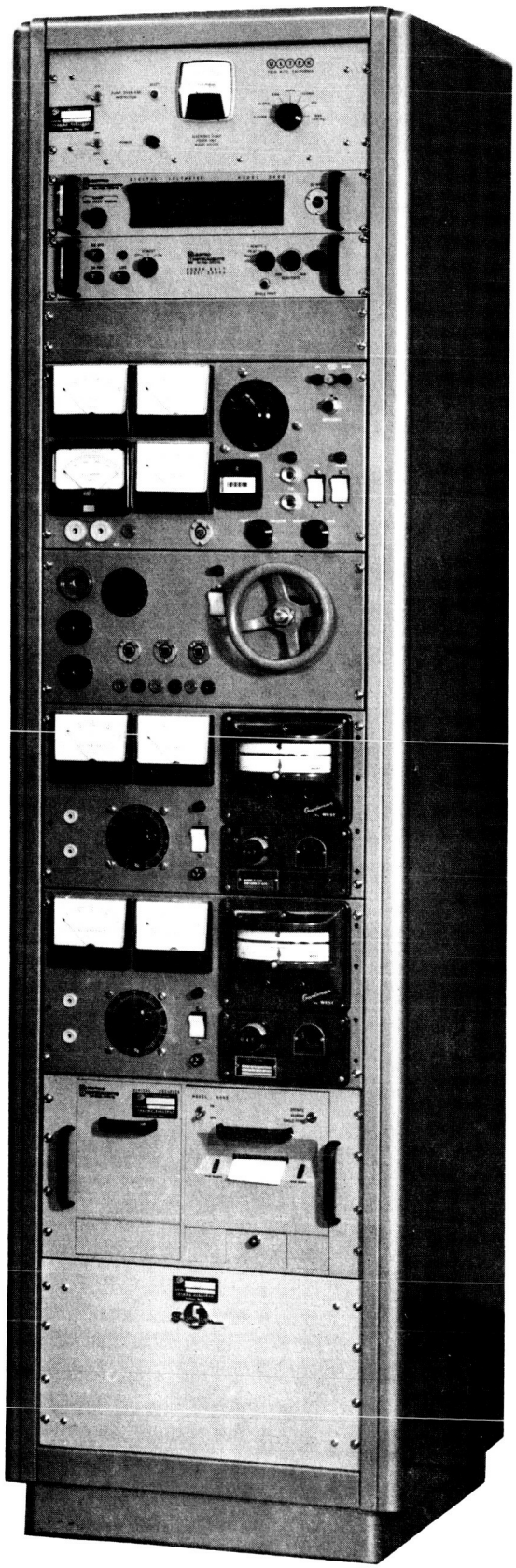

Figure 28. Instrument Console

controller, Model JBY, with a switching action to alternate between 80 and 100% of selected heater voltage.

Under the temperature controllers is an Electro Instruments 9053 digital recorder printer.

At the bottom, the console houses a Sorensen 100v-750 milliamperes regulated d c power supply used in conjunction with the electron bombardment control unit.

4.1.4 Micro Optical Pyrometer

All emitter temperature measurements made in this program were obtained with a Pyro Micro-optical pyrometer, No. 5217. In general, it is felt that emitter temperature measurements are still among the most critical to be made during converter testing and, therefore, careful measurement procedures should be adopted.

4.2 Converter Instrumentation

4.2.1 Emitter Temperature Measurement

To measure the emitter temperature, the converters were provided with a hohlraum .031 inch in diameter .250 inch deep with the centerline parallel to the emitter surface. The distance between this centerline and the emitter surface was .070 inch for the prototypes with a tantalum emitter, TE-100 and TE-101, and it was .075 inch for the remainder prototypes which had a pressure bonded rhenium emitter. The respective thermal resistances between the hohlraum and the emitter surface are .144°C/watt/cm^2 and .150°C/watt/cm^2.

The actual heat flux in the vicinity of the bottom of the hohlraum is calculated by adding the electron heat transfer at the emitter of 2.72 watts cm^2/ampere/cm^2 (see Section 4.4.3), the interelectrode radiation. The pyrometric measurement of the emitter temperature involves a temperature correction at the bell jar due to the non-ideal transmissivity of the glass. To minimize the value of this correction, the bell jar is cleaned, using a mixture of cerium oxide and ethyl alcohol. In this program, the bell jar temperature drop was calibrated when this cleaning procedure was still not in use and the temperature drops obtained at 1700°C observed temperature were between 21 and 25°C. The actual data used for the interpretation of all emitter temperature measurements is given in Figure 29 and was obtained from the National Bureau of Standards, Technical Paper No. 170 entitled "Pyrometric Practice."

4.2.2 Cesium Reservoir Thermocouples

To measure the temperature at the cesium reservoir, a nickel ring was brazed around the copper tubulation at the approximate level where the liquid-gas interface was expected and two stainless steel washers, each carrying a spot welded alumel-chromel thermocouple, were then mechanically fastened to this ring by means of a No. 0-80 screw, in the manner shown in Figure 6. With this method, the thermocouples can be easily demounted and replaced in case of thermocouple lead damage. Also, the use of the stainless steel washer enables the achievement of a relatively large heat transfer contact area between the thermocouple junction and the point of measurement, thus minimizing the effect of thermocouple lead conduction on

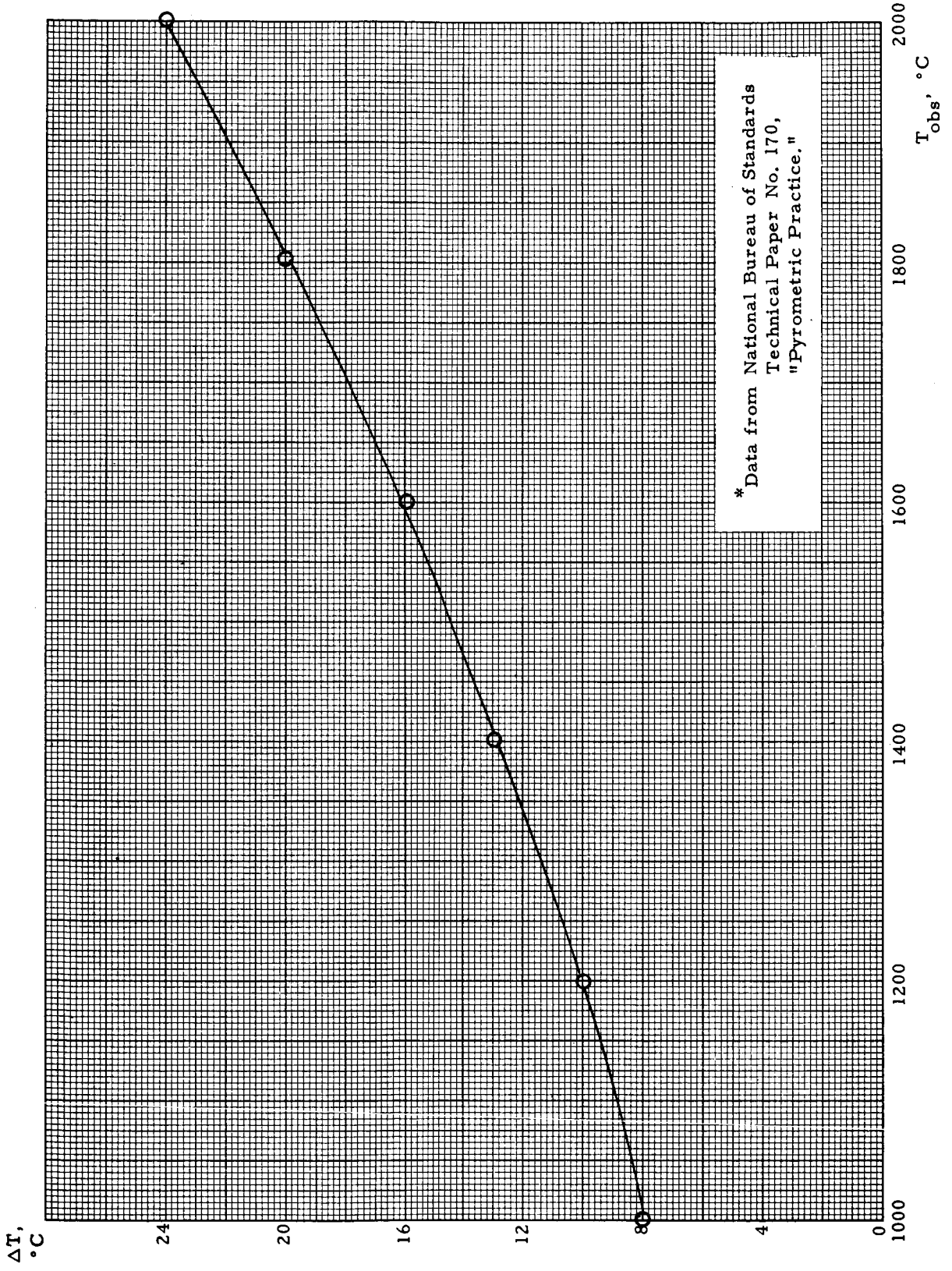

Figure 29. Corrections for Pyrometer Measurements through a Glass Bell Jar*

the temperature of the measuring junction.

4.2.3 Collector Thermocouples

In order to provide the same demountable features at the collector, the collector thermocouples were spot welded to a small collector thermal slug made of stainless steel and oxidized, and the assembly was mechanically positioned so that the thermal slug would be located at the bottom of a hole through the collector structure and only .080 inch away from the collector surface. The dimensions of the collector thermal slug were chosen so that its area would be sufficiently large to collect enough heat by radiation from the collector material to overcome the conduction loss in the thermocouple leads, and yet not be so massive as to require an unreasonable amount of time in reaching temperature equilibrium. At equilibrium, the temperature difference between the collector and the thermal slug is of the order of 6°C and the time required to reach this equilibrium is of the order of one minute.

4.2.4 Output Voltage Taps

The emitter potential was sensed by means of a .020 inch diameter copper wire clamped under Part 21, the emitter terminal nut. (In the case of converter TE-101, as mentioned in Section 3.3.8, the bond between Part 8, the emitter terminal post, and the outer seal flange, Part 2, was broken; in order to avoid a voltage measurement error, the emitter potential measurement in this converter was made by clamping the copper lead around the outer seal flange.)

The collector potential was measured on one of the radiator fins, Part 13, one different from that used as a negative current terminal.

4.3 Prototype Tests Conducted

As per the contract, prototype TE-100 was to be tested to thoroughly evaluate constructional features, thermal distribution, and interelectrode spacing. The specified testing procedure for converters TE-101 to TE-104 was more elaborate and consisted of the following:

(A) Operate for thirty (30) hours in steady-state conditions, at 1900°K ± 5°K emitter temperature. This temperature, as well as any other emitter temperature referred to hereinafter, shall be the temperature observed at the bottom of a pyrometric hole of 8 to 1 length-to-diameter ratio, after all corrections due to light losses and pyrometric errors. During this test, the converter shall operate with a total load of 0.075 ohm. Any signs of a change in power output shall be observed, investigated, and reported. If degradation in performance exceeds a 20% drop in output power at this load, all further testing shall be diagnostic.

(B) Evaluate the converter at an emitter temperature of 1800°K, 1900°K, and 2000°K and at output voltages of 0.4 volt, 0.6 volt, 0.8 volt, 1.0 volt and 1.2 volts. Emphasis shall be placed on the operation of the converter at optimum collector and cesium reservoir temperatures for the attainment of maximum power outputs. All data shall be recorded after a minimum of five (5) minutes of stable operation at the selected point. Data obtained by dynamic or other means of measurement shall be recorded as auxiliary information.

(C) At the emitter temperatures specified in paragraph (B) evaluate the maximum power output performance of the converters for a change of ± 5°C in cesium reservoir temperature and a change of ± 20°C in the collector temperature. This evaluation shall be conducted with the changes in temperature performed separately at output voltages of 0.6 volt, 0.8 volt, and 1.0 volt.

(D) Explore the operating characteristics of the converters as a function of λ/d ratio over an extended range of temperatures and current voltage character-

istics measurements. These temperatures shall include the normal operating emitter temperature conditions for maximum power output. Sufficient data shall be collected and analyzed to fully interpret the dependency of the characteristics of the converter on this parameter.

In this report, the sequential page by page discussion of the data recorded has been omitted in favor of the comprehensive, comparative description of the results of similar tests on all the prototypes. In this manner the results of the work conducted under this program can be made most apparent.

4.3.1 Steady-state Performance Optimization

The evaluation of constructional features and the thermal distribution observed during the test of converter TE-100 was already discussed in Section 3.2. Prototype TE-100 was subjected to additional tests to compare its output with that of previously constructed tantalum converters. Figure 30 shows the steady-state optimized performance of converter TE-100 at emitter temperatures of 1951°K and 1991°K (these are hohlraum true temperatures), and compares it with the equivalent performance of converter VI-S-15 at 2000°K (this performance is obtained by multiplying the actual observed performance in this converter by the ratio of the emitter areas of the converters). As may be observed, the current output of converter TE-100 is greater at output voltages above 1.05 volts.

Figure 31 shows the steady-state optimized performance observed at the beginning of the tests of prototype TE-101. The I-V characteristic is very similar to that observed for converter TE-100, and as may be seen, it crosses the equivalent characteristic of converter VI-S-15 again in the vicinity of 1.05 volts. The figure also shows the change in performance observed at 1900°K over a 33 hour period with a total load of .075 ohms. A substan-

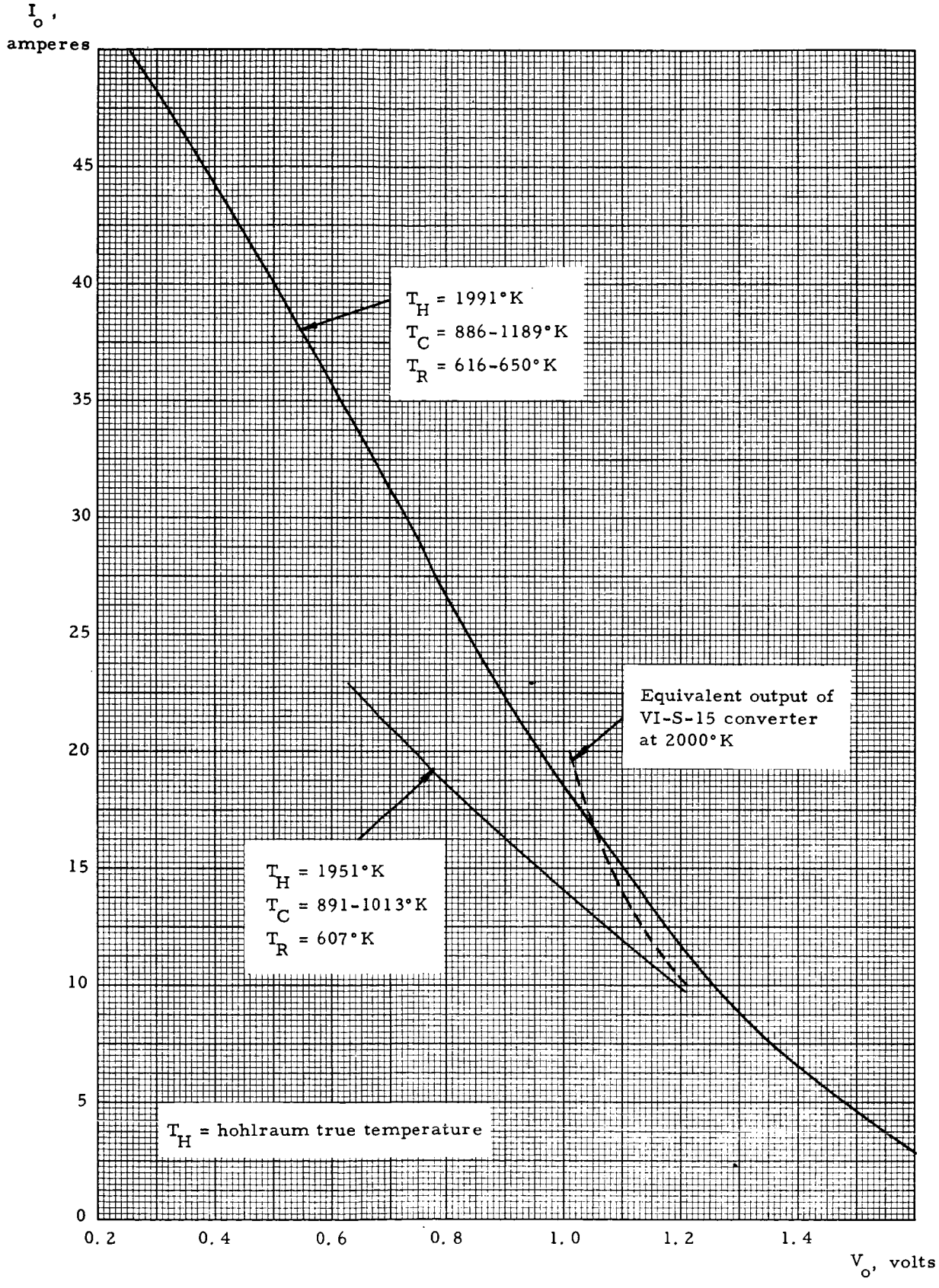

Figure 30. Steady-State Optimized Performance of Converter TE-100 (Data Sheets 4-9, 17-21)

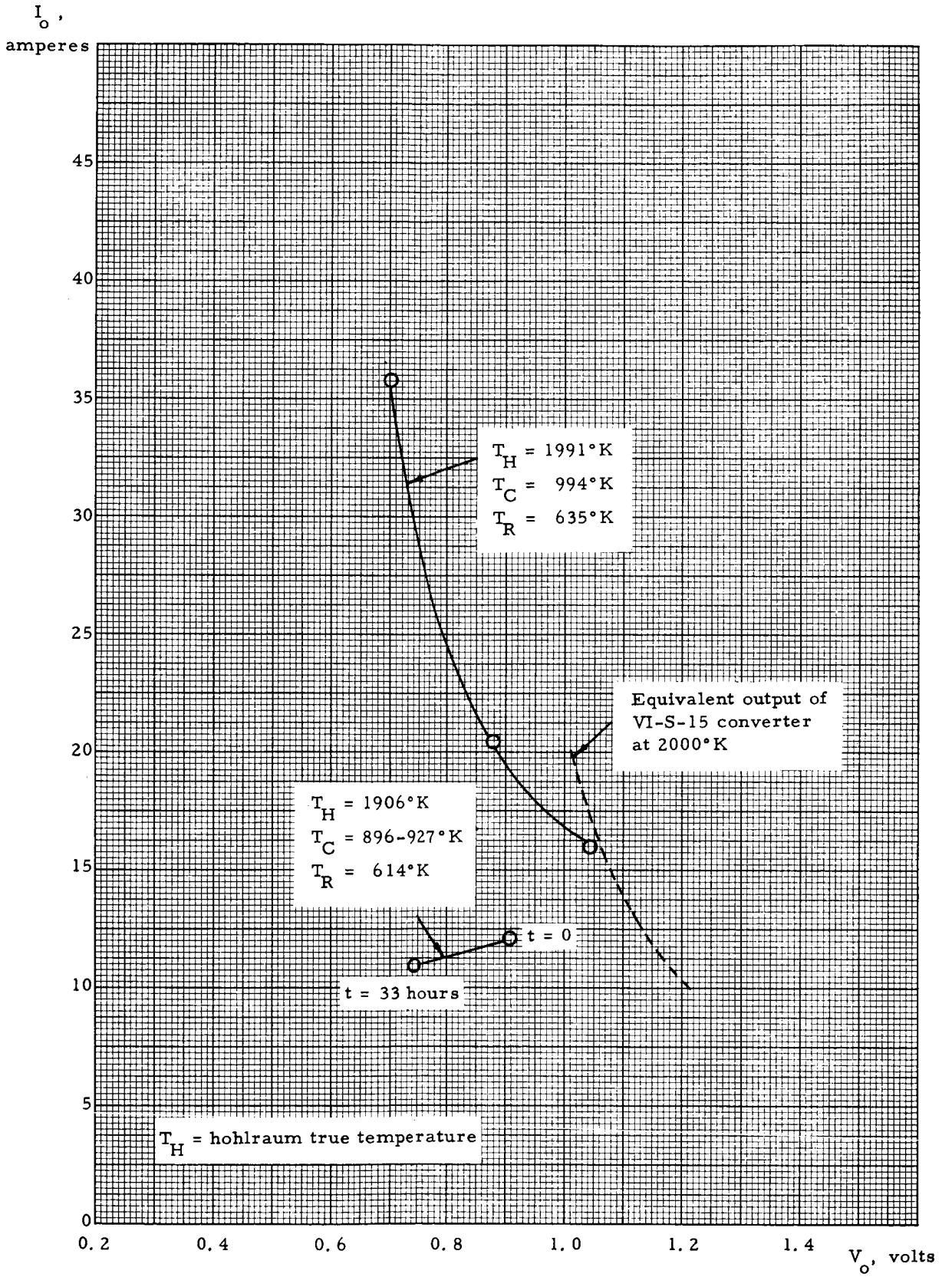

Figure 31. Steady-State Optimized Performance of Converter TE-101 (Data Sheet 1)

tial performance degradation occurred, and power loss corresponding to this degradation is 30%. Since it exceeded the 20% drop limitation in the test specification, all further testing on converter TE-101 was diagnostic. The additional tests, however, failed to reveal any unusual condition in the converter, and the converter was subsequently opened for examination. As already discussed in Section 3.2, a heavy collector deposit was found which is shown in Figure 11.

As previously mentioned, converter TE-102 was the first to incorporate a rhenium emitter, and the emitter was bonded to the substrate of tantalum using an intermediate layer of niobium .001 inch thick. During the initial 30 hours of steady-state operation, the converter was brought to 1929°K in 1.4 hours and allowed to reach an optimum in the following 3.6 hours of 14.0 amperes at 1.001 volts. At the end of 28.3 additional hours at this temperature, the output power had increased by .7% and the heating power required to maintain the same temperature had risen by 3%. Figure 32 shows the steady-state optimized performance of this converter at hohlraum temperatures of 1812°K, 1916°K, and 2023°K as observed at approximately 60 hours and 260 hours of testing. As it may be seen, a considerable increase in performance took place in the 200 hours elapsed between the measurement of the I-V characteristics. This increase in performance was discussed in Section 3.2 and is suspected to be related to the use of niobium at the rhenium-tantalum interface in the emitter structure. It may be interesting to observe that the changes in the optimized I-V characteristics were accompanied by corresponding changes in reservoir temperatures. These changes are tabulated in Table V, and they average about 15°K rise in cesium reservoir temperature over a period of 200 hours for all emitter

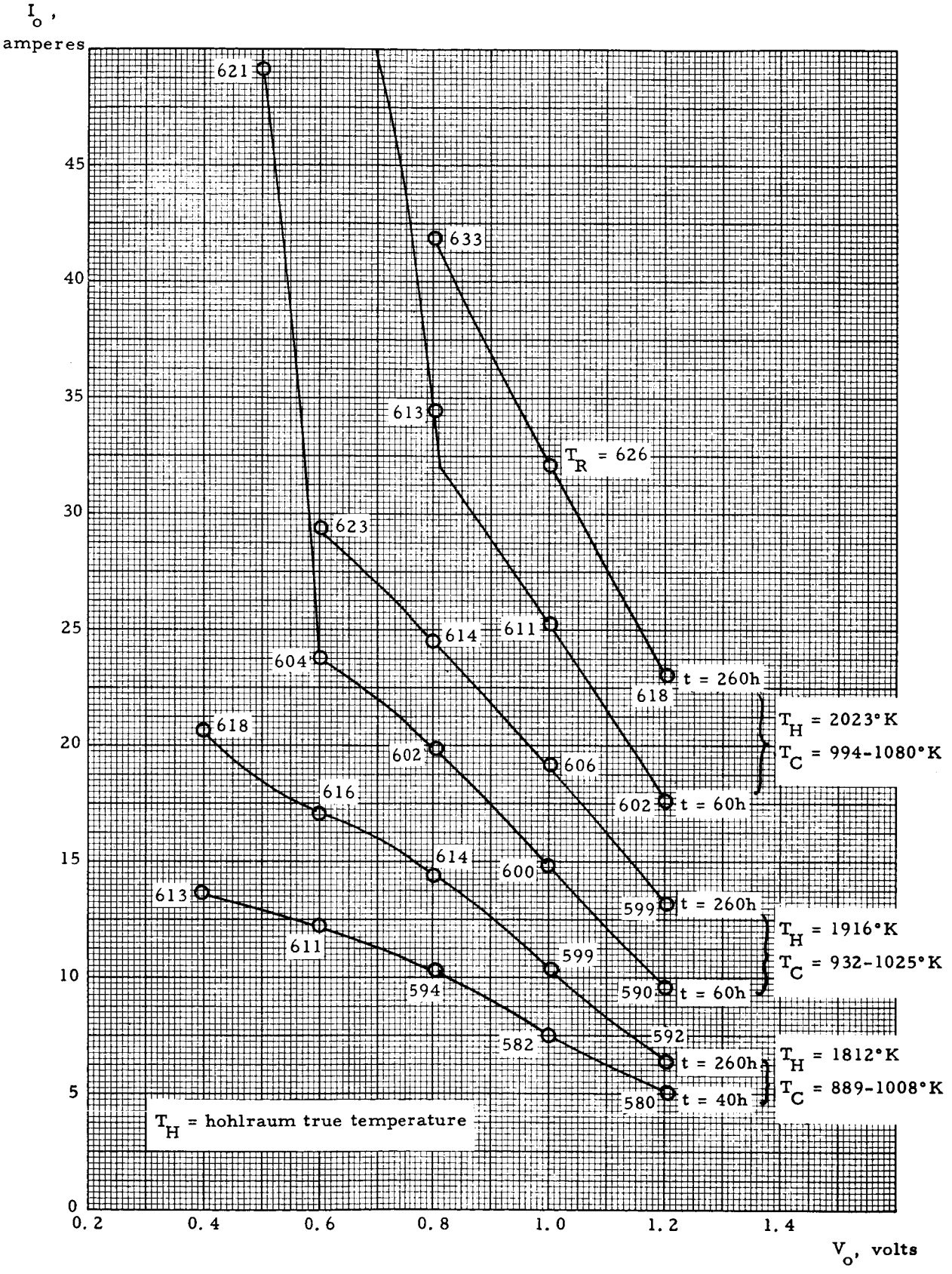

Figure 32. Steady-State Optimized Performance of Converter TE-102 (Data Sheets 2-7, 24, 25)

TABLE V

Optimum Reservoir Temperatures (°C) for Converter TE-102

(Data Sheets 2-6, 24-25)

	Initial	After 200 hours	ΔT_R
1800°K, 0.8v.	321	341	+20
1.0	309	326	+17
1.2v.	307	319	+12
1900°K, 0.8v.	329	341	+12
1.0v.	326	333	+ 7
1.2v.	317	326	+ 9
2000°K, 0.8v.	341	360	+19
1.0v.	338	353	+15
1.2v.	329	345	+16

temperatures (taking into account that there exists an uncertainty in the optimum cesium reservoir temperature of about ± 3°C).

The steady-state run for converter TE-103 was conducted at 2000°K emitter temperature rather than the previously specified 1900°K. It was felt that converter TE-103 might display a gradual decrease in output, such as observed in converter TE-102, and the higher test temperature would then enable the acceleration of this process. Also, the steady-state run was conducted for 67.6 hours, rather than 30 hours. The test indicated that, over this period of time, the output at 1.2 volts decreased by .3% and the power required to maintain a 2000°K hohlraum temperature increased by .5%. Thus, converter TE-103 did not exhibit the tendency to the gradual increase in output of converter TE-102, and since this converter was built without the use of a niobium shim between the rhenium and the tantalum substrate and the emitter structure, this result reinforces the tentative conclusion that the drift observed in the performance of converter TE-102 was related to the use of the niobium shim. The steady-state optimized performance of converter TE-103 is shown in Figure 33 for hohlraum temperatures of 1794°K, 1896°K, 1998°K and 2023°K. The comparison between this performance and that observed in converters TE-102 and TE-104 is made in more detail in Sections 4.4.1 and 4.4.8.

As for converter TE-103, in the initial test of converter TE-104, the emitter temperature was set at 2000°K rather than 1900°K to accelerate the process of performance stabilization. During the first 15.8 hours, the converter was operated at an output of 14.3 amperes at 1.200 volts. It was then optimized and, at the same output voltage, the output current increased to 15.0 amperes. At the end of 23.6 hours of further running under auto-

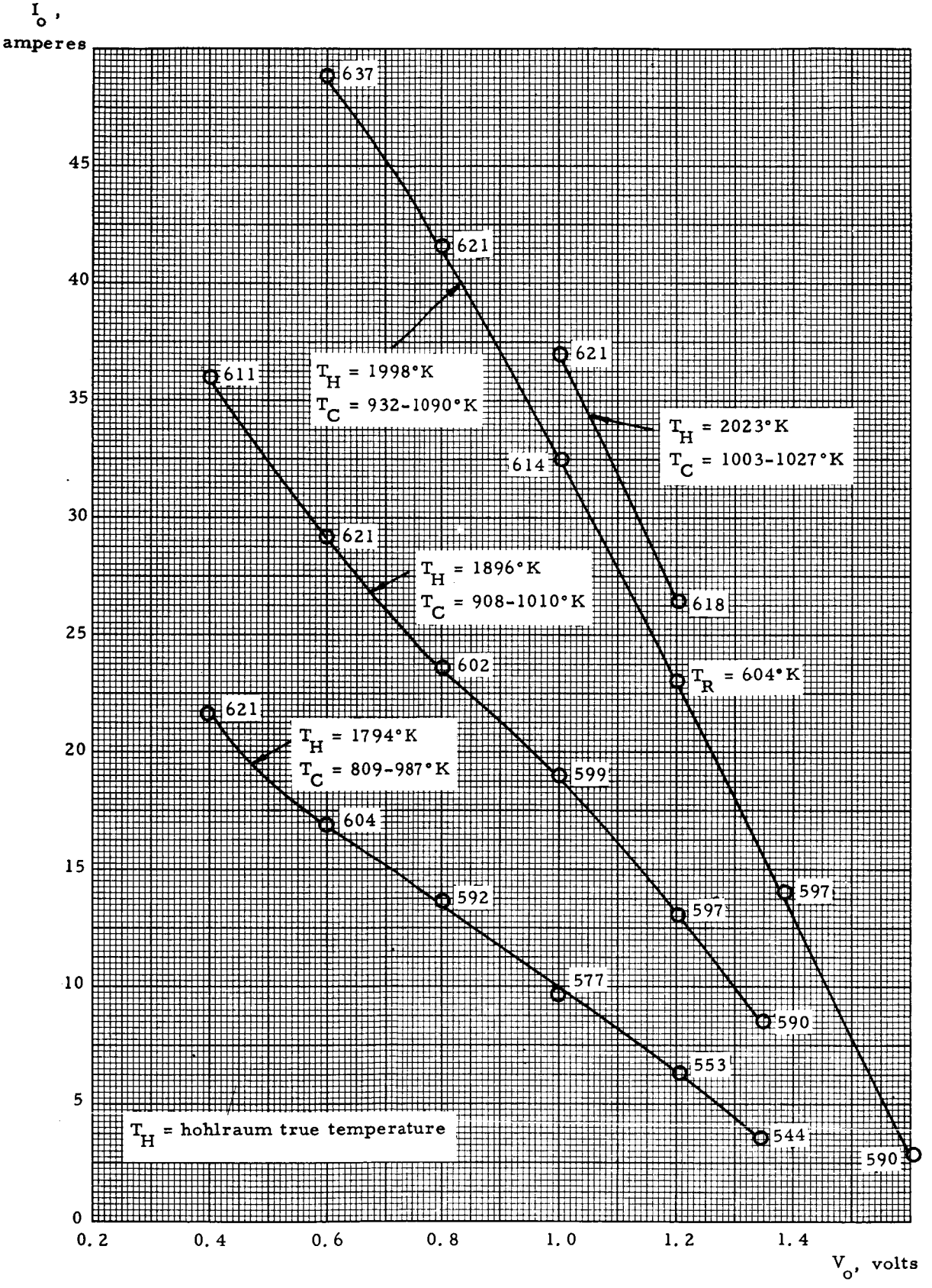

Figure 33. Steady-State Optimized Performance of Converter TE-103 (Data Sheets 2-5)

matically controlled conditions, the output was still 15.0 amperes at 1.200 volts. Therefore, no tendency to a change in performance was detected. The output of 15.0 amperes at 1.200 volts was, however, considerably lower than that observed in the tests of converters TE-102 and TE-103 which at the same voltage and similar emitter temperature had delivered 23.0 and 23.1 amperes, respectively. As already discussed in Section 3.2, the lower performance observed in converter TE-104 is suspected to be related to a broken drill fragment which had been inadvertently left unremoved in the emitter structure. The steady-state optimized performance of prototype TE-104 at 1794°K, 1896°K and 1998°K hohlraum temperatures is presented in Figure 34.

4.3.2 Effect of Reservoir and Collector Temperature Variations

During the tests of converter TE-102, the effect of a $\pm$ 5°C change in reservoir temperature and of a $\pm$ 20°C temperature change in the collector was evaluated separately at output voltages of .6, .8, and 1.0 volts at emitter temperatures of 1800°K, 1900°K, and 2000°K. Table VI shows the corresponding per cent changes in output observed. As it can be realized, the observed changes in performance are rather scattered and erratic. In some instances, particularly with regard to collector temperature variations, it is found that the converter was not completely optimized before the temperature variation. It was then concluded that the output response to reservoir and collector temperature variations cannot be adequately evaluated by means of this type of test. Consequently, in the test of converter TE-103, the response to reservoir and collector temperature variations were evaluated at a single optimized point, but the emphasis was placed on collecting more data with greater accuracy. Figure 35 shows the results of the tests

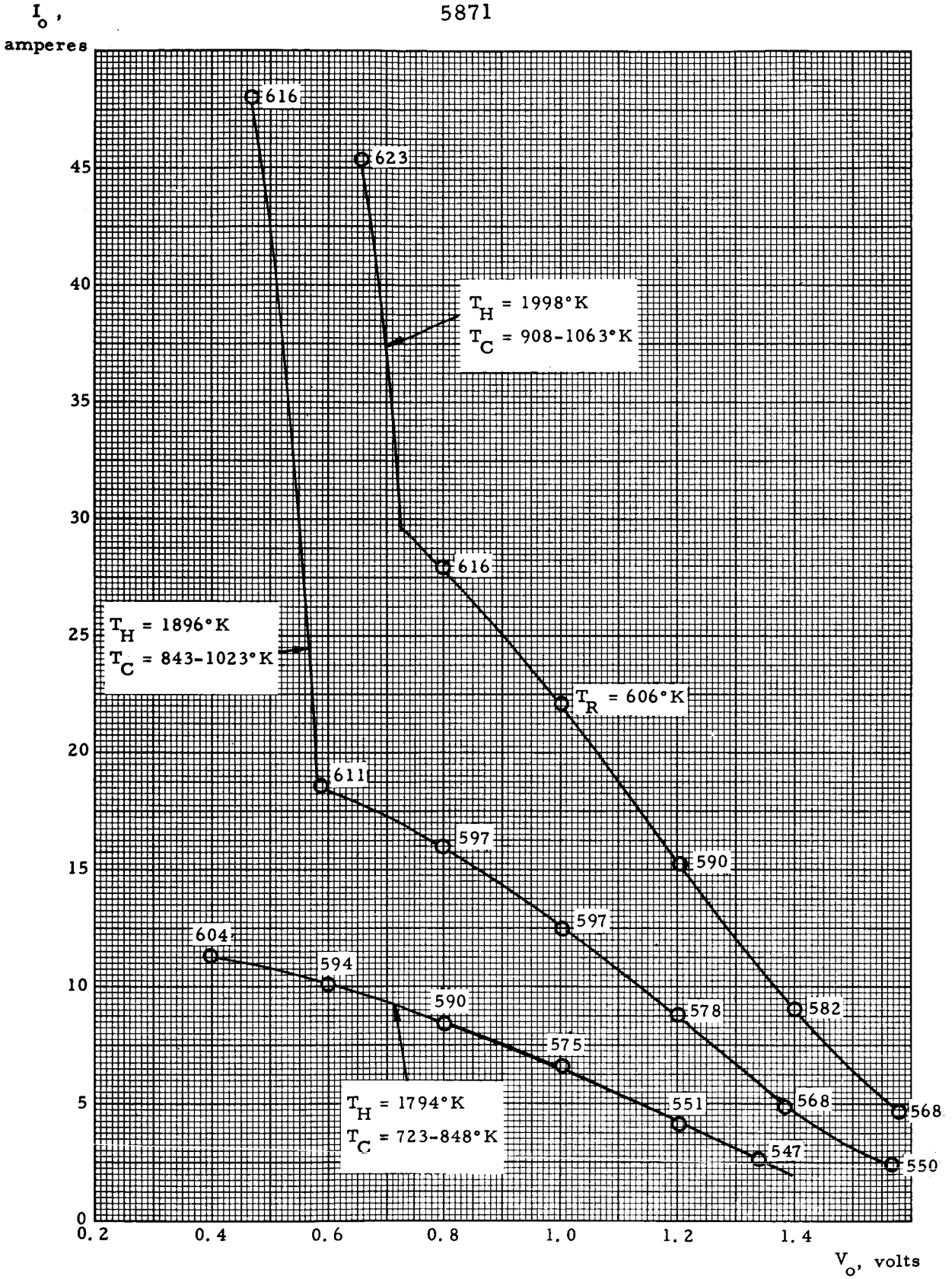

Figure 34. Steady-State Optimized Performance of Converter TE-104 (Data Sheets 3-5)

TABLE VI

Response in the Output of Converter TE-102
to Reservoir and Collector Temperature Variations

(Data Sheets 2 to 7)

Output Voltage	T_R - 5°C	T_R + 5°C	T_c - 20°C	T_c + 20°C
		1800°K		
0.6v	- .8	-3.3	-2.5	+ .8
0.8v	0	0	-1.0	+2.0
1.0v	-2.7	-2.7	-1.3	-1.3
		1900°K		
0.6v	- .4	-1.7	- .9	+1.3
0.8v	-1.0	-1.5	-2.0	+ .5
1.0v	-1.3	-2.0	-2.0	+ .7
		2000°K		
0.6v	-	-	-	-
0.8v	-1.5	-3.7	-1.8	-3.3
1.0v	0	-1.6	+ .8	+ .4

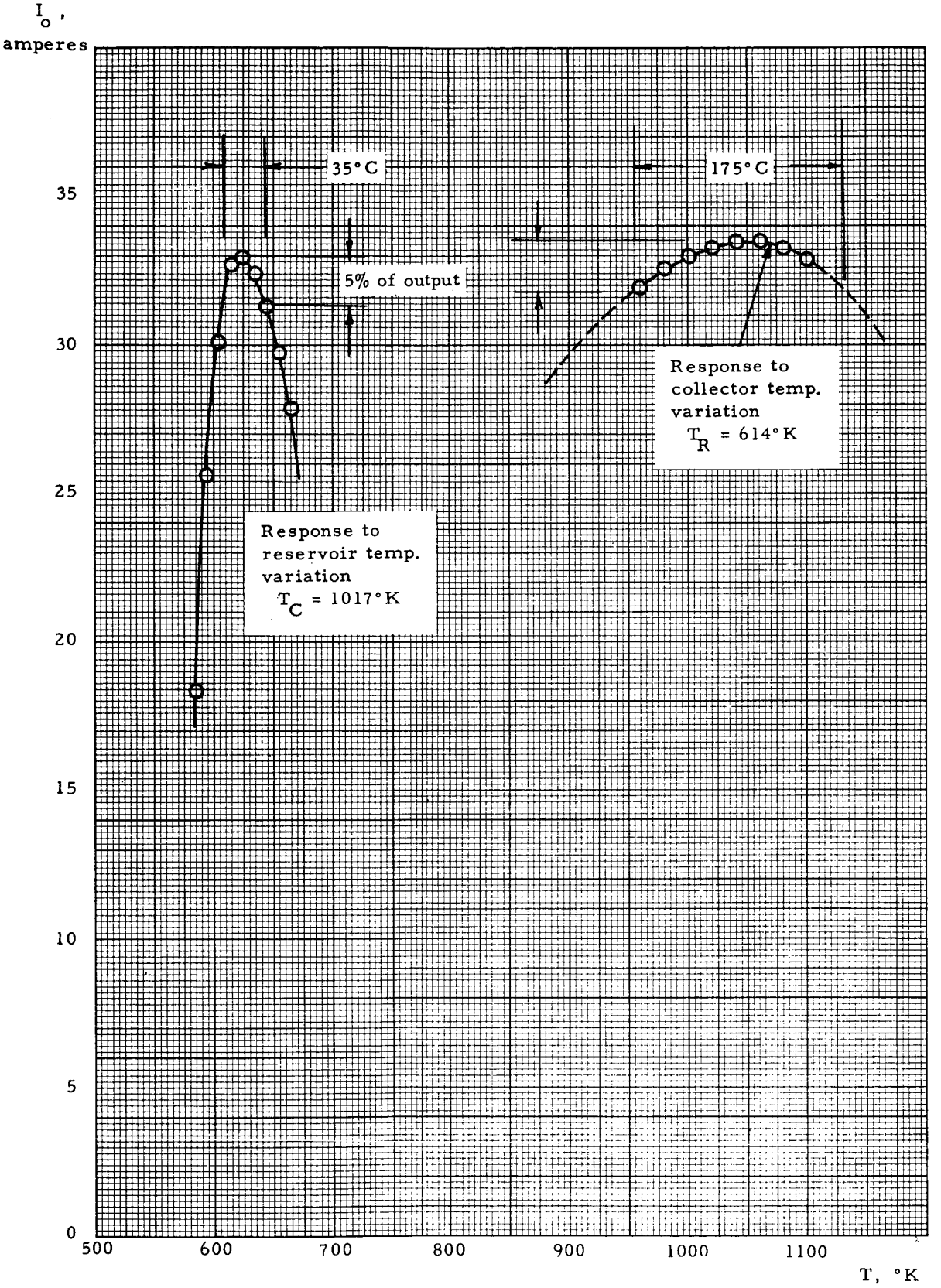

Figure 35. TE-103 Output vs T_C and T_R Output at 1.000 volt, 2000°K Hohlraum (Data Sheets 9 and 10)

conducted. It can be noted that to decrease the performance by 5%, it is necessary to change the reservoir temperature by ± 17°C, and the collector temperature by ± 87°C. Similar tests on converter TE-104 were not performed.

4.3.3 Measurement of Cesium Conduction

Cesium conduction data was obtained from converters TE-100, 102 and 104 in order to infer the values of interelectrode spacing achieved in these converters. The data was obtained by measuring accurately the power input required to maintain a given emitter temperature (monitored automatically by means of a temperature sensor, previously discussed, to within ± 2°K (while the cesium reservoir temperature was increased from approximately 520°K to 680°K). The data obtained is analyzed in Section 4.4.5.

4.3.4 Dynamic Measurement of I-V Characteristics

In order to obtain I-V characteristics at constant cesium reservoir temperature and at smaller output voltages than can be realized under steady-state testing conditions, the I-V characteristics were measured dynamically by placing the converter in series with the low voltage secondary of a transformer powered at 60 cycles. The oscillographs obtained for converters TE-102, 103 and 104 are presented in Figures 36, 37, and 38, respectively. These are useful for the interpretation of the dependency of the characteristics of the converter on the mean-free-path to spacing ratio λ/d, and they are discussed in Section 4.4.7. The data was obtained at true emitter temperatures as follows:

For converter TE-102, T_E = 1900°K

For converter TE-103, T_E = 2000°K

For converter TE-104, T_E = 2000°K, 1900°K, 1800°K, 1700°K

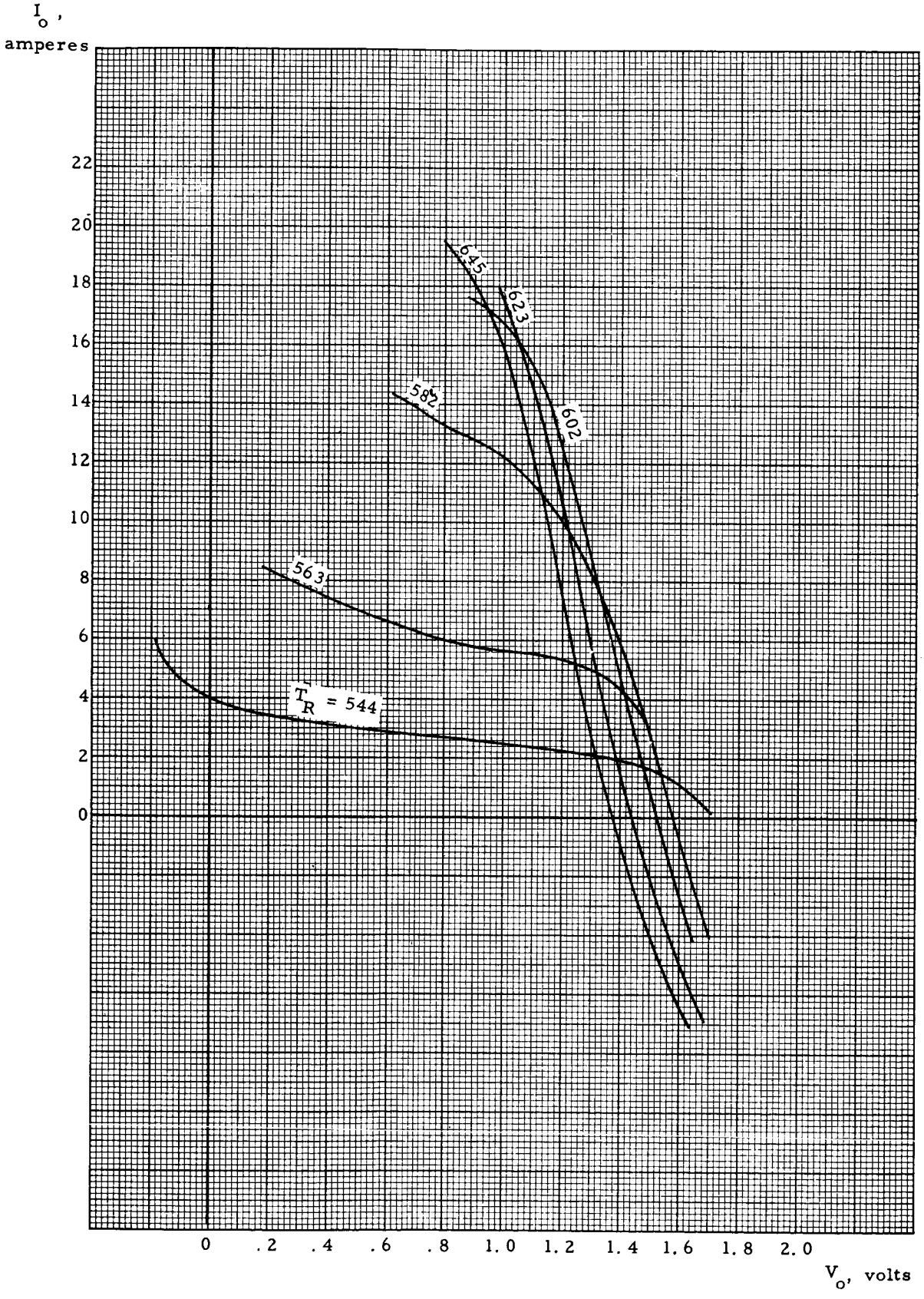

Figure 36. Dynamic I-V Characteristics of Converter TE-102, T_E = 1900°K, T_C/T_R = 1.667 (Data Sheets 28, 29)

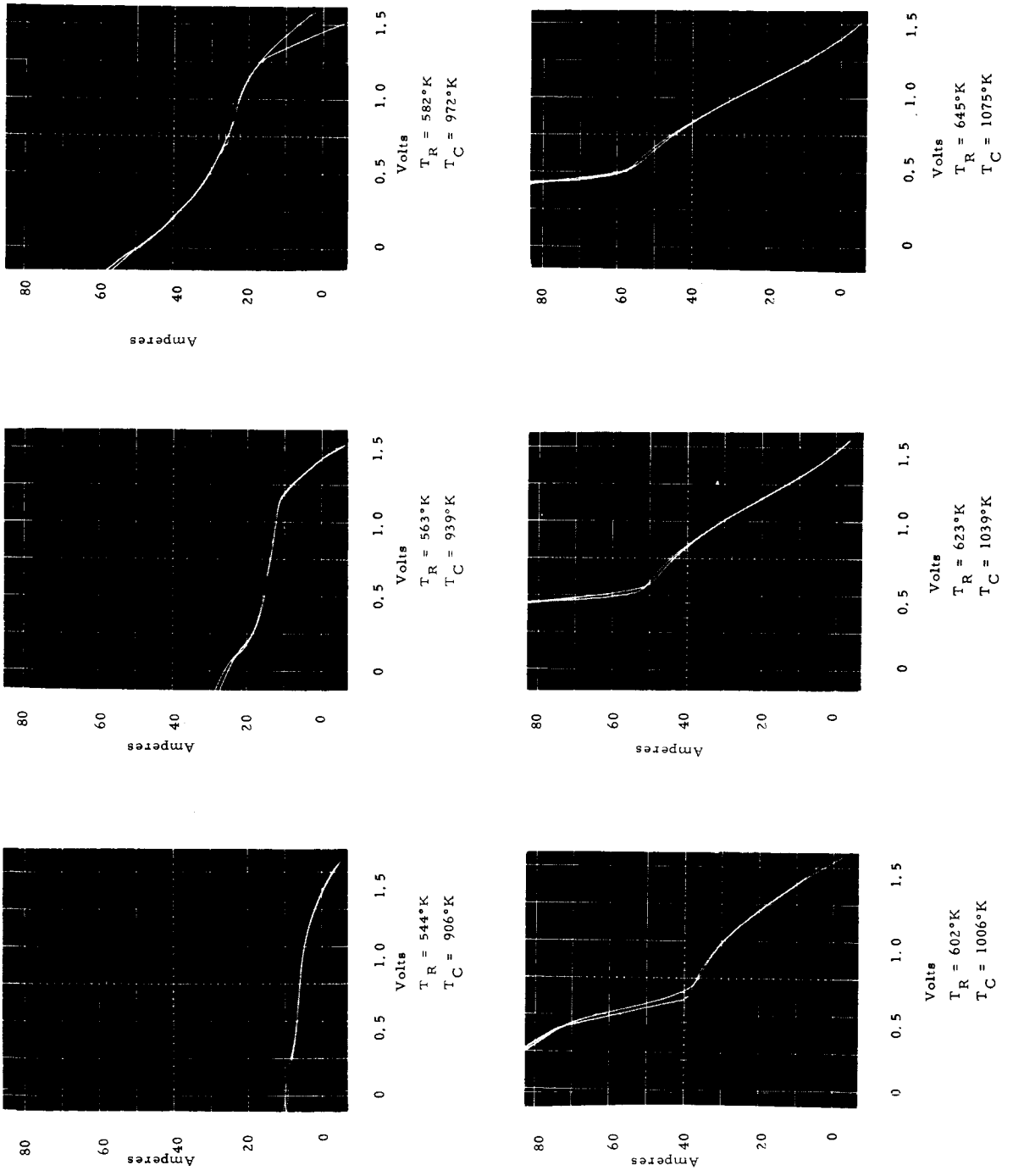

Figure 37 Dynamic I-V Characteristics of Converter TE-103
T_E = 2000°K (Data Sheets 11-12)

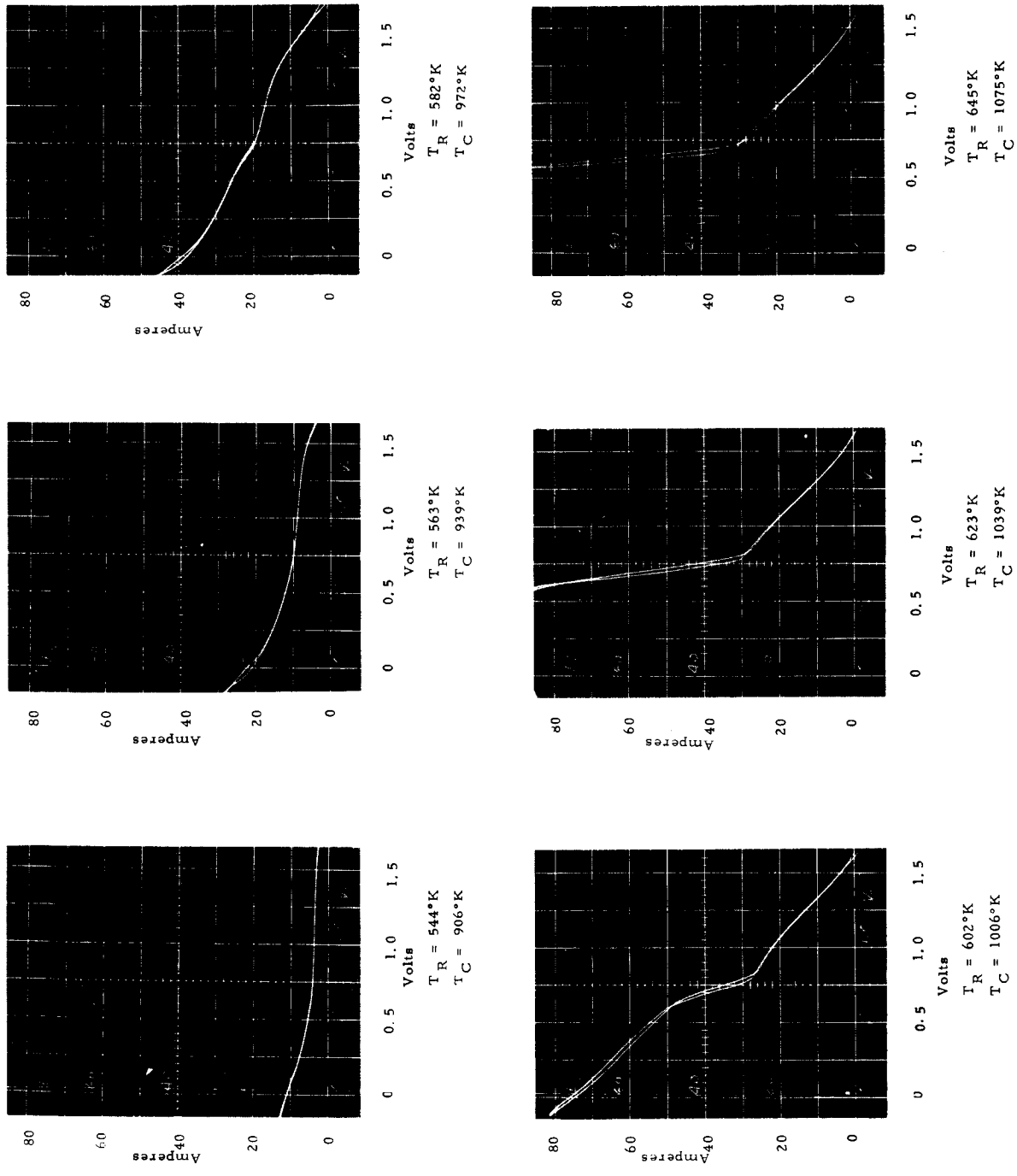

Figure 38a Dynamic I-V Characteristics of Converter TE-104

$T_E = 2000^{\circ}K$ t = 46 hours (Data Sheet 6)

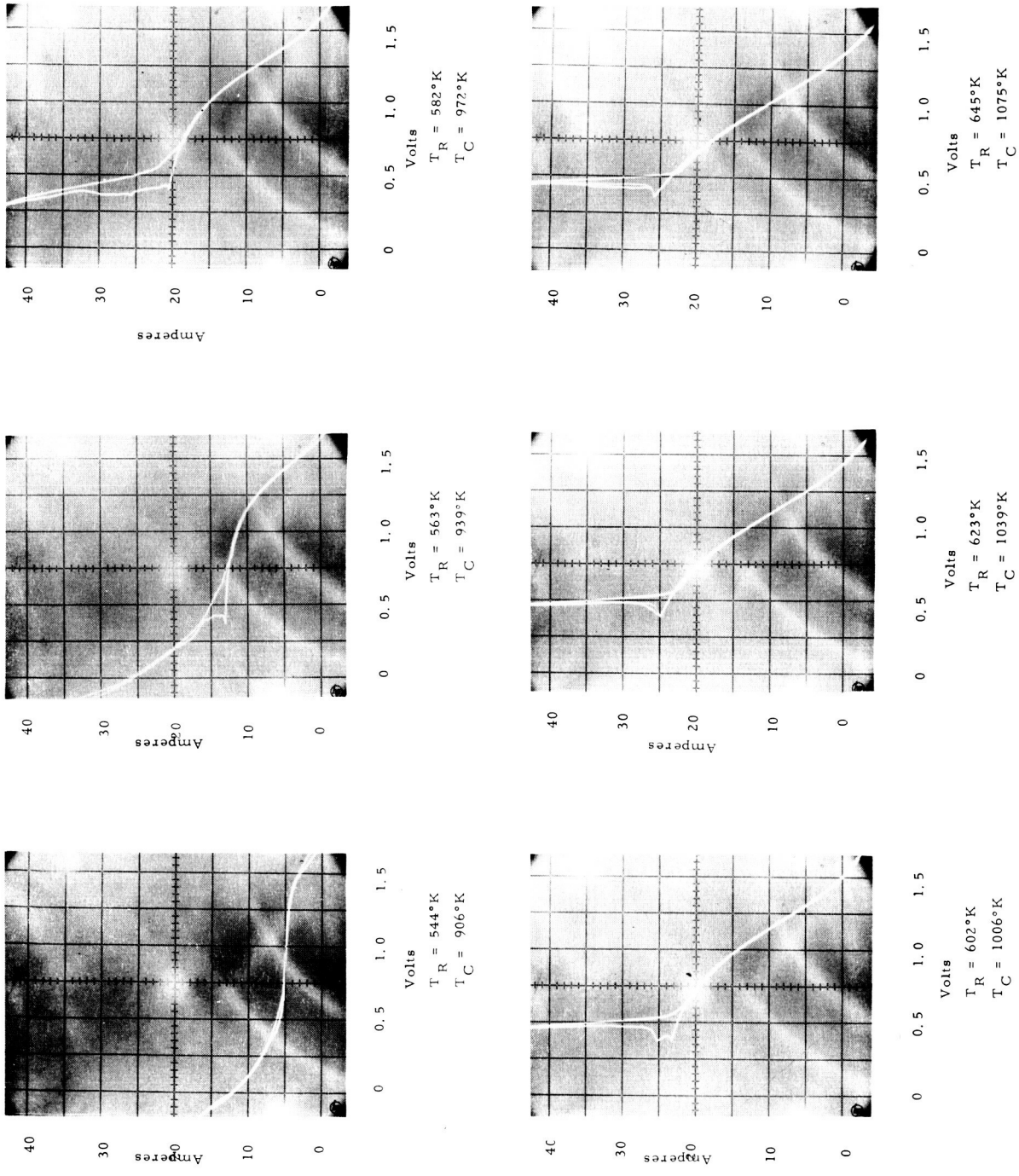

Figure 38b Dynamic I-V Characteristics of Converter TE-104

T_E = 1900°K t = 214 hours (Data Sheet 7

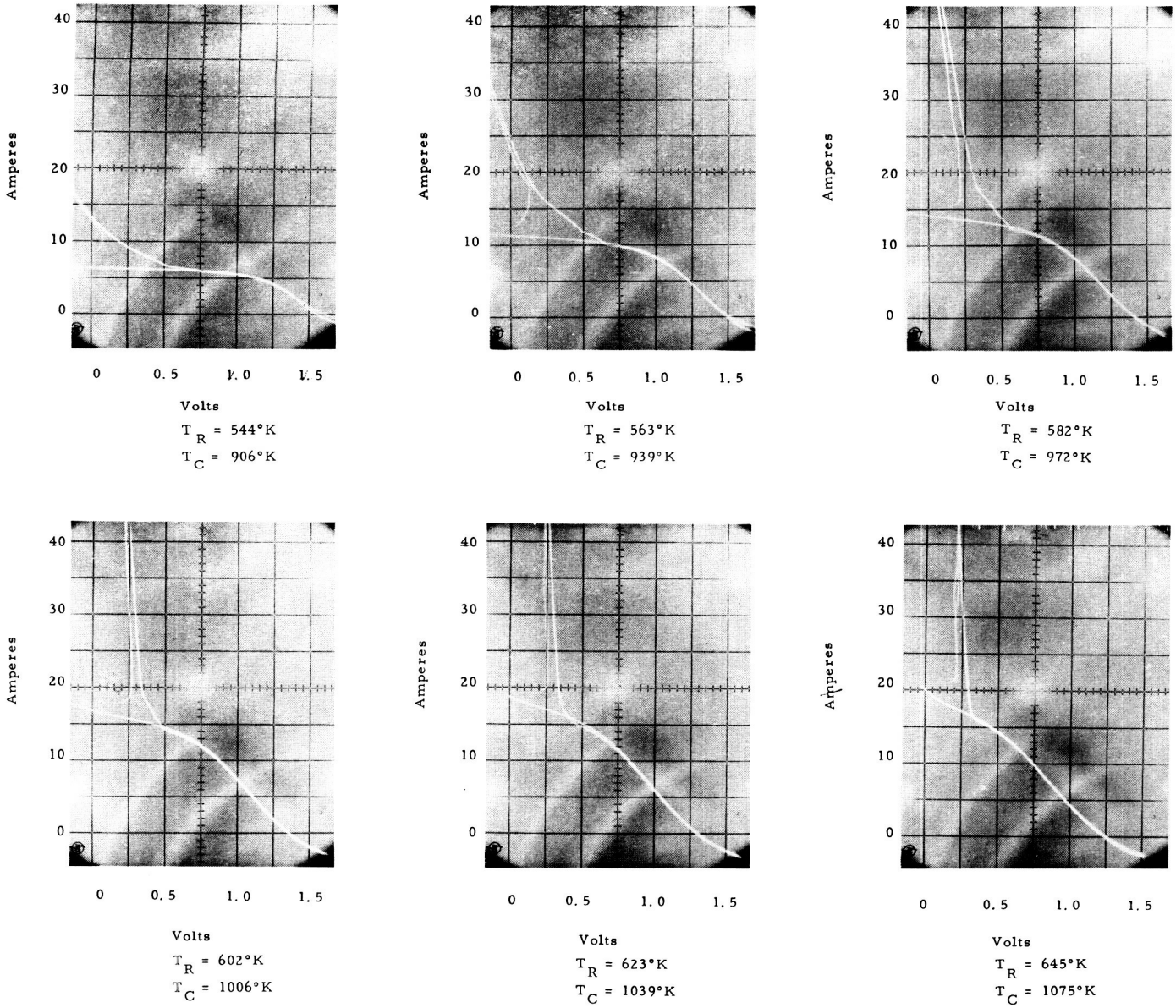

Figure 38c Dynamic I-V Characteristics of Converter TE-104

T_E = 1800°K t = 215 hours (Data Sheet 8)

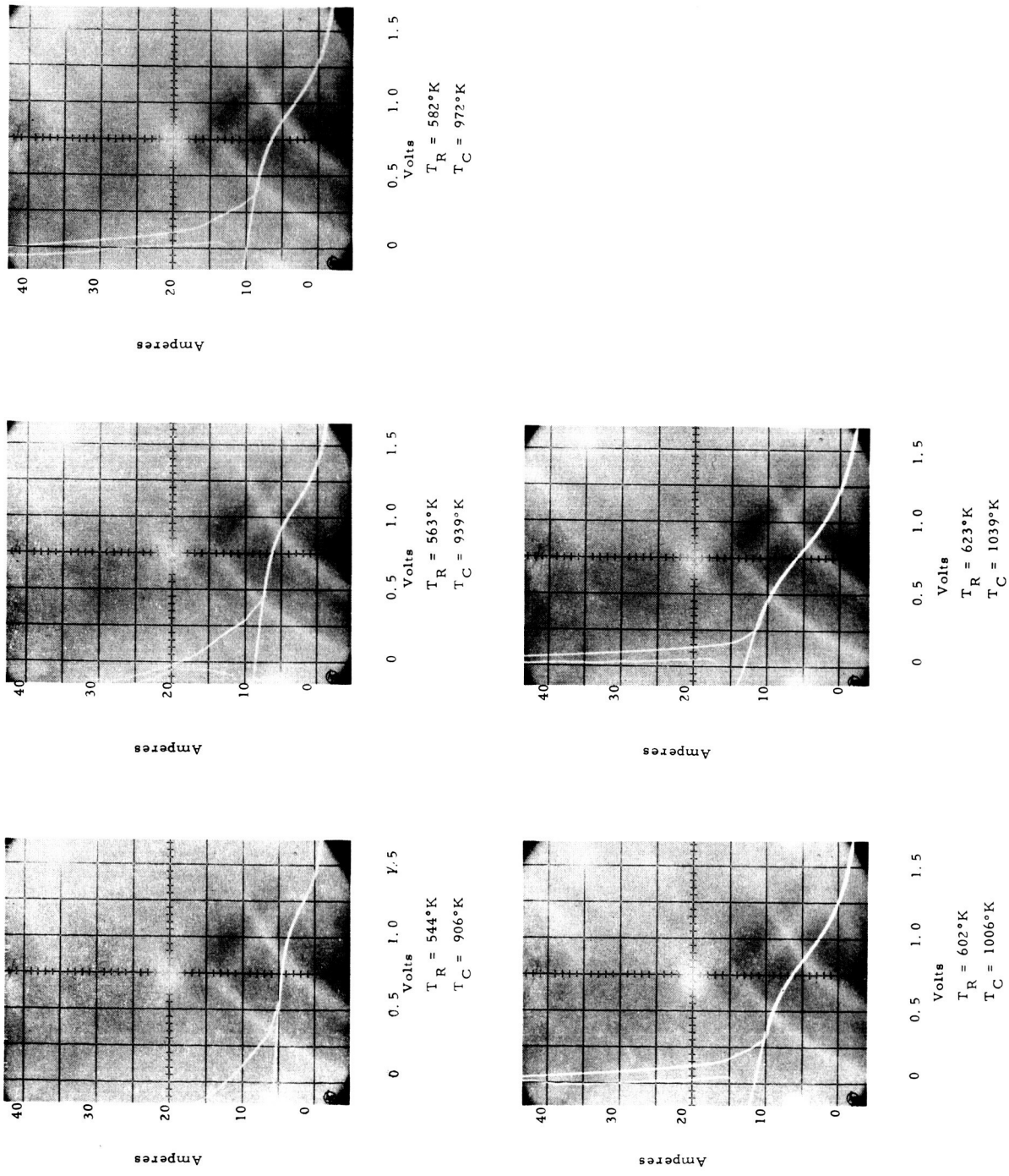

Figure 38d Dynamic I-V Characteristics of Converter TE-104

T_E = 1700°K t = 215 hours (Data Sheet 9)

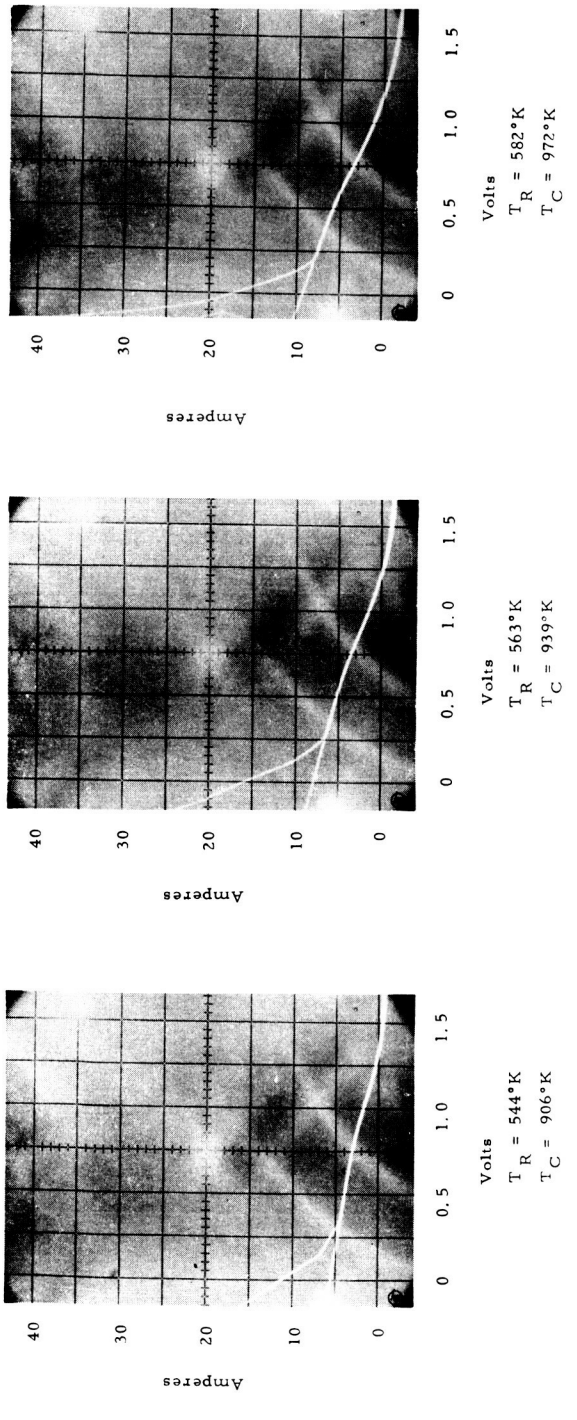

Figure 38e Dynamic I-V Characteristics of Converter TE-104

T_E = 1600°K t = 216 hours (Data Sheet 10)

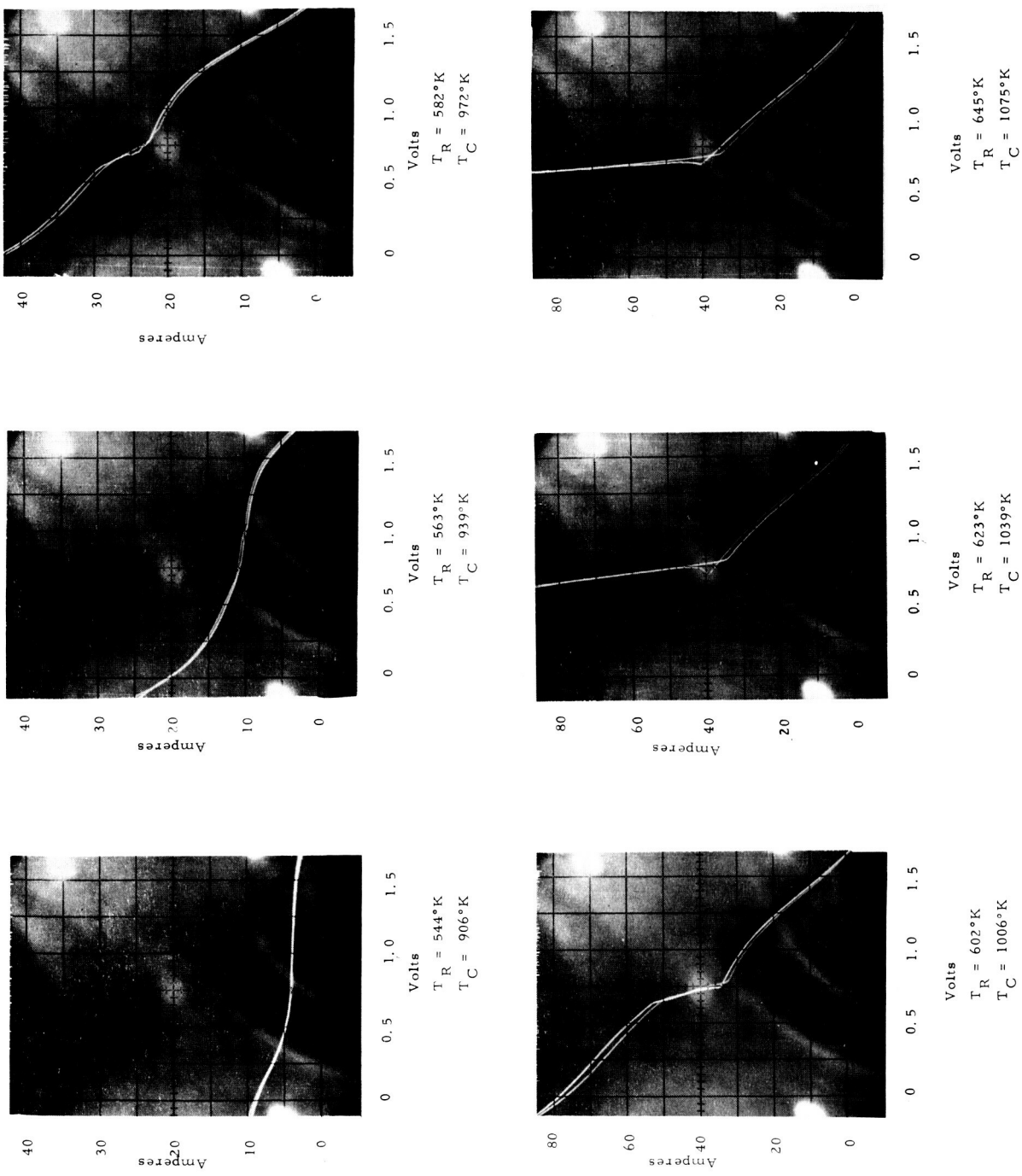

Figure 38f Dynamic I-V Characteristics of Converter TE-104

T_E = 2000°K t = 451 hours (Data Sheet 12)

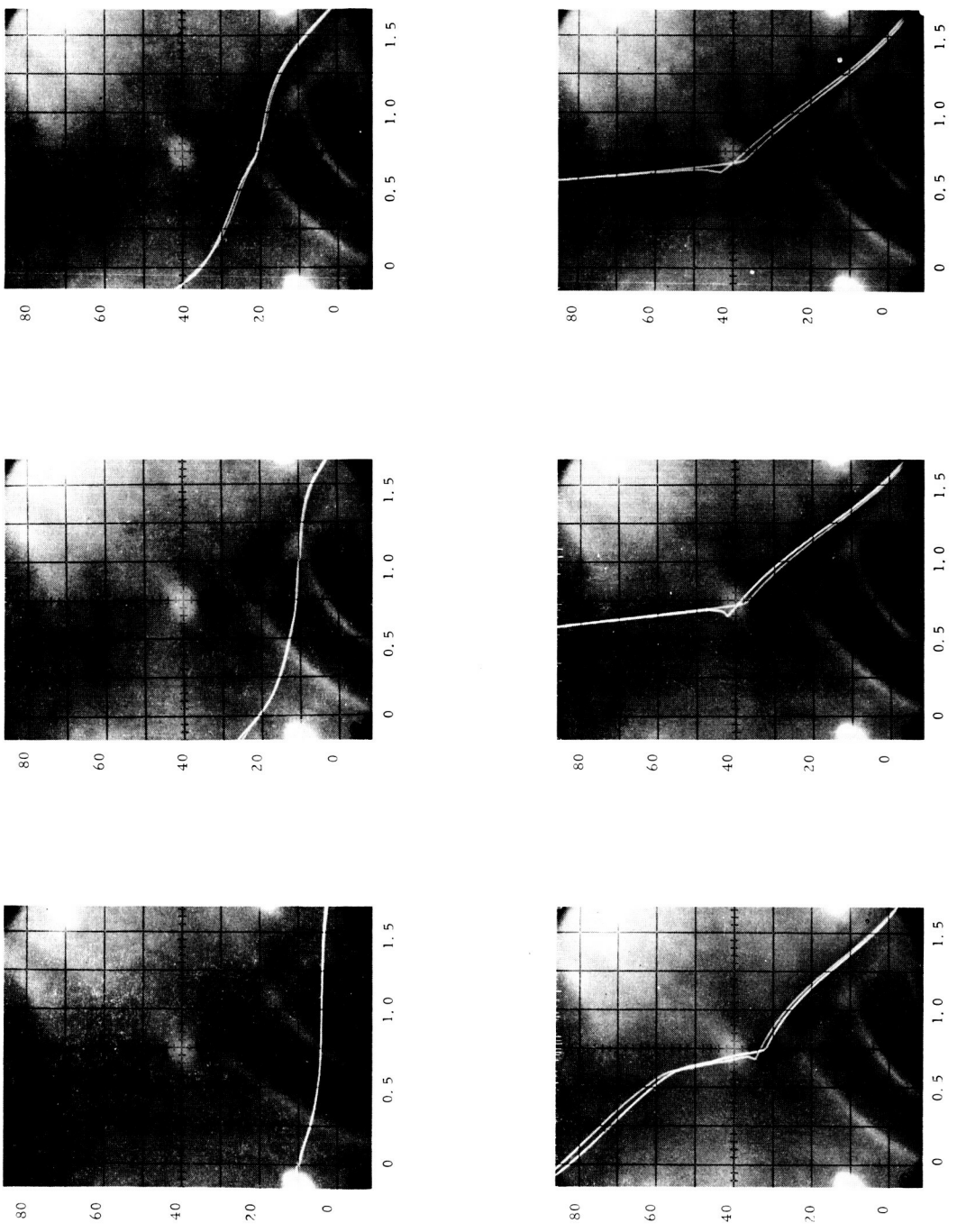

Figure 38g Dynamic I-V Characteristics of Converter TE-104
T_E = 2000°K t = 470 hours (Data Sheet 13)
(After Taking Collector to 865°C for 17 hours)

and 1600°K.

The oscillographs presented in Figures 38f and 38g were obtained on converter TE-104 at 2000°K after subjecting the collector of converter TE-104 to a high temperature, high current cycle, as explained below, to investigate the effect of this treatment on converter performance.*

Figure 38f: The collector was taken to 865°C for 7 hours at 50 amperes output. Static measurements (Data Sheet 11) indicated an output voltage increase at constant output current of .198, .121 and .088 volts at the respective I-V points 27.9A, 0.8V; 22.1A, 1.0V, and 15.3A, 1.2V. But, before the dynamic records of Figure 38f were made, the converter was cooled to clean the bell jar.

Figure 38g: After the measurements shown in Figure 38f were made, the collector was taken to 865°C, 50 amperes for 17 hours and the measurements presented in Figure 38g were made. This test was made to determine whether further changes in performance could be obtained with this treatment and whether the cycle to room temperature after the first collector heat treatment had had any effect. As may be seen, the output observed after this second heat treatment is practically identical to that observed after the first.

Further discussion of the effect of collector heat treatment is presented in Section 4.4.9.

4.3.5 Collector Work Function Data

Collector work function data was gathered under the form of retarding plots and dynamic characteristics. It will be explained later in Section 4.4.6 that the retarding plots are actually worthless for the measure-

*This treatment was found to be effective in partially retaining the performance of SET converters with a tantalum emitter after a degradation in performance had been observed.

ment of collector work function due to the overriding importance of edge effects when making these measurements. The lack of value of the retarding I-V characteristics was clearly demonstrated in the case of converter TE-101 when such a diagnostic test failed to give any indication of a collector abnormalty when, in fact, later inspection disclosed that the collector was covered with a thick deposit. It is for this reason that most of the retarding I-V data will not be given further notice in the body of this report. To serve the purpose of further discussions presented in Section 4.4.6, Figures 39 and 40 show typical retarding plots obtained for converters TE-102 and TE-104, respectively. Figure 41 shows the data for a different approach at measuring collector work function, which was devised and used for the first time during the test of converter TE-104. This data is also discussed in Section 4.4.6.

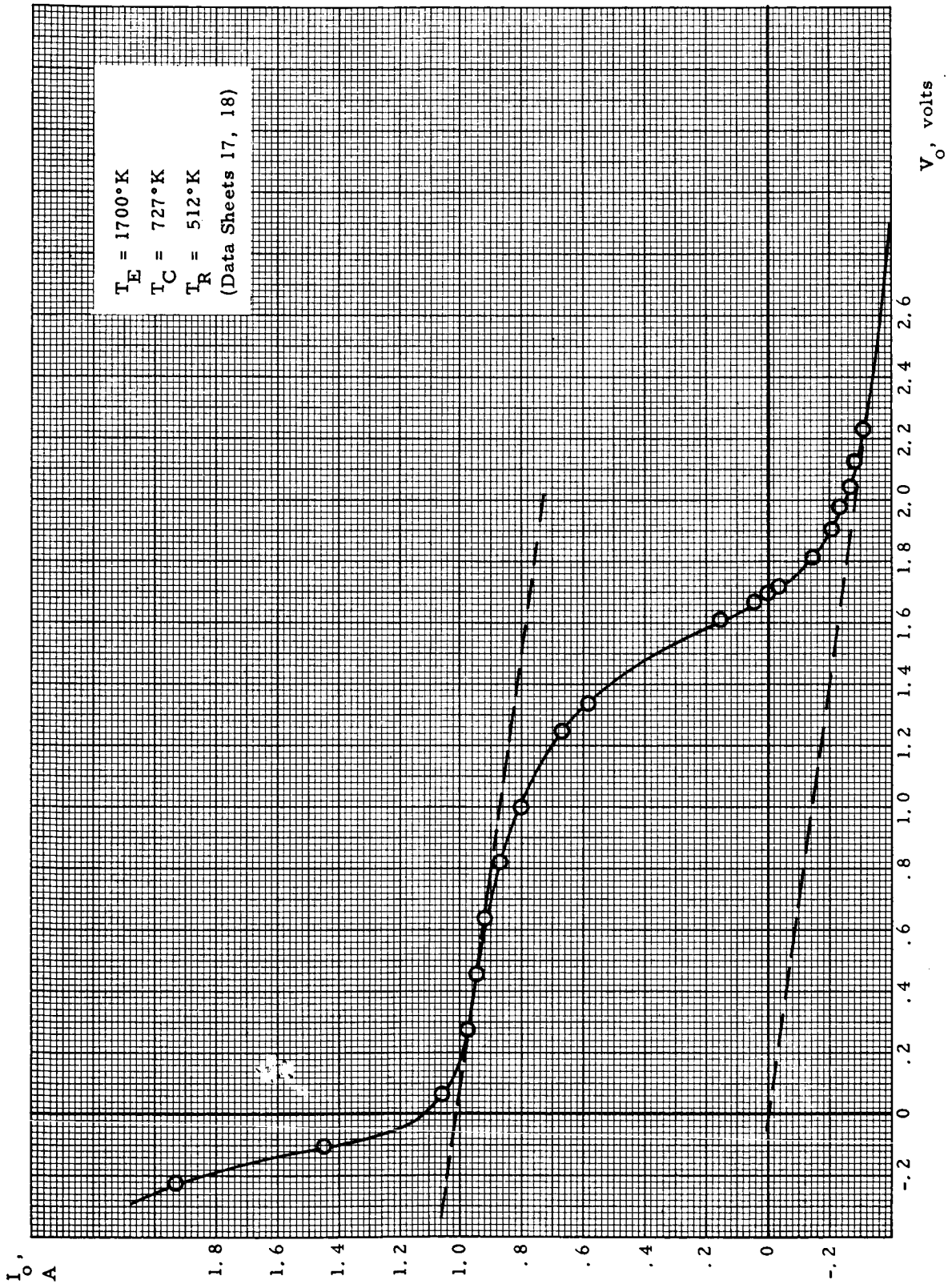

Figure 39. Retarding Plot for Converter TE-102

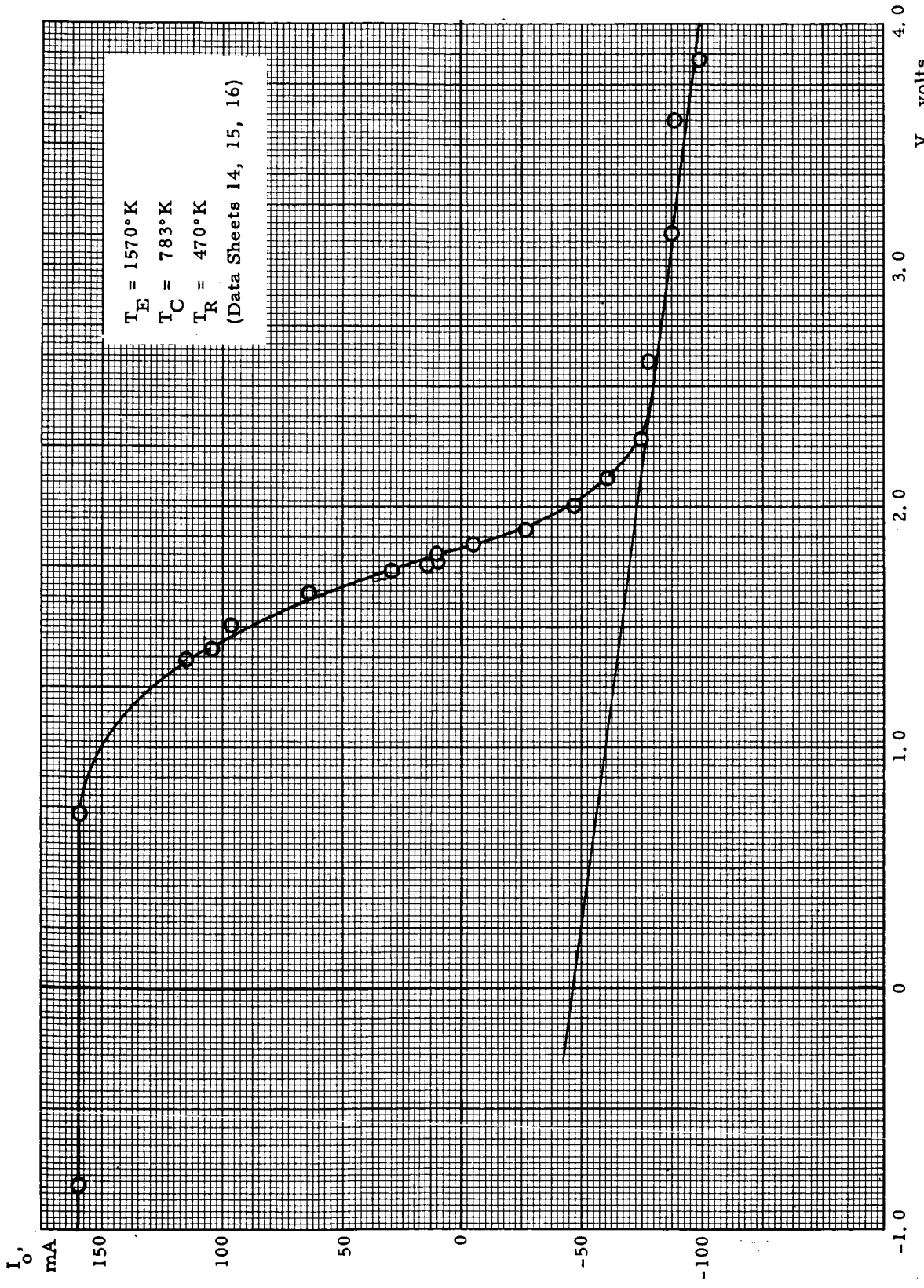

Figure 40. Retarding Plot for Converter TE-104

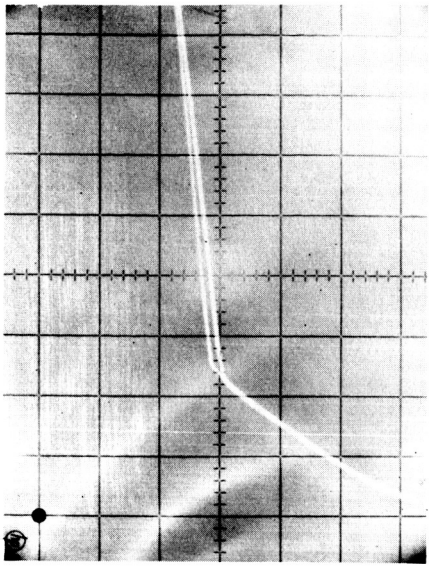

T_C = 942°K

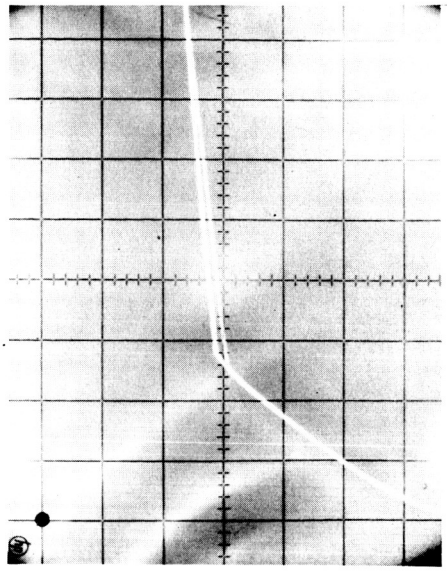

T_C = 992°K

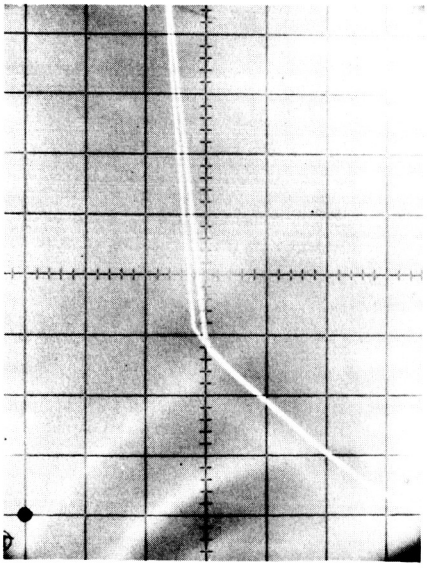

T_C = 1042°K

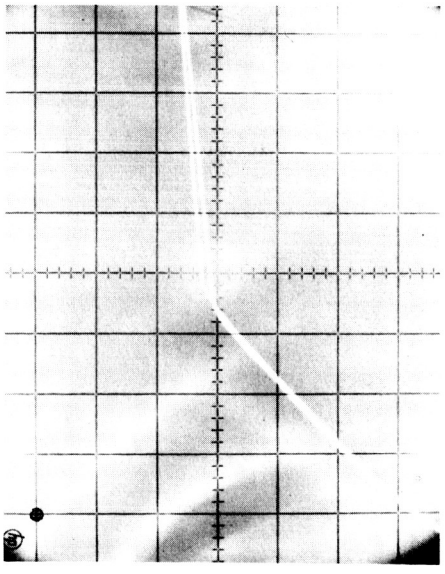

T_C = 1092°K

Figure 41. TE-104 I-V Characteristics at pd = 20

T_E = 2000°K, T_R = 683°K

(Data Sheet 16; Vertical Scale: 10 A/cm, Horizontal Scale: 0.25 V/cm)

4.4 Interpretation of Data

4.4.1 Performance Comparison with Research Data and SET VIII Converter Data

The steady-state optimized performance at 2000°K for converters TE-102, 103 and 104 which was presented in Figures 32, 33 and 34, is re-plotted in Figure 42 for 1 cm^2 of emitter area. This figure also gives the observed performance in two research converters and in SET converters VIII-P-2A and VIII-P-3. Unfortunately, not all the data extends to the higher values of output voltage, where the comparison is of greatest interest. For instance, at voltages above 1.55 volts, converter TE-104, which had a relatively low output compared with the other TE-100 converters, appears to exceed the performance of all other converters presented in this figure. In the intermediate range of voltages, from .7 volt to 1.5 volt, converter TE-103 is clearly the best of the TE-100 converters. At a voltage below .7 volt the performance of converter TE-104 tends to exceed the performance of converter TE-103, because converter TE-104 reaches ignition at about .73 volts, while converter TE-103 has not yet ignited at a voltage as low as .6 volt. Of the two curves representing the research data, that provided for converter No. 1 is the most meaningful, because it applies to a converter with the same spacing as that of converters TE-100 and run at the same emitter temperature and at optimum reservoir temperature, although the collector temperature was not fully optimized. The second curve, that for research converter No. 2, applies to a smaller spacing and is for a higher emitter temperature and, therefore, can only be used as an upper bound for the performance that could have been expected out of all the hardware converters represented in the figure. Above .8 volt, the data for research converter No. 1 is considerably lower than that obtained in converter TE-103, and it is pre-

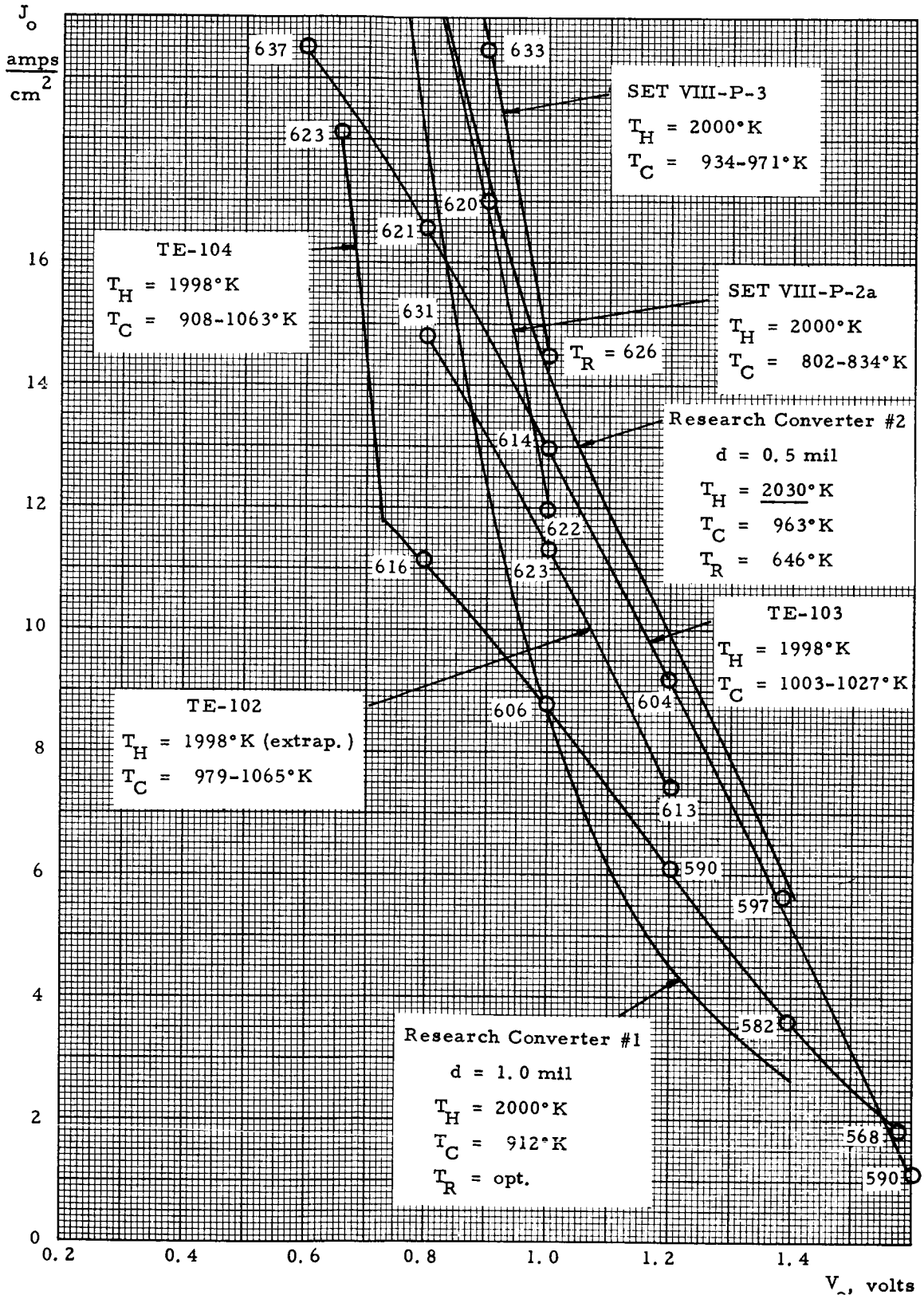

Figure 42. Comparison of Performance of TE-100 Converters with Research Data and SET VIII Data

assumed that this difference is due to the presence of significantly larger edge effects in the hardware converters* which increase the actual electrode area, thus yielding deceivingly high values of current density when these are computed on the basis of the planar electrode area only. It can be noted that the curves for converters VIII-P-2A and VIII-P-3 parallel closely the curve for research converter No. 1 and it is likely that the difference between these curves can be largely ascribed again to the greater importance of edge effects in hardware converters.

Another important feature appearing in Figure 42 is that the ignition of the research converters and the SET VIII converters takes place at a substantially higher value of voltage than that of converter TE-104 which is the only one of the TE-100 converters to exhibit ignition in Figure 42. The lower value of ignition voltage in the TE-100 converters can be due to a higher collector work function, or a larger value of internal voltage drop. Further discussion of collector work function and internal voltage drop characteristics is presented in Section 4.4.6.

4.4.2 Measured Overall Efficiency

Figure 43 shows the measured overall efficiency for converters TE-102, 103, 104 and VIII-P-3. The overall efficiency was obtained by dividing the observed converter power output by the actual electron bombardment power input (the power required to heat the filament of the electron bombardment unit was not included however, because simple calculations show that only a minute fraction of this power is absorbed by the emitter). It is striking to notice in this figure, that in spite of its lower power density, converter TE-103 achieves a higher efficiency than converter VIII-P-3 at all voltages above .8 volt. Also, converter TE-103 has a substantially broader efficiency curve; for instance, it exceeds 10% efficiency for the voltage range from .7 to 1.3 volts, while converter VIII-P-3 exceeds 10% efficiency only over the range from .63 volt to .95 volt. The main factors accounting for

*A deliberate attempt is made, in all research converters, to minimize any contribution to the measured output from the edge of the electrodes.

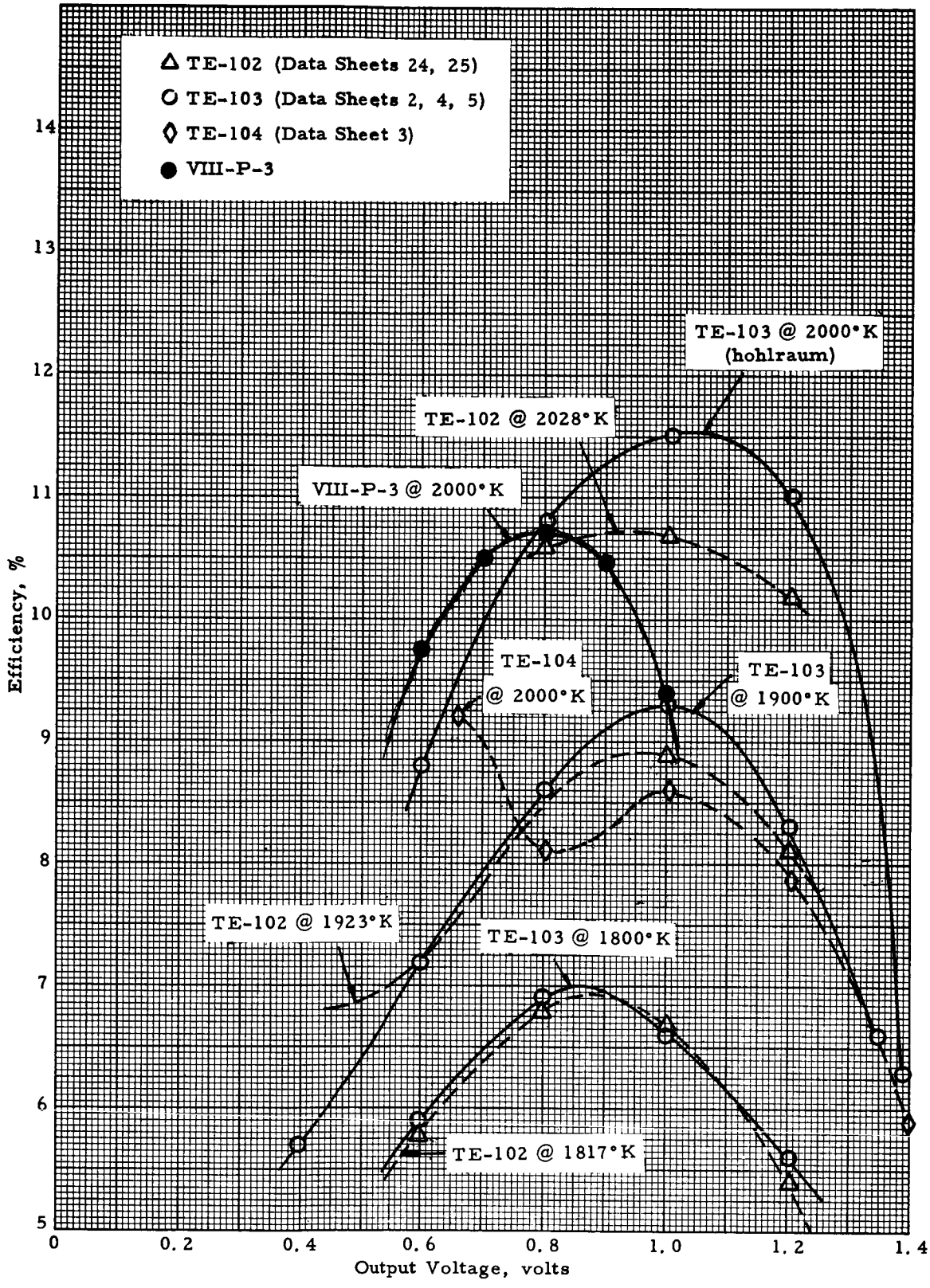

Figure 43. Overall Measured Efficiency

the lower heat losses of converter TE-103 are:

(1) the lower radiation losses of the re-entrant emitter support structure, and

(2) the lower radiation losses from the top of the emitter piece which is polished and hence does not incorporate the higher emissivity, grooved, cavity configuration used on converter VIII-P-3.

The curves in Figure 43 also tend to show that for every 100°K rise in emitter temperature, the maximum efficiency increases by approximately 2 points, and the voltage at maximum efficiency shifts to the right by approximately .1 volt. The curve for converter TE-104 at 2000°K has 2 maxima, because converter TE-104 has 2 points at which maximum power occurs; one in the unignited mode, and one in the ignited mode.

4.4.3 Electron Heat Transfer Correlation

One of the most interesting experimental results obtained under this program is presented graphically in Figure 44. This is a plot of the power required to operate prototypes TE-102, 103 and 104 at maximum output in the unignited mode (excluding the cesium conduction heat transfer) as a function of the current density at the respective maximum power points, at 2000°K, 1900°K, and 1800°K. Since the power input value plotted does not include the cesium heat transfer, changes in its value can only be accounted by the changes in electron heat transfer that occur as the current output is varied. What is of interest in Figure 44, is that the data shows electron heat transfer to be a linear function of output current independent of cesium reservoir temperature and even of emitter temperature. Thus, at least in the case of prototypes TE-102, 103 and 104, the electron heat transfer is independent of emitter work function when the converter is operated at maximum power output in the unignited mode. The straight lines traced through the data points in Figure 44 indicate that the value of electron heat transfer

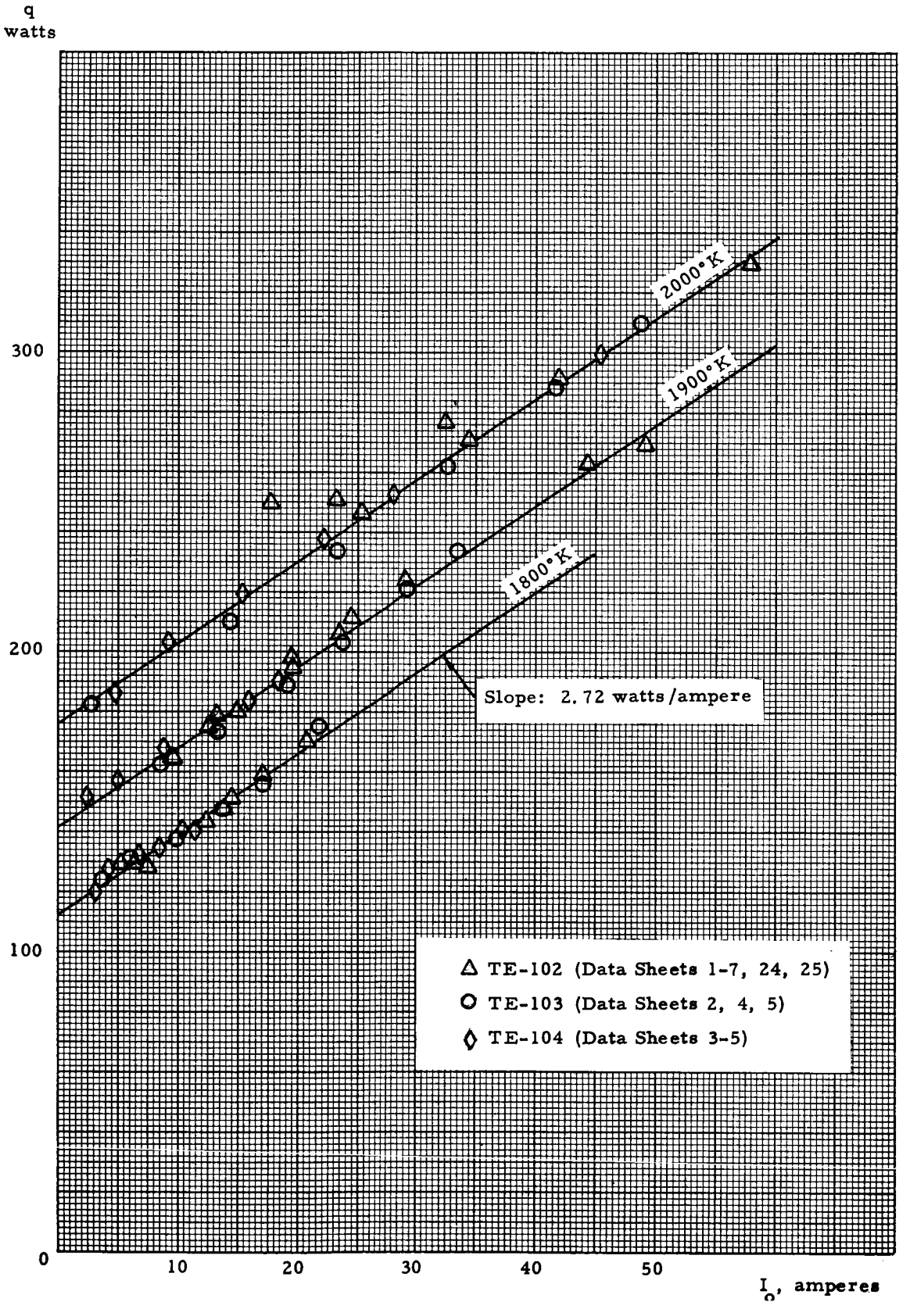

Figure 44. Electron Heat Transfer in Prototypes TE-102, 103 and 104

is equal to 2.72 watts per ampere of net current delivered by the converter.

4.4.4 Account of Converter Heat Losses

The intercept of the straight line for an emitter temperature of 2000°K with the vertical axis in Figure 44, occurs at a value of power input of 176 watts. This means that, in the absence of cesium conduction and electron heat transfer, the TE-100 converter structure requires a power input of 176 watts to achieve an emitter temperature of 2000°K. This value is of great interest in the thermal design of solar thermionic generators and its usefulness can be enhanced if its magnitude can be accounted for by the sum of individual heat loss terms. In the case of prototype TE-100, there are four major components of heat loss in the structure. These are: (1) the conduction loss in the emitter support structure of 58 watts, (2) the inter-electrode radiation of 33.5 watts, (3) the radiation from the top of the emitter structure which is calculated as follows:

diameter of the top of the emitter structure: 1.86 cm

area of top of emitter structure: 2.7 cm^2

heat loss/cm^2 of top of the emitter structure: 21.2 watts
(Kohl, "Materials and Techniques for Electron Tubes", p. 334)

heat loss at the top of the emitter structure = 2.7 x 21.2 =

57.5 watts

(4) the heat loss from the unshielded lateral area of the emitter structure. Since the first three losses add up to 149 watts, the fourth loss, the radiation loss from the unshielded lateral area of the emitter, must equal 176-149 = 27 watts. A value of 27 watts for this fourth loss can be justified by assuming that the lateral unshielded area radiates an amount of heat equal to 85% of that which it would radiate if it were unobstructed by the re-entrant emitter support and by the radiation shield usually placed there, as follows:

Mean diameter of lateral unshielded area, 1.84 cm

Height of lateral unshielded area, .26 cm

Area of lateral unshielded surface, 1.5 cm^2

Heat loss from lateral unshielded surface =

$1.5 \times 21.2 \times .85 =$ 27 watts

Table VII gives this breakdown of converter heat losses and gives an example of how the power input required at an arbitrary operating condition can be predicted using the electron heat transfer data derived in the previous section, 4.4.3, and the cesium conduction data given below and plotted in Figure 45.

4.4.5 Analysis of Cesium Conduction Data

The values of cesium conduction heat transfer obtained for converter TE-100, 102 and 104 were normalized for an emitter-collector temperature difference of 1000°K, and they are plotted as a function of reservoir temperature in Figure 45. This figure also shows the predicted heat transfer characteristics for an interelectrode spacing of .8, 1.0, 1.2 and 1.4 mils and an effective heat transfer area of 2.75 cm^2. As may be seen in the figure, the data for converter TE-100 tends to show that interelectrode spacing achieved in this converter is of the order of 1.4 mils. The data for converters TE-102 and TE-104 indicates that the interelectrode spacing achieved in these converters is of the order of 1.05 mils, and it is in surprisingly good agreement with the value of interelectrode spacing predicted by the relative thermal expansion calculations.

The reason for the larger interelectrode spacing of converter TE-100 offered in Section 3.2 is that the electrodes of this converter were not in good intimate contact during the subassembly braze (described in Section 3.4.4) because of accumulated mechanical tolerances and the lack of a posi-

TABLE VII

Account of Heat Lost by Emitter at 2000°K

Conduction to Emitter Support		58 watts
Interelectrode Radiation		33.5 "
External Radiation	Top Face	57.5
	Lateral	27.
Total Fixed Losses @ 2000°K		176 watts

Add: Cesium conduction as given in Figure 45

Electron Heat Transfer at 2.72 watt/amp.

Example:

Data Point #2 Sheet No. 3, Converter TE-103

T_R = 614°K I_o = 32.5 Amps Q = 282 watts

From Figure 45, Q_{cs} = 20.5 watts

Electron Heat Transfer = 32.5x2.72 = 88.3 watts

Predicted Power Input Required:

Q = 176 + 20.5 + 88.3 = 284.8 watts

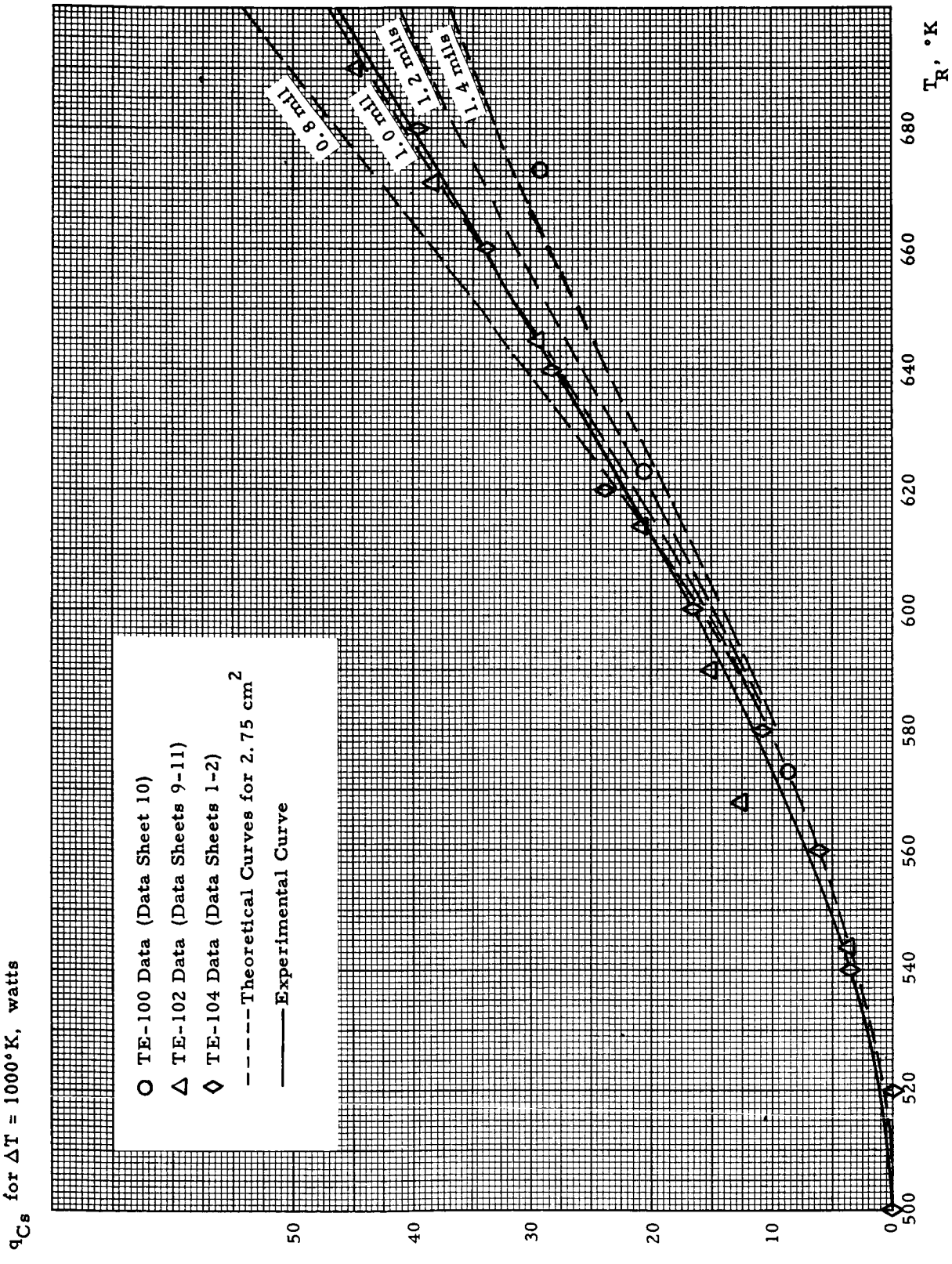

Figure 45. Cesium Conduction Data

tive clamping force between the electrodes during this operation. It is seen here that this must indeed have been the case since converters TE-102 and 104 appear to have achieved a closer interelectrode spacing, and for these converters a positive clamping force between the electrodes was applied by means of a compression jig.

4.4.6 Interpretation of Collector Work Function Data

As it was stated in Section 4.3.5, the collector work function data gathered was in the form of retarding plots and dynamic characteristics. Retarding plots were presented for converters TE-102 and TE-104 in Figures 39 and 40, and collector work function dynamic characteristics for converter TE-104 were presented in Figure 41.

The first step in the interpretation of retarding plot data is to identify the net forward emission of the emitter by drawing the assymptotic limits of the I-V characteristics, as shown in Figures 39 and 40. The next step is to plot this net forward current as a function of output voltage on a semi-logarithmic plot, such as shown in Figure 46. On such a plot, the retarding portion of the I-V characteristics is expected to approach assymptotically the Boltzmann line with the slope corresponding to the emitter temperature. It can be proven that, under ideal conditions, the potential barrier which retards the current to the value at any particular point on the Boltzmann line is equal to the sum of the collector work function and the output voltage at that particular point on the Boltzmann line. Thus, for instance, one assumes ideally that the 100 milliamperes point of the Boltzmann line appearing in Figure 46 corresponds to a current density of 40 milliamperes/cm^2 which, for an emitter temperature of 1700°K, in turn corresponds to a voltage barrier, as seen from the Fermi level of the emitter, equal to 3.36 volts. Since the output voltage at this particular point on the Boltzmann line

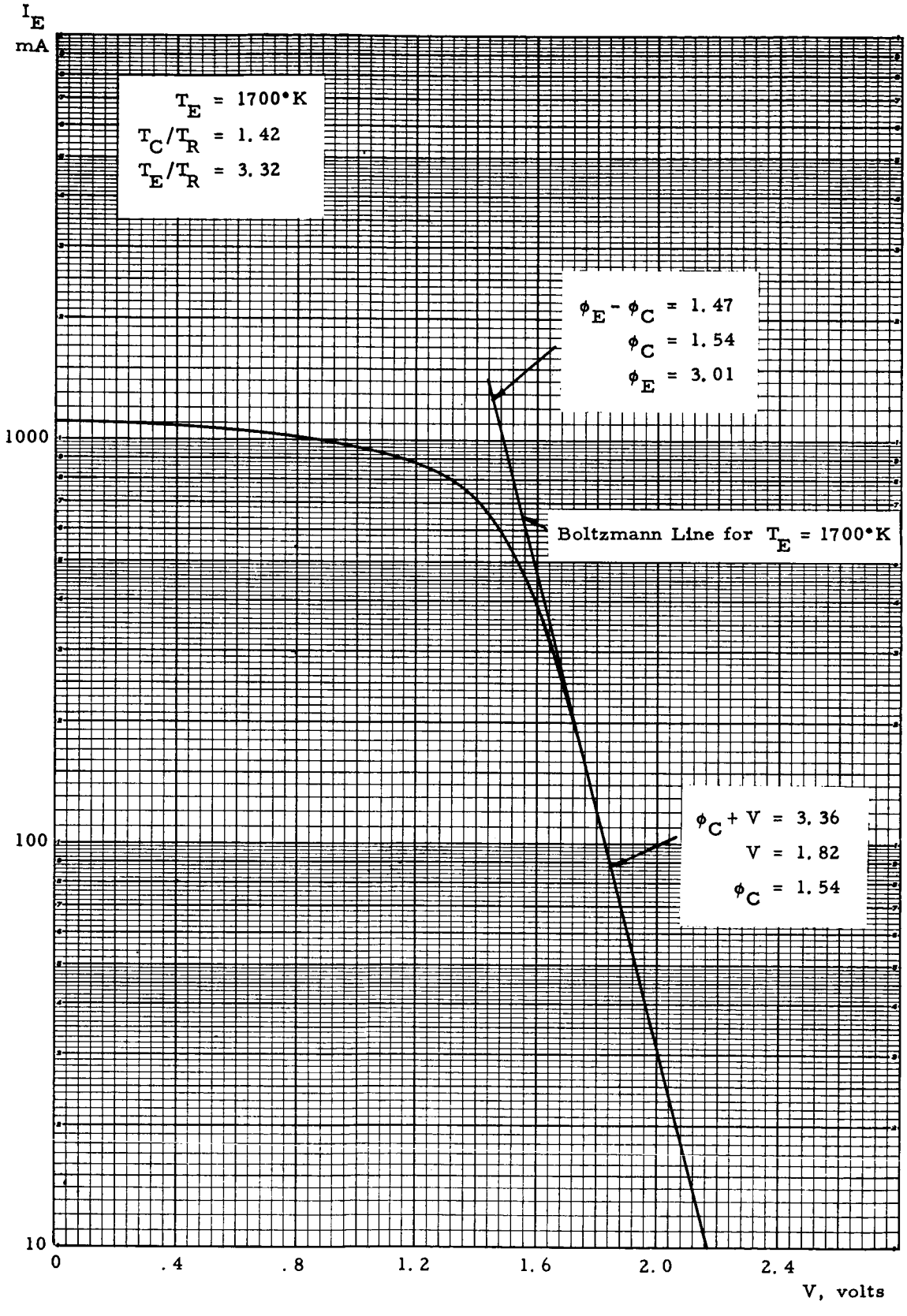

Figure 46. Boltzmann Line for TE-102 Collector

in Figure 46 is 1.86 volts, it is deduced that the collector work function is equal to 3.36 - 1.82 = 1.54 electron volts. Figure 47 gives the correlation of collector work function measurements made on a molybdenum collector by the Research Department at Thermo Electron, and it can be seen that for a collector to reservoir temperature ratio of 1.42 (which is the value for which the data for Figure 46 is given), the expected collector work function measured using the retarding plot technique would be just about 1.54 ev. Figure 48 shows the Boltzmann line corresponding to the data of Figure 40 for converter TE-104. The collector work function computed is again 1.54 ev, but to arrive at this value, it was assumed that the electrode area was equal to the total emitter area, including the inner emitter support sleeve, and equal to 6.86 cm^2. If a value of electrode area of 2.5 cm^2 had been used, as in the calculation of the data for converter TE-102, the collector work function calculated would have been 1.25 electron volts, clearly an unrealistically low value. The actual collector work function value predicted by Figure 48 for the collector to reservoir temperature ratio of 1.667 is of the order of 1.48 electron volts. If the assumptions made in the correlation of work function measurements made, using the retarding plot technique, are examined critically, it clearly appears that they cannot hold true for converters with the configuration of TE-100 and that whatever fitting of the data points with proper Boltzmann lines can be achieved in certain instances is rather fortuitous. In particular, in order for the collector work function measurement to be meaningful, it is necessary that most of the current measured in the retarding plot originate at the planar emitter electrode and be collected by the planar collector electrode. It can easily be seen that, in actual fact, a small portion of the measured current is actually contributed by this portion of the emitter surface. For instance, it is calculated that

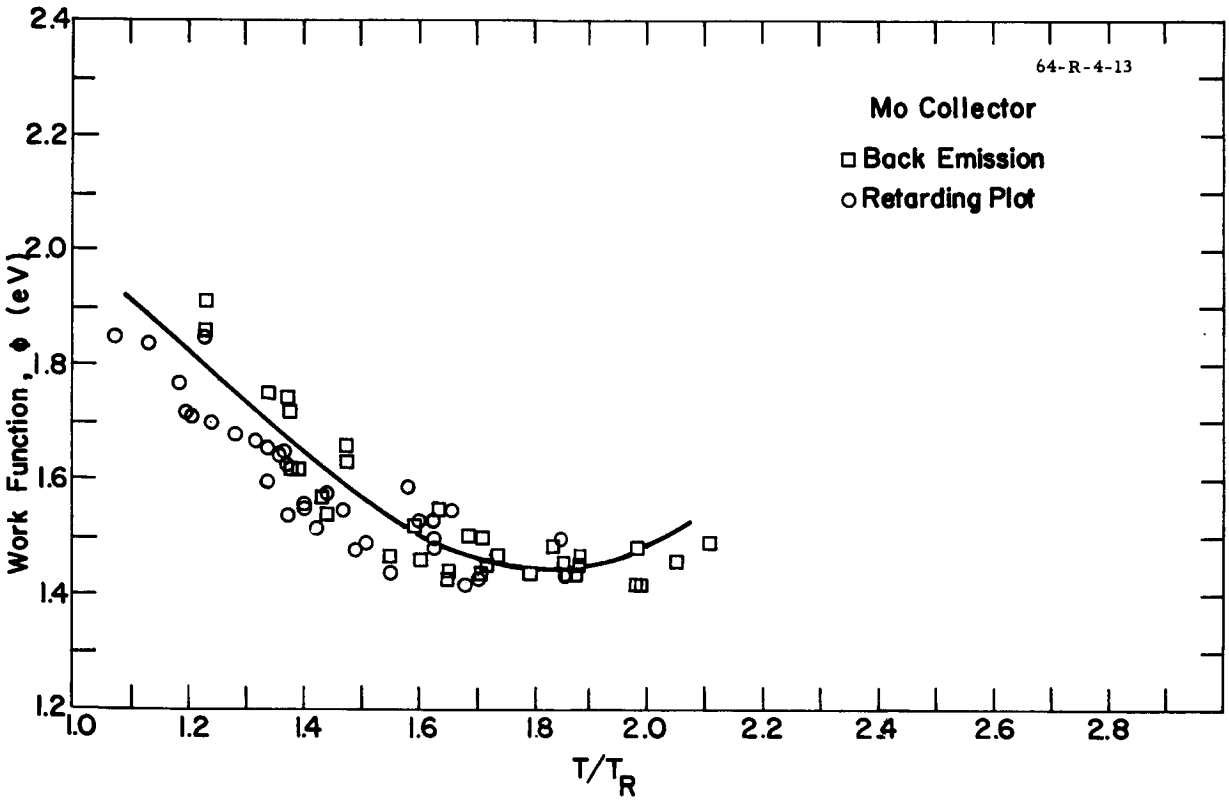

Figure 47. Correlation of Collector Work Function (Research Department Data)

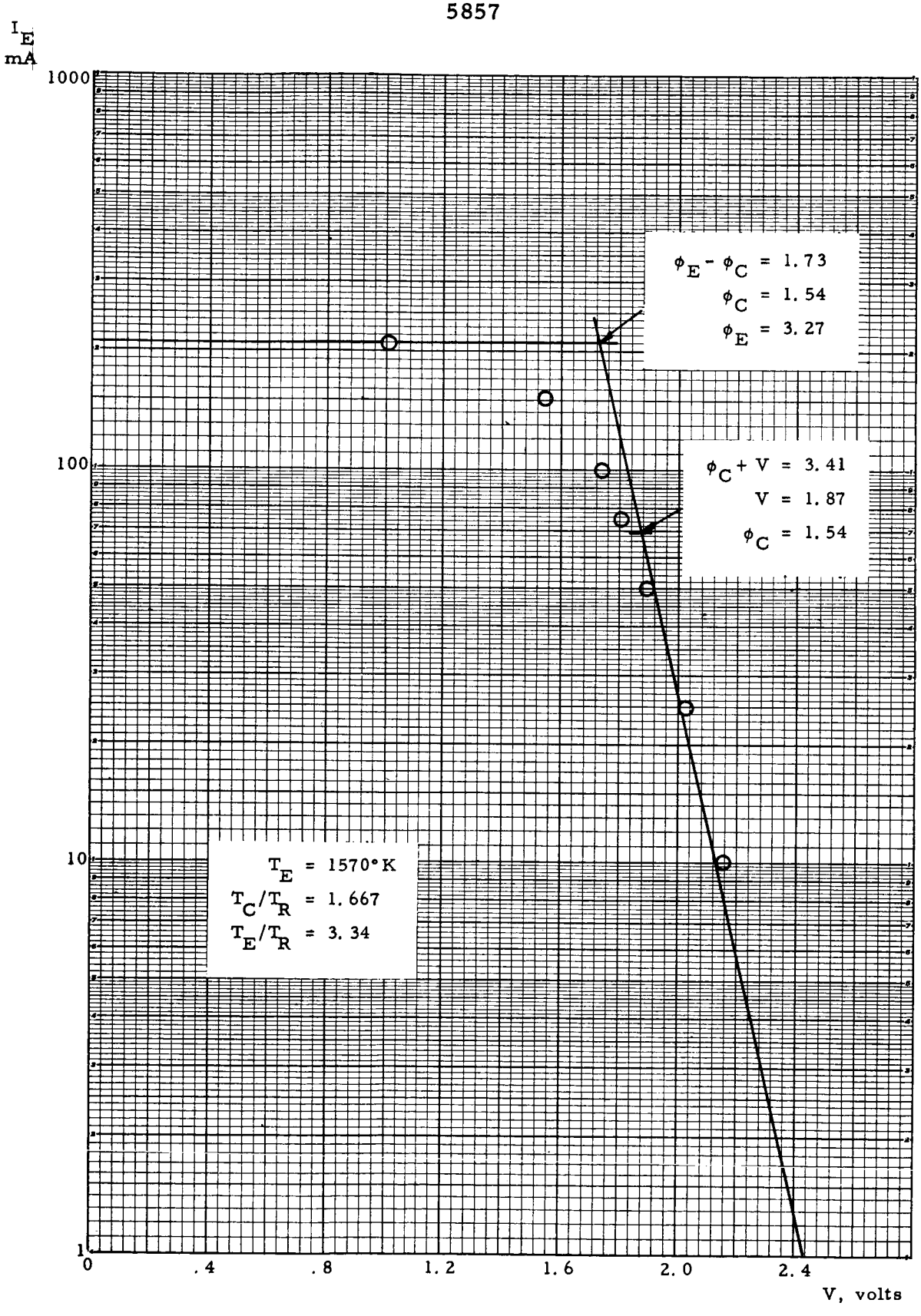

Figure 48. Boltzmann Line for TE-104 Collector

for an emitter temperature of 2000°K, the inner sleeve of the re-entrant emitter structure operates at an average temperature of 1805°K. If we take rhenium data as being representative of the emission properties of the surface of this piece, at any practical cesium reservoir temperature the emission density at the sleeve surface can be expected to be 50% higher than that at the emitter surface. Since the sleeve area is 70% greater than the emitter-planar area, 72% of the total current emitted will be contributed by the emitter support, rather than the emitter, and such collector work function measurements are, therefore, not valid.

In order for the measurements to have a greater resolution in de-determining the work function of the actual operating area of the collector, it is desirable to make the work function measurements at high current densities so that only the areas designed to handle a substantial rate of heat transfer can participate in the emission and collection of a high electron current. This is basically the approach followed in making the measurements presented in Figure 41. From a large number of measurements made in research converters, it is known that in the ignited mode an internal voltage drop takes place in the plasma, which is almost uniquely determined by the value of the pd (pressure times spacing) parameter, provided that the value of pd is above 20 mil-torrs. Figure 49 shows the dependence of the internal voltage drop, V_d, on pd as established by Thermo Electron's Research Department for a large body of thermionic data. For a value of pd of 20, this voltage drop reaches a minimum which is approximately equal to .48 volt. Since the position of the ignited branch of the I-V characteristic along the voltage axis is a function of the collector work function and the internal voltage drop, the oscillographs of Figure 41 provide a relative measurement

63-R-12-121

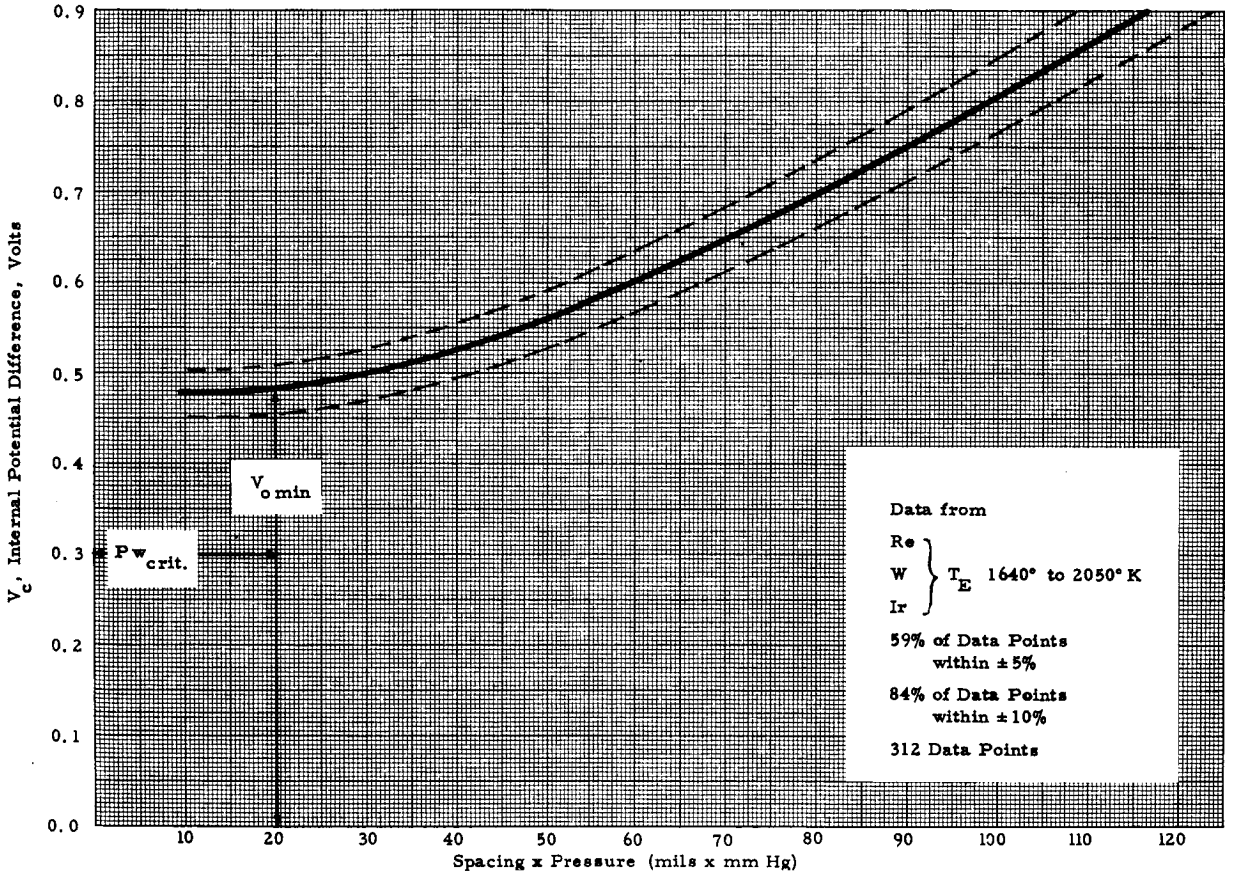

Figure 49. Voltage Drop in Cesium Plasma Versus Internal Potential Difference

of collector work function which can be compared with similar measurements on other converters. Figure 41 shows oscillographs for four different collector temperatures, and it would have been expected that the ignited branch of the I-V characteristics would move to the right with increases in collector temperature, thus signalling a decrease in collector work function, as predicted by the correlation presented in Figure 47. Actually, it was found that all four ignited branches occupied practically the same relative position, thus implying that the collector work function had not changed with collector temperature. This seemingly paradoxical fact tends to confirm the latest analytic results on collector back emission developed by N. S. Rasor, which predict that above a certain collector temperature, the increase in back emission causes a sheath to be created at the collector which offsets the decrease in collector work function which would otherwise have occurred.

In order to facilitate the calculation of emission currents at collector and emitter temperatures, Figure 50a and 50b present the plot of Richardson's Equation for the current range of 100 mA to 1000 A/cm^2.

4.4.7 Effect of pd on I-V Characteristics

The static data obtained from converter TE-103 at 1900°K, and the dynamic I-V characteristics at constant cesium temperature presented in Figures 36, 37, 38a and 38b for converters TE-102, 103, and 104, have been plotted in semi-logarithmic form in Figures 51a to 52a to f. The specific data sheet references for these figures are given in Table VIII. These figures also include a postulated I-V characteristic, calculated from a simple analysis of collision-free performance and including back emission effects. The sequence of figures permits the evaluation of the extent to which ideal performance is approached as the cesium pressure is gradually in-

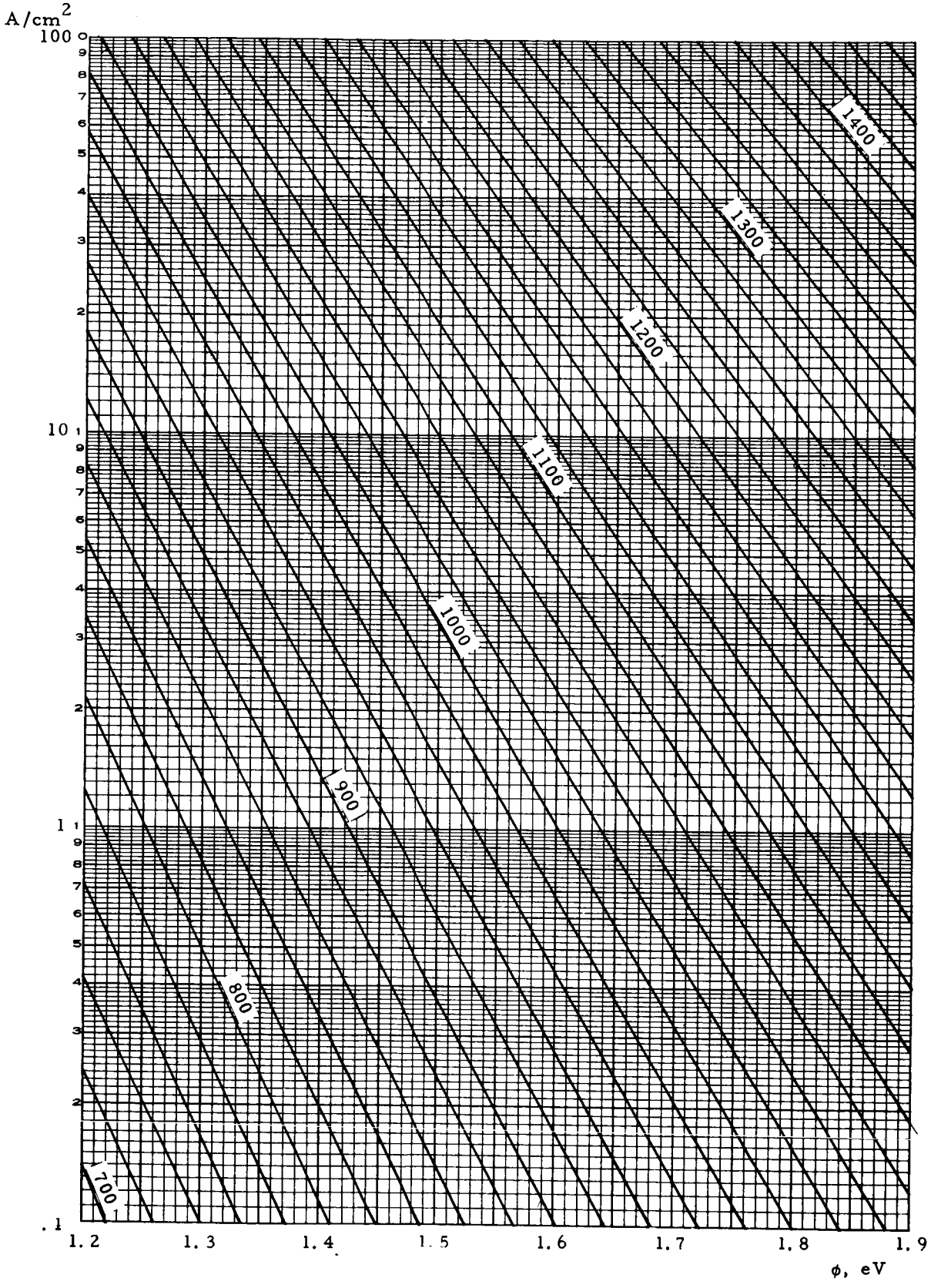

Figure 50a. Richardson's Equation (°K), ϕ = 1.2 to 1.9 eV

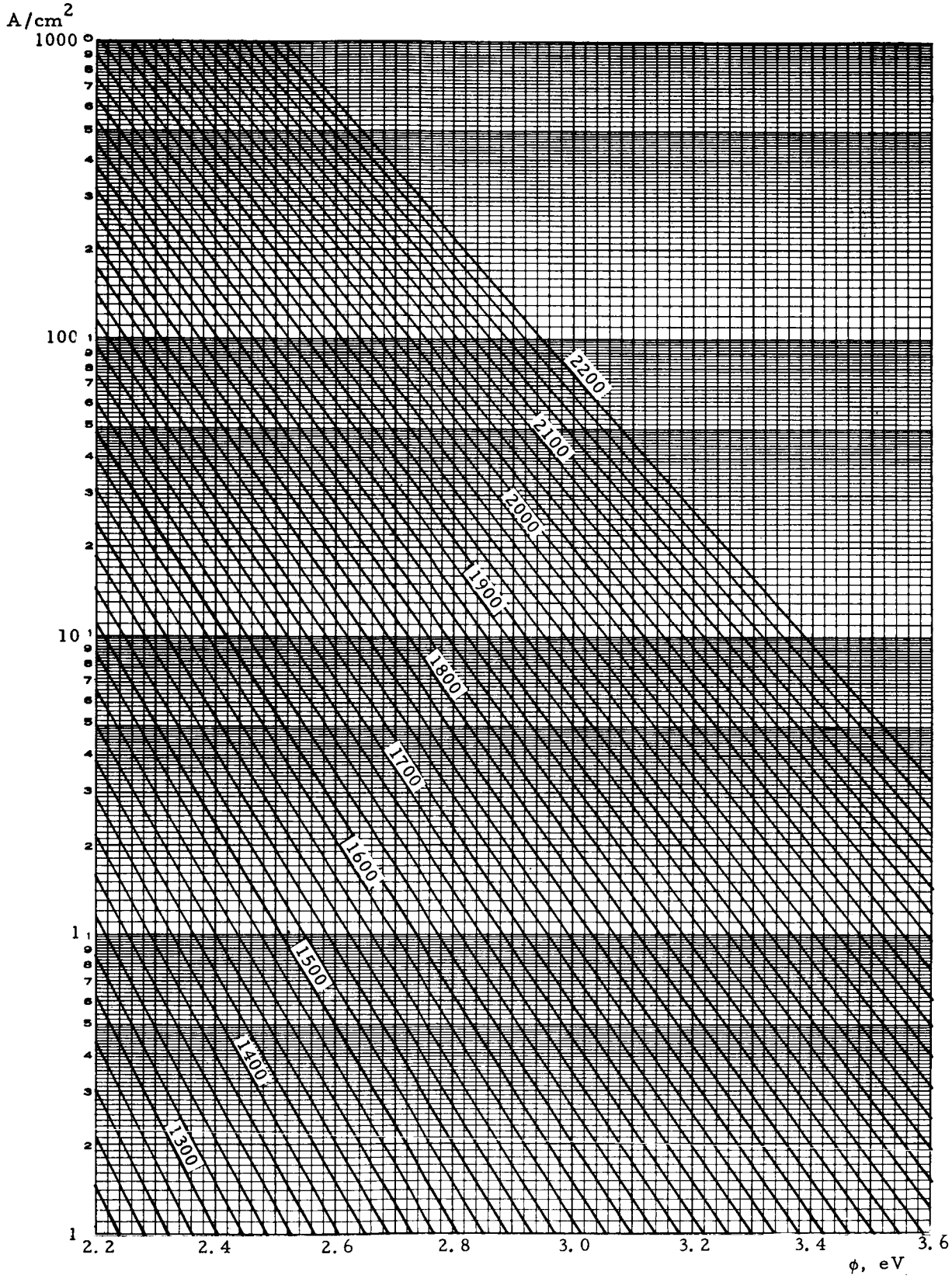

Figure 50b. Richardson's Equation (°K), ϕ = 2.2 to 3.6 eV

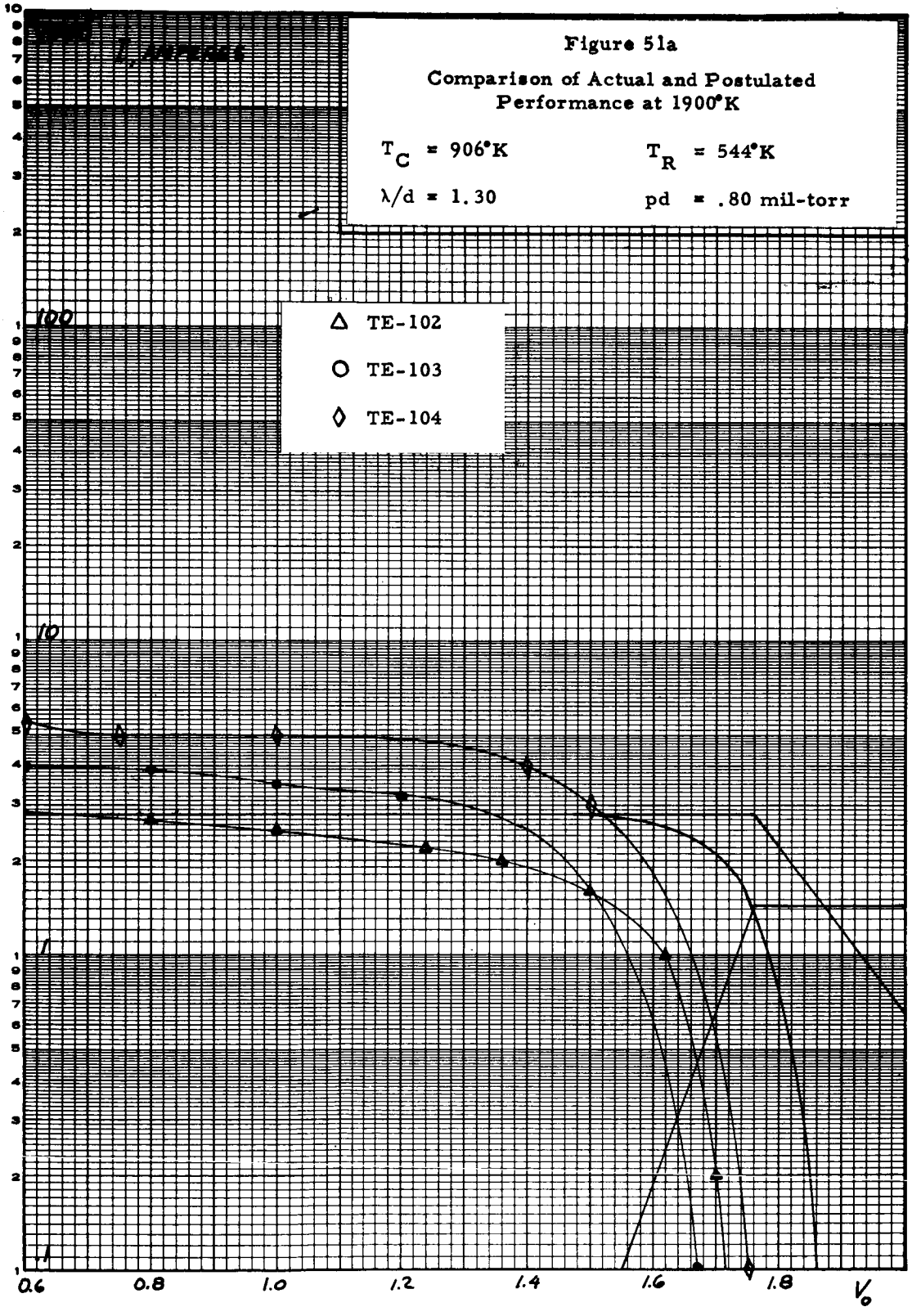
Figure 51a
Comparison of Actual and Postulated Performance at 1900°K
T_C = 906°K
T_R = 544°K
λ/d = 1.30
pd = .80 mil-torr
TE-102
TE-103
TE-104
100
10
1
.1
0.6
0.8
1.0
1.2
1.4
1.6
1.8
V_o

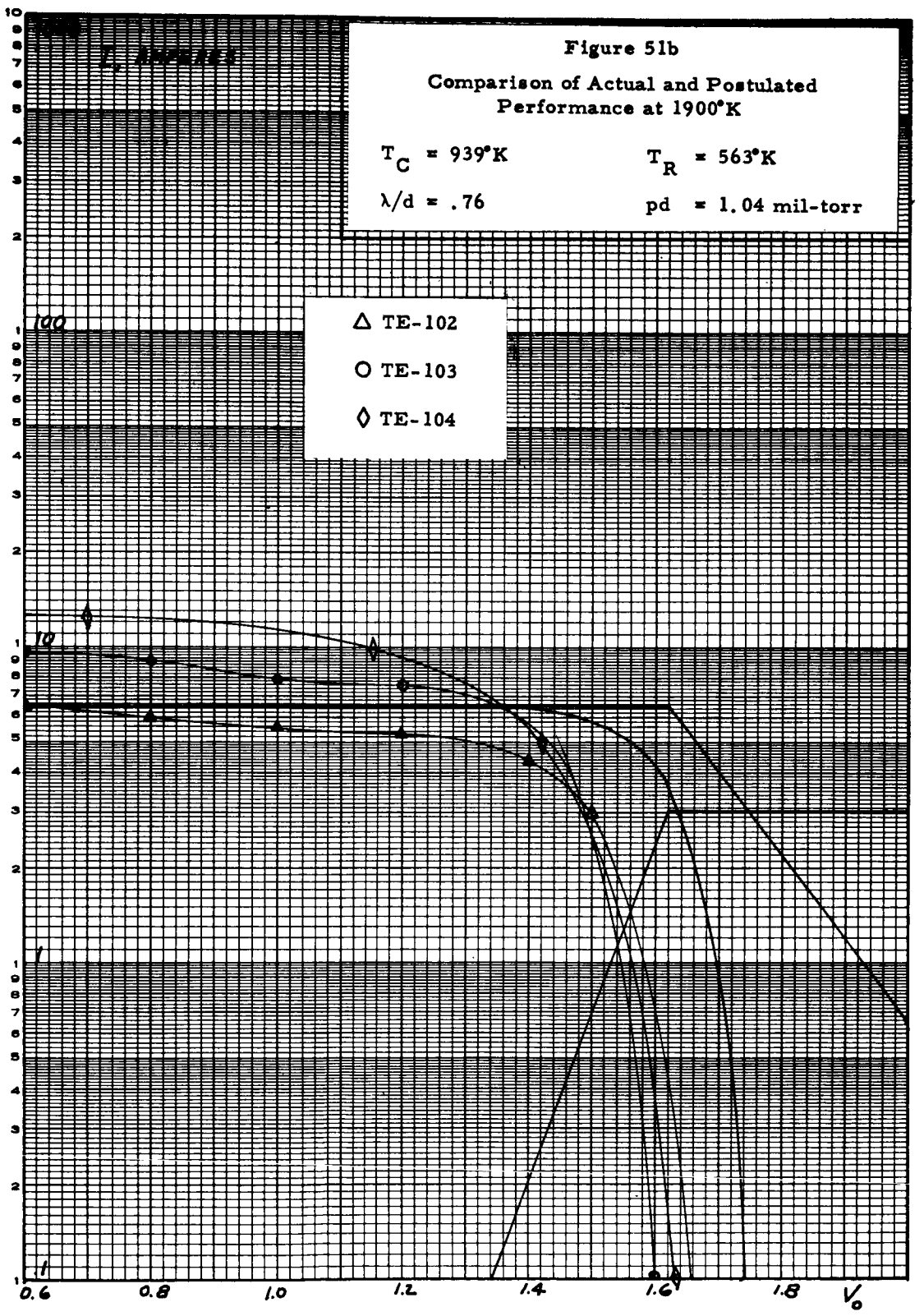
Figure 51b
Comparison of Actual and Postulated Performance at 1900°K
T_C = 939°K
T_R = 563°K
λ/d = .76
pd = 1.04 mil-torr
△ TE-102
○ TE-103
◊ TE-104
100
10
1
.1
0.6
0.8
1.0
1.2
1.4
1.6
1.8
V_o

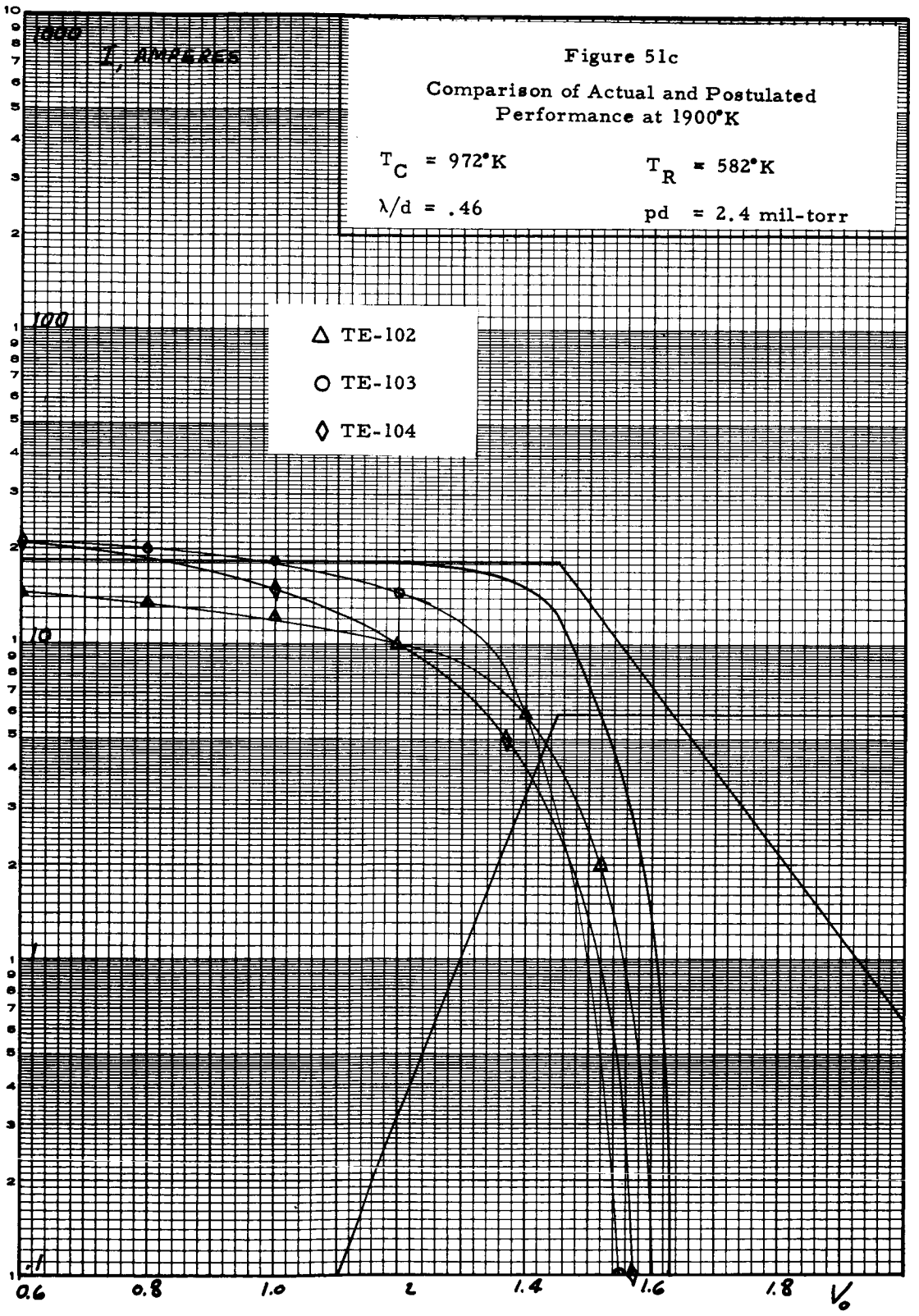

Figure 51c

Comparison of Actual and Postulated Performance at 1900°K

T_C = 972°K T_R = 582°K

λ/d = .46 pd = 2.4 mil-torr

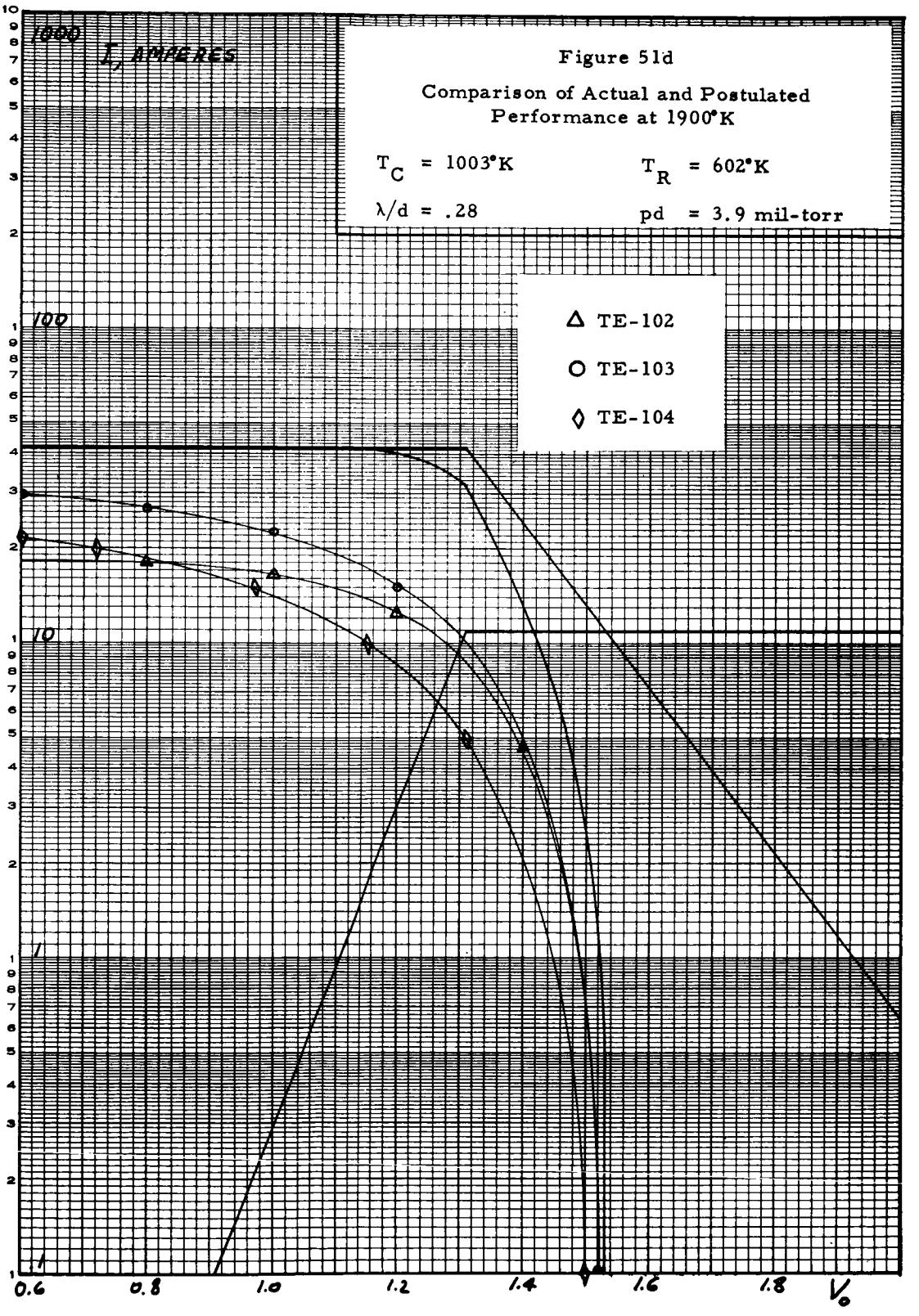
1000
I, AMPERES
100
10
1
.1
0.6
0.8
1.0
1.2
1.4
1.6
1.8
V₀
Figure 51d
Comparison of Actual and Postulated Performance at 1900°K
T_C = 1003°K
T_R = 602°K
λ/d = .28
pd = 3.9 mil-torr
△ TE-102
○ TE-103
◊ TE-104

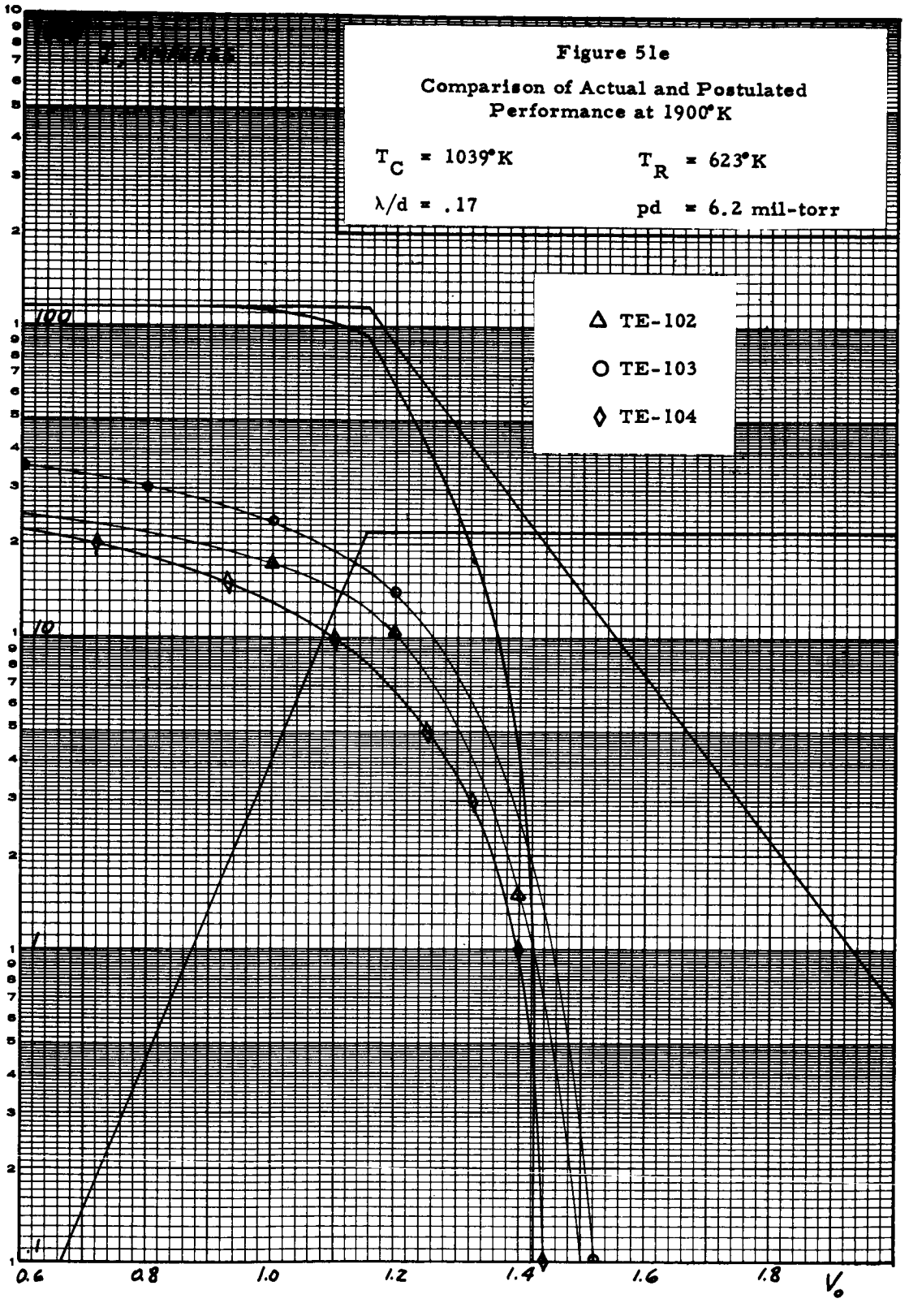
Figure 51e
Comparison of Actual and Postulated Performance at 1900°K
T_C = 1039°K
T_R = 623°K
λ/d = .17
pd = 6.2 mil-torr
△ TE-102
○ TE-103
◊ TE-104
100
10
1
.1
0.6
0.8
1.0
1.2
1.4
1.6
1.8
V_o

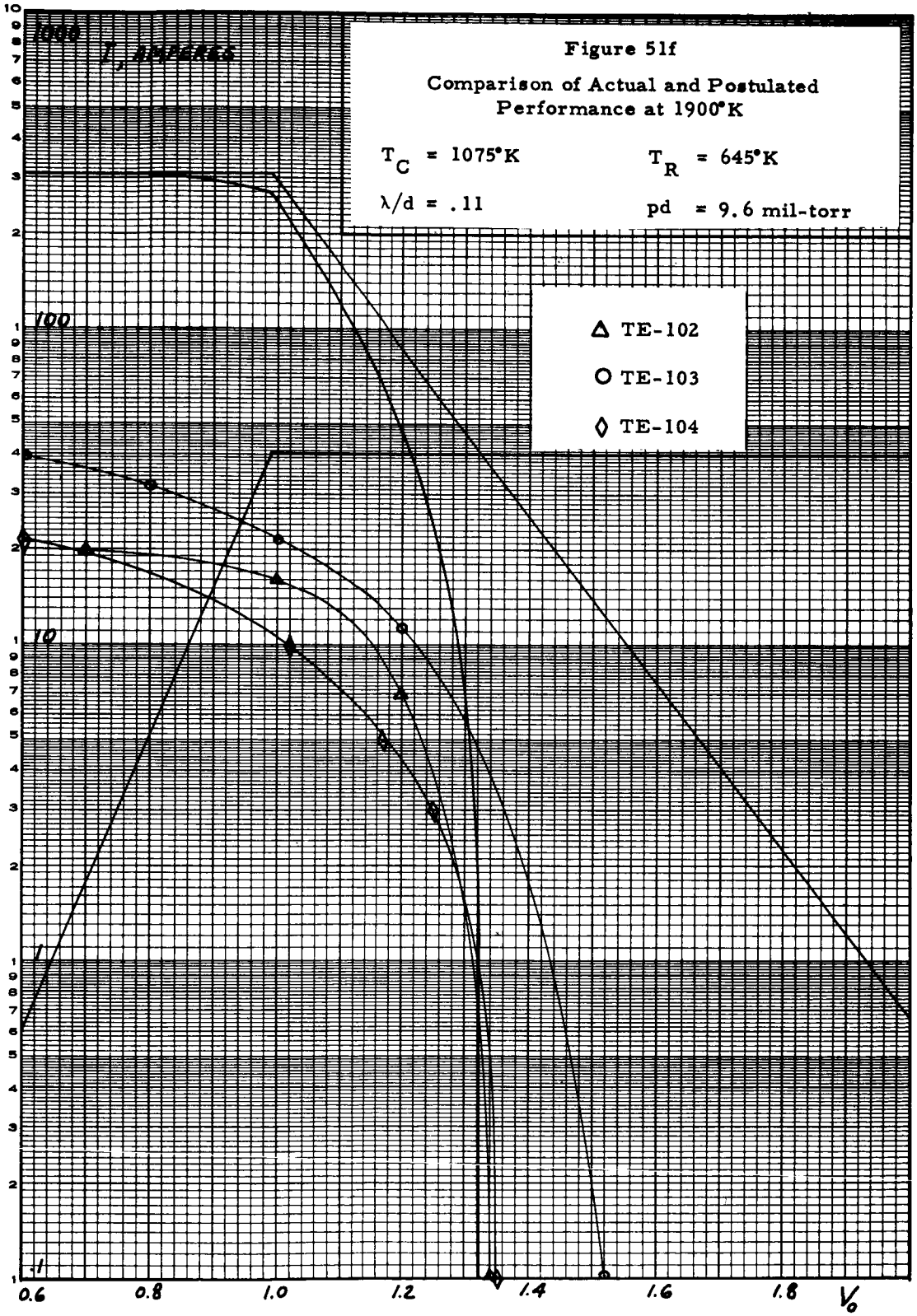
1000
I_p, AMPERES
100
10
1
.1
0.6
0.8
1.0
1.2
1.4
1.6
1.8
V_0
Figure 51f
Comparison of Actual and Postulated Performance at 1900°K
T_C = 1075°K
T_R = 645°K
λ/d = .11
pd = 9.6 mil-torr
△ TE-102
○ TE-103
◊ TE-104

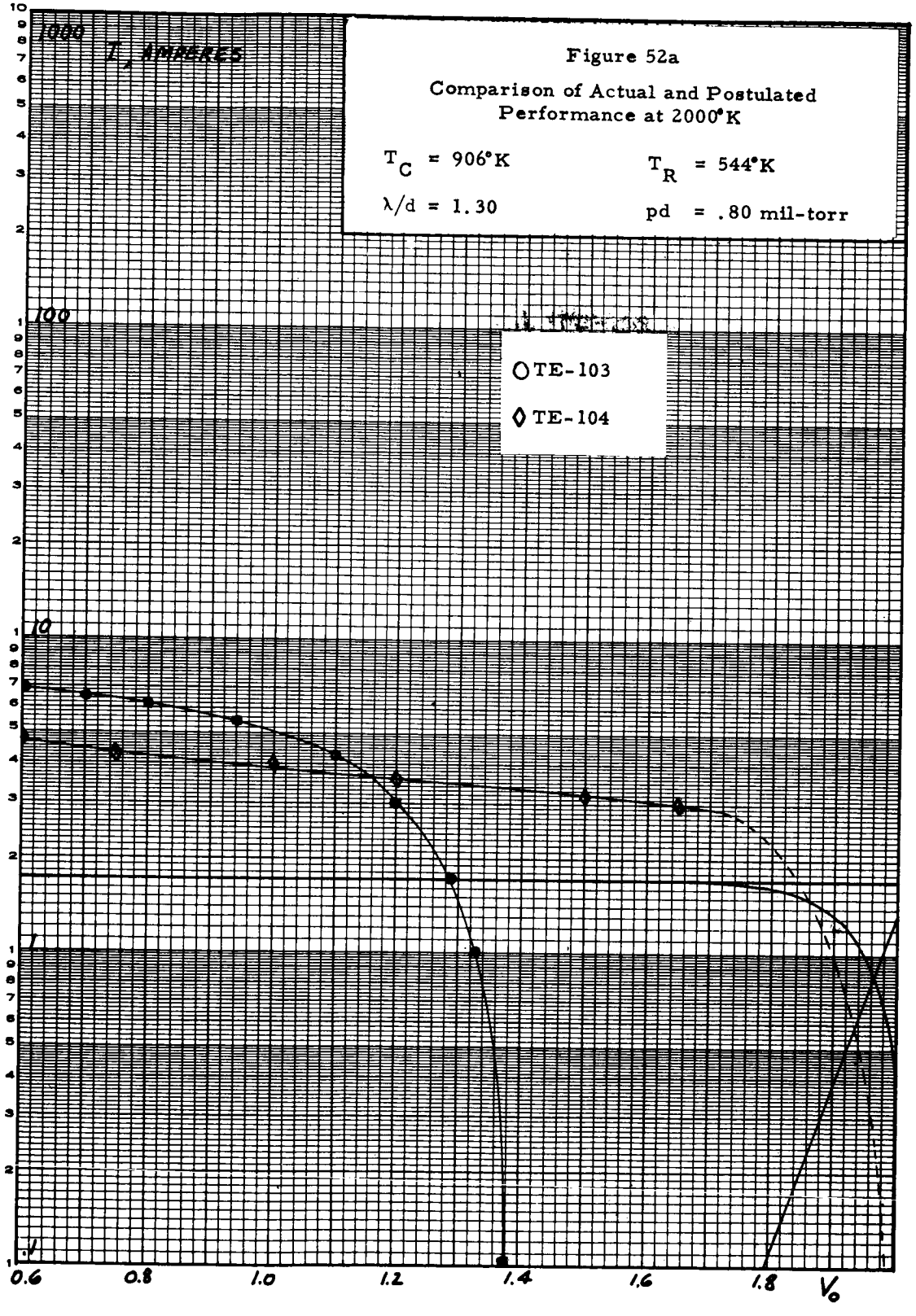

Figure 52a

Comparison of Actual and Postulated Performance at 2000°K

T_C = 906°K T_R = 544°K

λ/d = 1.30 pd = .80 mil-torr

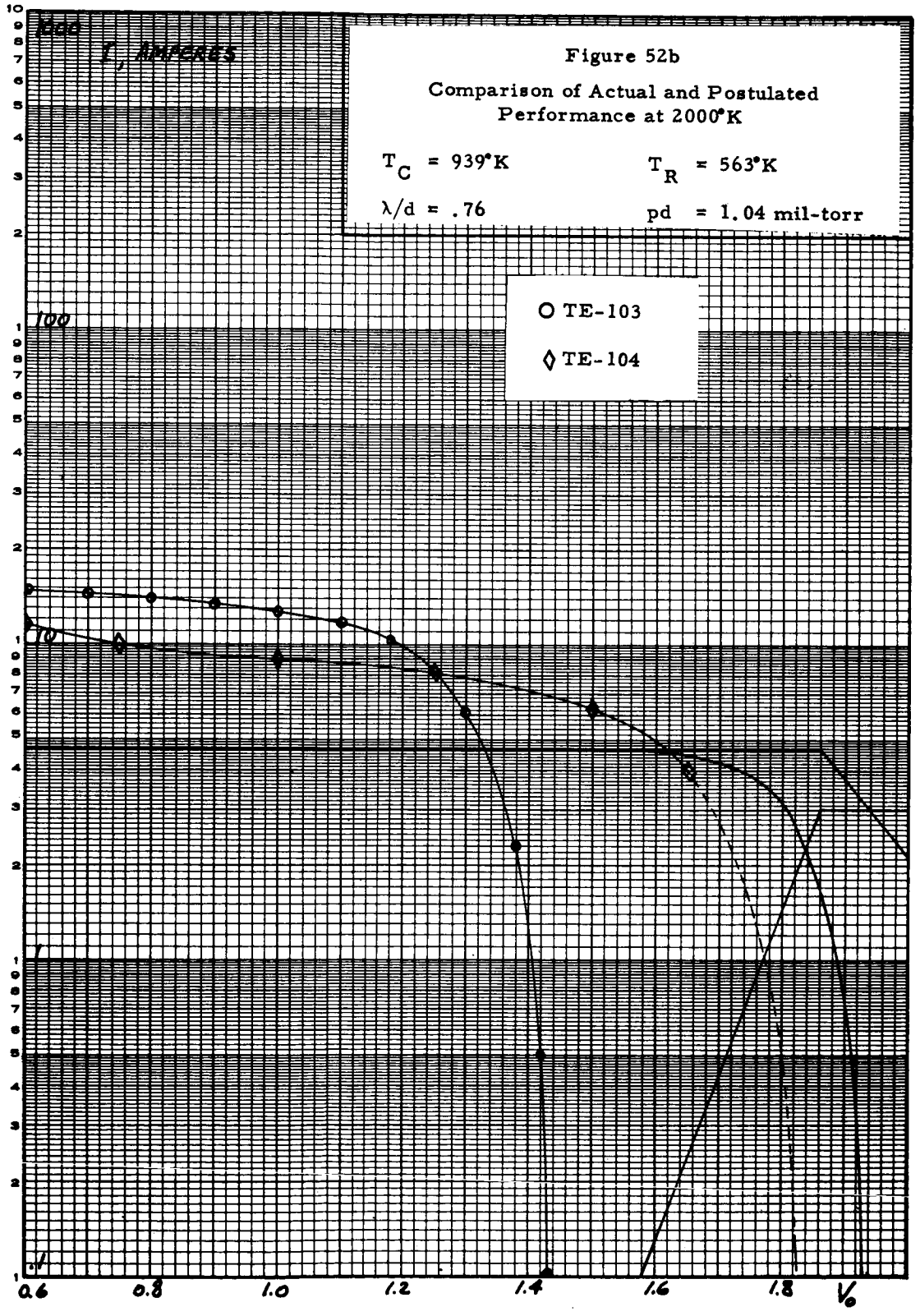
Figure 52b
Comparison of Actual and Postulated Performance at 2000°K
T_C = 939°K
T_R = 563°K
λ/d = .76
pd = 1.04 mil-torr
O TE-103
◊ TE-104
I, AMPERES
100
10
1
0.6
0.8
1.0
1.2
1.4
1.6
1.8
V_o

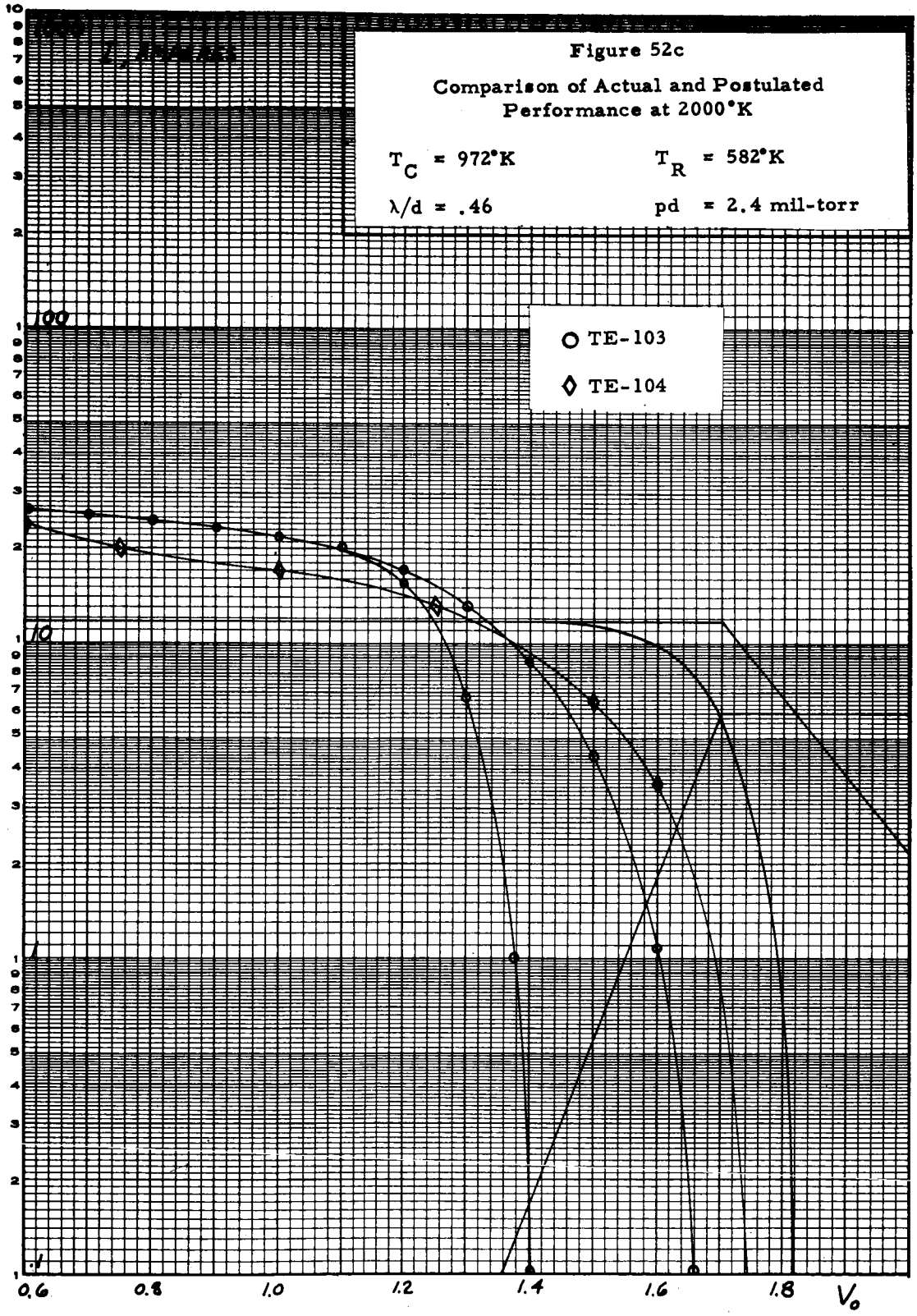
Figure 52c
Comparison of Actual and Postulated Performance at 2000°K
T_C = 972°K
T_R = 582°K
λ/d = .46
pd = 2.4 mil-torr
TE-103
TE-104
100
10
1
0.6
0.8
1.0
1.2
1.4
1.6
1.8
V_o

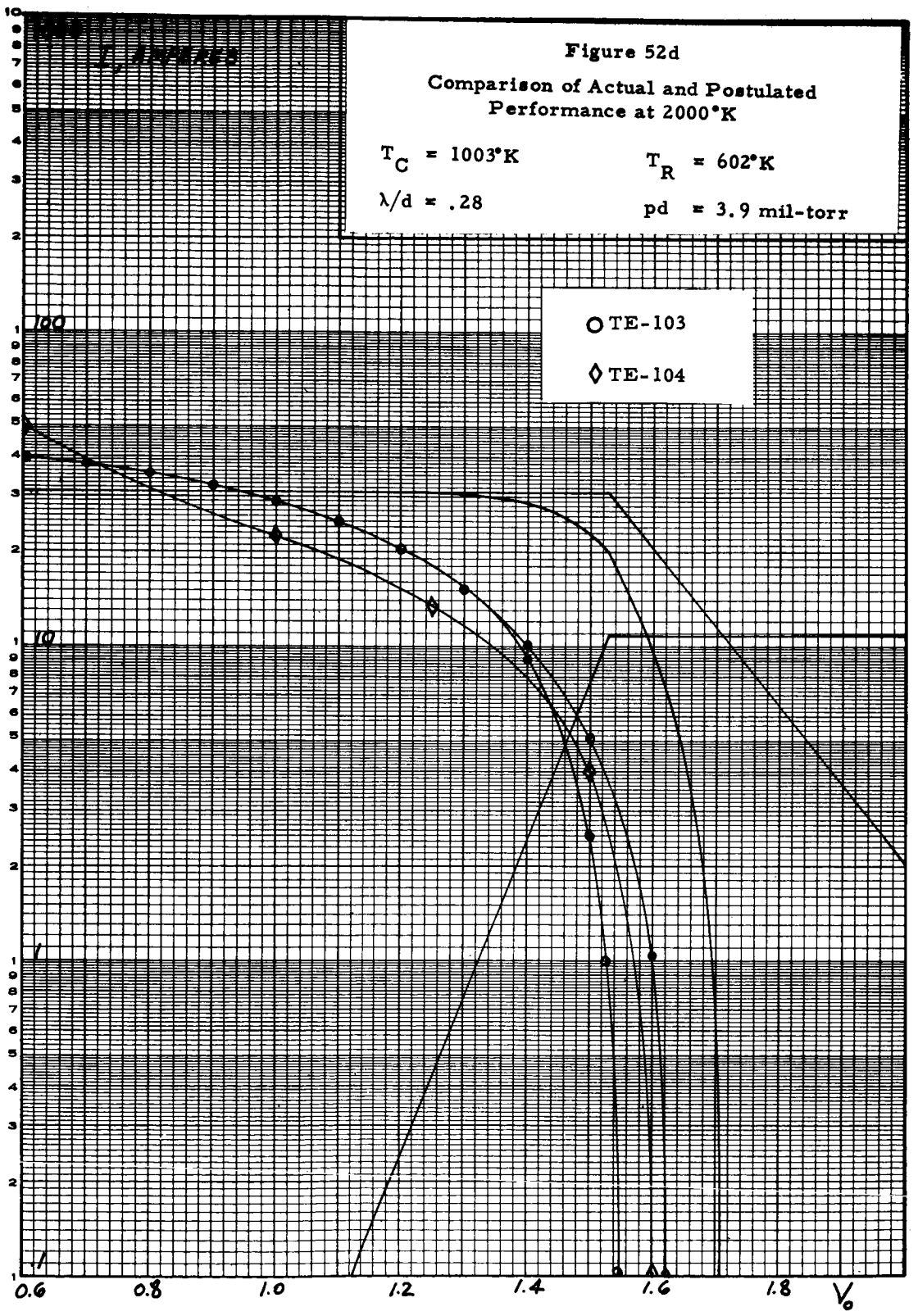
Figure 52d
Comparison of Actual and Postulated Performance at 2000°K
T_C = 1003°K
T_R = 602°K
λ/d = .28
pd = 3.9 mil-torr
TE-103
TE-104
100
10
1
.1
0.6
0.8
1.0
1.2
1.4
1.6
1.8
V_o

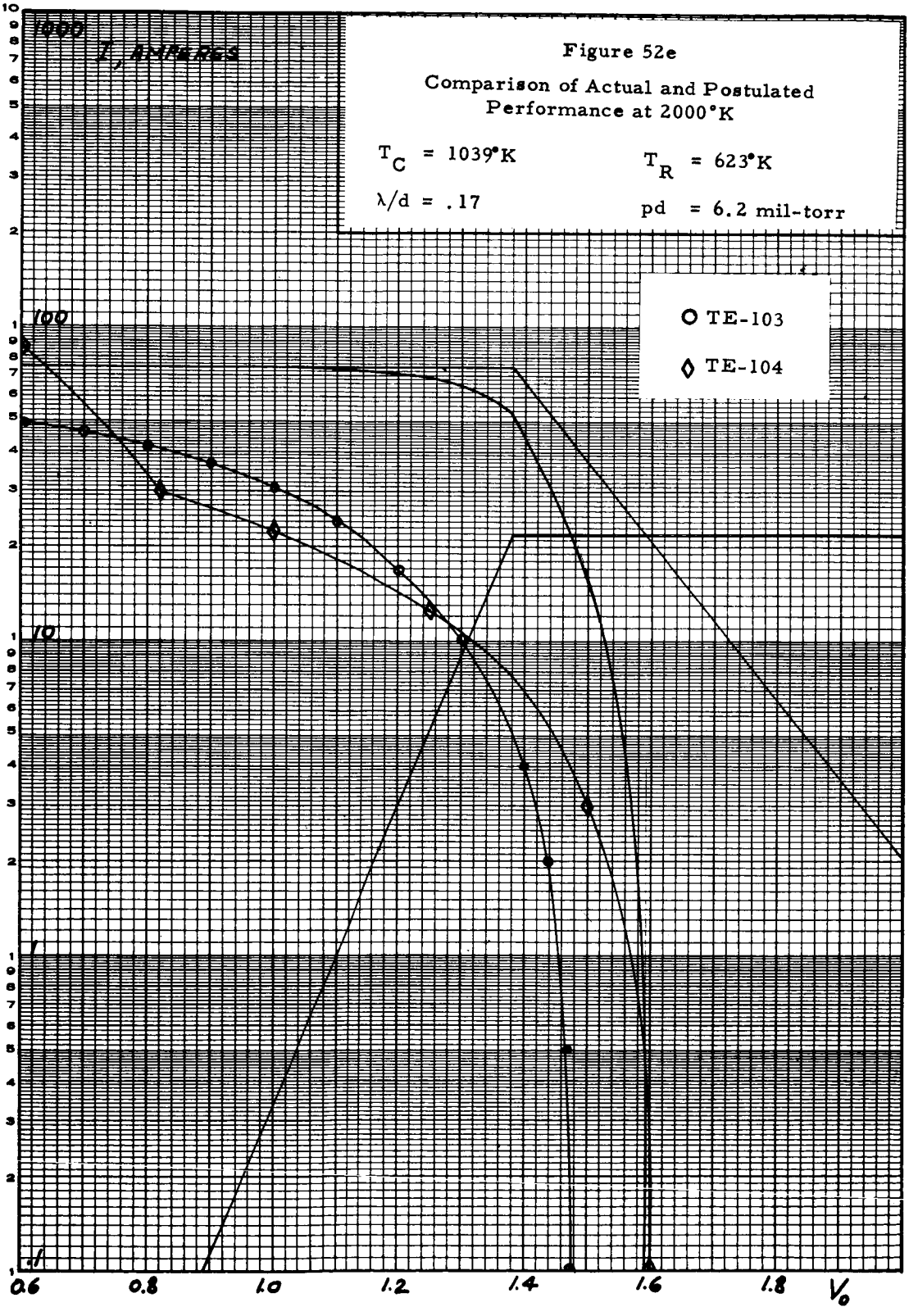

Figure 52e

Comparison of Actual and Postulated Performance at 2000°K

T_C = 1039°K T_R = 623°K

λ/d = .17 pd = 6.2 mil-torr

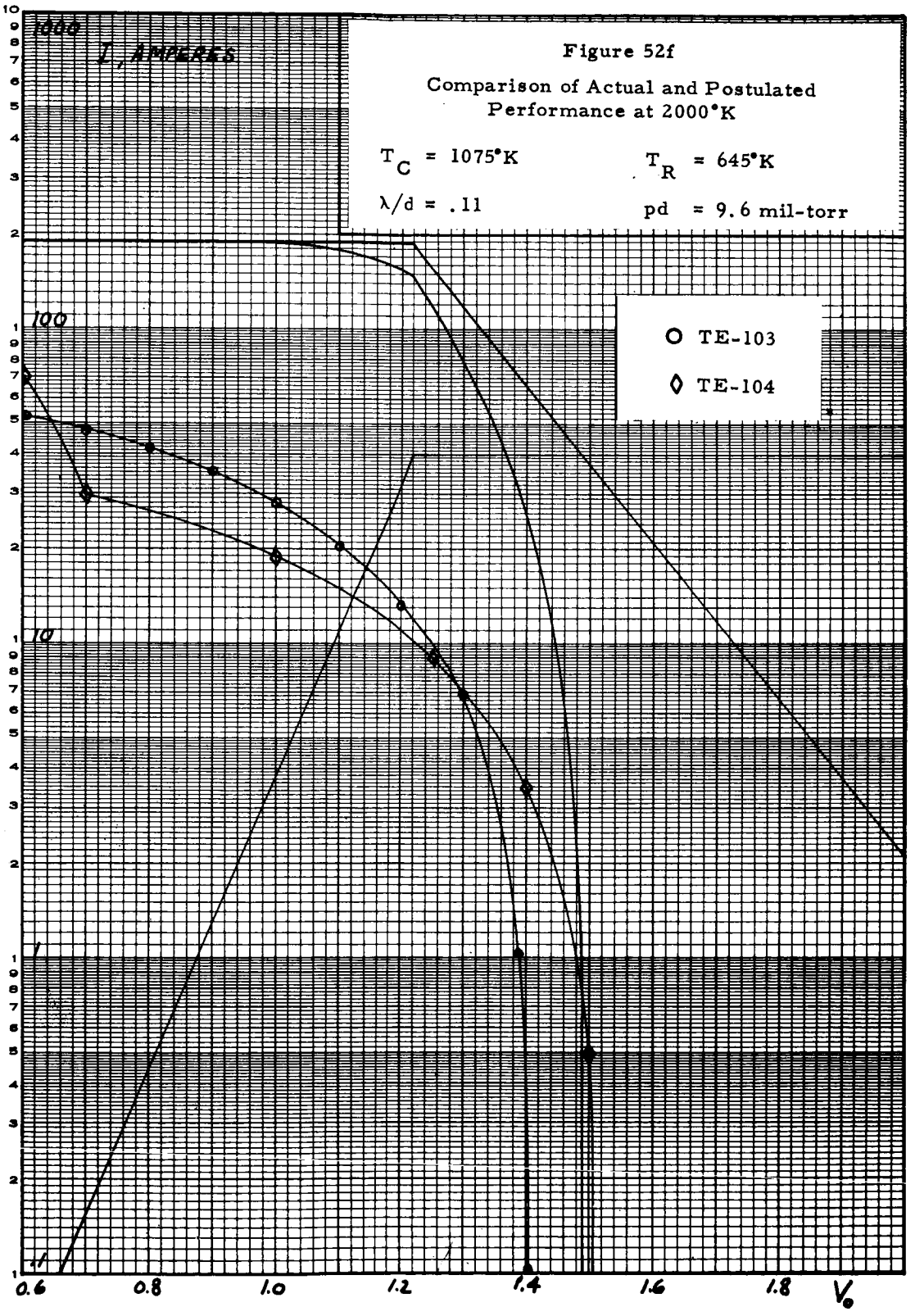
1000
I, AMPERES
100
10
1
0.1
0.6
0.8
1.0
1.2
1.4
1.6
1.8
V₀
Figure 52f
Comparison of Actual and Postulated Performance at 2000°K
T_C = 1075°K
T_R = 645°K
λ/d = .11
pd = 9.6 mil-torr
O TE-103
◊ TE-104

TABLE VIII

Data Sheet References for Figures 51 and 52

Figure 51 (a, b, c, d, e, f)

Converter	Data Sheets	Figure
102	28, 29	36
103	6, 7, 8	-
104	7	38b

Figure 52 (a, b, c, d, e, f)

Converter	Data Sheets	Figure
103	11, 12	37
104	6	38a

creased so that the ratio of mean-free-path to interelectrode spacing is decreased. They show that in order for ideal performance to be approached λ/d should have a value of no less than about 1.30. Figure 52a is of particular interest because it strikingly shows the improvement in high voltage performance which was obtained in converter TE-104 by the removal of the internal radiation shield. Figure 52e corresponds to the maximum power output conditions in the vicinity of 1 volt at 2000°K, and it can be seen that the converter output at that particular value of λ/d of .17 is substantially below ideal performance. The fact that the actual characteristics in some instances surpass the postulated I-V characteristics is probably due to a combination of (1) the effective emitter area is greater than 2.5 cm^2 due to edge effects, (2) the actual emitter work function may have been lower [redacted], and (3) the cesium reservoir temperature may have been slightly higher than recorded.

4.4.8 Comparison of Observed Performance in Converters TE-102, 103 and 104

Converters TE-102, 103 and 104 all incorporated a rhenium emitter and differed primarily in the following respects:

1. The emitter of converter TE-102 was pressure bonded, using a niobium shim.
2. Converter TE-103 was pressure bonded without the use of a niobium shim, and had a collector lateral area of more than double that of converter TE-102.
3. Converter TE-104 was fabricated without the internal radiation shield, but a broken drill fragment was left in the emitter structure inadvertently and must have subsequently melted and diffused in the emitter structure.

The use of a niobium shim in converter TE-102 was already mentioned as

being the probable cause of a continuous and gradual increase in the performance of converter TE-102 over the period of its test. Neither converter TE-103 nor converter TE-104, which did not include this niobium shim, exhibited a similar increase in performance. The highest performance reached by converter TE-102 under static conditions, and the corresponding performance of TE-103 were already compared at 2000°K in Figure 42. It is probable that the higher performance level achieved by converter TE-103 is due to the use of a larger collector lateral area in that converter. The lower performance of converter TE-104 compared to either TE-102 or TE-103 is attributed to the presence of the drill fragment in the emitter structure mentioned above. It is of interest, however, that in spite of this generally lower performance level, converter TE-104 exceeds the performance of TE-102 and TE-103 at both low and high voltages. The superior performance at low voltages is due to the ability of converter TE-104 to reach the ignited mode at a higher value of voltage than converter TE-103. This is made quite evident in Figures 37 and 38a where it can be observed that the ignition of converter TE-104 tends to occur at a voltage about 0.25 volt higher than that of converter TE-103. Although the pd values for these characteristics do not attain the region of validity of pd $>$ 20 (the highest pd being 9.6 mil-torrs) for the internal voltage drop correlation, it is rather evident that the difference in ignition voltages must be due primarily to a difference in collector work functions in favor of converter TE-104. It is then difficult to explain why the output of converter TE-104 is lower than that of TE-103 in the unignited mode. At this time, it appears that the difference might be attributed to a higher emitter work function in converter TE-104, but to answer the question with reasonable certainty, additional converters should

be built and tested. The better performance of converter TE-104 at high output voltage is most likely due to the absence of the internal radiation shield which, being previously connected at collector potential, must have contributed significantly to the loss of output by back-emission.

4.4.9 Effect of Collector Heat Treatment

It was mentioned in Section 4.3.4 that the collector of converter TE-104 was subjected to a heat treatment by taking it to 865°C while drawing a current of 50 amperes from the converter. Figures 38f and 38g presented apparently identical dynamic characteristics at 2000°K after successive heat treatments of 7 and 17 hours respectively. The actual effect of the collector heat treatment can actually be judged from a comparison of Figures 38a and either 38f or 38g. As may be noted, the ignited branches of the I-V characteristics were unaffected by the collector heat treatment, but the unignited portions of the curves underwent a pronounced pivotal displacement about the open circuit voltage point with a consequent improvement which was greatest in the vicinity of the ignition point. This is again a rather surprising phenomenon. It seems, however, that the improvement in performance observed is rather stable and this treatment should deserve further consideration in future work.

5. CONCLUSIONS AND RECOMMENDATIONS

In this first year of effort in the development of the TE-100 converter, the converter structure has been designed, prototype tested and improved to the extent that a reliable device with a 1 mil interelectrode spacing is now available for performance investigations and for further refinements of the structure such as those required for generator fabrication.

The observations that can be made from these tests are as follows:

a) Converter TE-100 tests were significant in evaluating the initial TE-100 design from a heat transfer standpoint and in discovering the tendency of the converter electrodes to remain out of parallel if left free during assembly.

b) The test of converter TE-101 emphasized once again the great care that must be used in assembling converters with a tantalum emitter if performance degradation is to be avoided.

c) The steady improvement in the performance of converter TE-102 indicated that it is likely for niobium at a pressure-bonded emitter interface to have a deleterious effect on initial converter performance.

d) Converter TE-103 pointed to the need for more precise alignment of converter parts during assembly, in order to avoid side electrical shorts between the emitter and the collector. It also demonstrated the high level of performance stability that can be achieved with rhenium emitters, and exhibited a high power output at relatively large values of output voltage. Its thermal efficiency was considerably higher than that of any previous series of SET converter structures (including Series VIII).

e) The test of converter TE-104 is relatively inconclusive. It has demonstrated that a beneficial effect on performance is obtained by omitting the internal radiation shield of the converter and, possibly, by heat treatment of the collector. However, the performance level achieved is rather paradoxical at this time: in the ignited mode, the maximum power output is about 40% higher than that of converter TE-103, but in the unignited mode, the maximum power output of converter TE-103 exceeds that of TE-104 by about 17%. Although the difference can conceivably be ascribed to the effect of the additional lateral collector area in converter TE-103, the omission of the internal radiation shield in converter TE-104

and the fact that a drill fragment was present, melted and diffused in the emitter structure of this converter, it is clear, however, that more prototypes need to be built and tested to better understand the performance characteristics of TE-100 converters.

The development of the TE-100 converter series is judged to be of importance because of the numerous improvements that the converter incorporates, and because with its smaller interelectrode spacing it can lead to significant increases in conversion efficiency. This converter is the backbone of any future progress in the area of solar thermionics, and Thermo Electron earnestly recommends that its development be given a high priority.